Comprehensive Cardiovascular Phenotyping of Children with Renal Disease

Dr Mun Hong Cheang
A dissertation submitted in fulfilment of the requirements for the degree of

MD (Res)

of

University College London

Institute of Cardiovascular Science

2018

I, Mun Hong Cheang, confirm that the work presented in this thesis is my own. Where information has been derived from other sources, I confirm that this has been indicated in the thesis.

Acknowledgements

I would like to thank my primary supervisor Dr Vivek Muthurangu for his support and advice throughout my research. With his guidance, I have learnt one of the most valuable lessons in my career; the importance of an inquisitive mind for the pursuit of knowledge.

I want to thank Dr Jennifer Steeden, my secondary supervisor, for her constant support, sensible advice and imparting her vast knowledge of MRI physics which has been crucial for this project.

I also want to express my gratitude to Professor Andrew Taylor for giving me the opportunity to work in this department, Dr Nathaniel Barber, my research counterpart, for his unwavering support throughout my project, Wendy Norman, Rod Jones, and Steven Kimberley for their endless support and help with the logistics of this project. I would like to especially thank Dr Daljit Hothi and Dr Kjell Tullus and the renal department in Great Ormond Street Hospital for their help with patient recruitment and renal expertise.

I am also grateful to Kids Kidney Research for funding this project. This work would not have been possible without their assistance.

Finally, I want to thank my parents, my sisters and my partner Chris for their love, support and patience. This thesis is dedicated to them.

Abstract

Children with chronic kidney disease (CKD) have significantly increased cardiovascular mortality. The reasons for this remain unclear, as the pathological effects of renal disease have not been well characterised. This is because current methods of assessment like echocardiography have significant limitations. Cardiovascular magnetic resonance imaging (CMR) is the reference standard method for cardiovascular assessment. Therefore, the aim of this thesis is to investigate the utility of CMR for the cardiovascular assessment of children with renal disease.

Three separate studies were carried out to comprehensively characterise the cardiovascular phenotype in the following groups: pre-dialysis CKD, dialysis dependent CKD and renovascular hypertension. They were compared with a control group of healthy and essential hypertension children. All subjects underwent a CMR study with non-invasive blood pressure measurements. The protocol included novel sequences that assessed diastolic function and myocardial velocity, in addition to conventional measures. Between group ANOVA comparisons were performed as described; mild, moderate and severe pre-dialysis CKD (n=100) versus healthy children (n=20), Haemodialysis (n=9), peritoneal dialysis (n=8), pre-dialysis CKD stage 5 (n=10) versus healthy children (n=10), and renovascular hypertension (n=15), essential hypertension (n=15) versus healthy children (n=15).

Blood pressure and systemic vascular resistance (SVR) were elevated while total arterial compliance was normal in all renal patients. There was also evidence of left ventricular remodelling without hypertrophy in pre-dialysis and renovascular children. Diastolic dysfunction was present in all renal patients. Systolic myocardial velocity was impaired only in CKD but not in renovascular hypertension.

In conclusion, CMR offers valuable insight into the cardiovascular characteristics of renal disease. Hypertension in renal disease is predominantly secondary to elevated SVR. Diastolic impairment preceded left ventricular hypertrophy. Sub-clinical systolic dysfunction was also present in renal dysfunction. Further studies are warranted to investigate the future role of CMR for cardiovascular risk assessment in paediatric renal disease.

Table of contents:

List of figures:

List of tables:

List of abbreviations:

A = Peak late diastolic (mitral inflow) velocity

A’ = Peak late diastolic LV myocardial velocity

ACE = Angiotensin converting enzyme

ANOVA = Analysis of variance

AoC = Ascending aortic compliance

AoMax = Maximum ascending aortic diameter

AoMin = Minimum ascending aortic diameter

AoS = Ascending aortic strain

AT2 = Angiotensin 2

BB = Beta blocker

BP = Blood pressure

BSA = Body surface area

CAKUT = Congenital abnormalities of kidney and urinary tract

CCB = Calcium channel blocker

cIMT = Carotid intimal medial thickness

CV = Cardiovascular

CKD = Chronic Kidney Disease

CMR = Cardiovascular Magnetic Resonance Imaging

CO = Cardiac output

DBP = Diastolic blood pressure

E = Peak early diastolic (mitral inflow) velocity

E’ = Peak early diastolic LV myocardial velocity

ECG = Electrocardiography

ECHO = Two-dimensional Echocardiography

EDV = End-diastolic volume

EF = Ejection Fraction

eGFR = Estimated Glomerular Filtration Rate

eHTN = Essential hypertension

ESRF = End stage renal failure

ESV = End-systolic volume

ET = Ejection time

FOV = Field of view

GOSH = Great Ormond Street Hospital

HB = Haemoglobin

HC = Healthy controls

H-CKD = Hypertensive CKD cohort

HD = Haemodialysis

HR = Heart rate

HTN = Hypertension

ICT = Isovolumic contraction time

IRT = Isovolumic relaxation time

K-T SENSE = K-space and time sensitivity encoding

LAA = Left atrial area

Long = Longitudinal

LV = Left Ventricle

LVH = Left ventricular Hypertrophy

LVM = Left ventricular mass

$LVMht^{2.7}$ = Left ventricular mass indexed to height to the power of 2.7

LVOT = Left ventricular outflow tract

MBP = Mean blood pressure

MDT = Multi-disciplinary team

MR = Magnetic resonance

MRI = Magnetic resonance imaging

MVR = Mass volume ratio

N-CKD = Non-hypertensive CKD cohort

NRES = National Research Ethics Service

PCMR = Phase contrast magnetic resonance

PD = Peritoneal dialysis

PP = Pulse pressure

PTH = Parathyroid Hormone

PWV = Pulse wave velocity

RA = Renal artery

RAA = Right atrial area

Rad = Radial

RAS = Renal artery stenosis

RAAS = Renal angiotensin aldosterone system

RF = Radiofrequency

RH = Renovascular hypertension

ROI = Region of interest

RRT = Renal replacement therapy

S’ = Peak systolic LV myocardial velocity

SAX = Short axis

SBP = Systolic blood pressure

SENSE = Sensitivity encoding

SPAMM = Spatial modulation of magnetization

SV = Stroke volume

SVR = Systemic vascular resistance

TAC = Total arterial compliance

TE = Echo time

TEI = Myocardial performance index

TPM = Tissue Phase Mapping

TR = Repetition time

UNFOLD = Unaliasing by fourier-encoding overlaps using temporal dimension

VENC = Velocity Encoding (maximum measurable velocity range)

β = Beta coefficient

1 Introduction

Chronic kidney disease (CKD) is associated with a significantly higher mortality risk in adults (1). This risk increases as renal function deteriorates (Figure 1.1). Cardiovascular (CV) mortality is one of the leading causes of death in end-stage renal disease (2). This is because CV risk factors like essential hypertension and diabetes mellitus are common co-morbidities in the adult population. In fact, they are the two main causes of renal disease in adults (3) and are independently associated with adverse long-term CV effects. However, the confounding effect of these conditions has made it difficult to study the pathophysiological impact of renal disease on the CV system. While epidemiological studies have clearly demonstrated an independent link between CKD and CV risk (1), the mechanistic relationship between CKD and CV effects remain poorly understood.

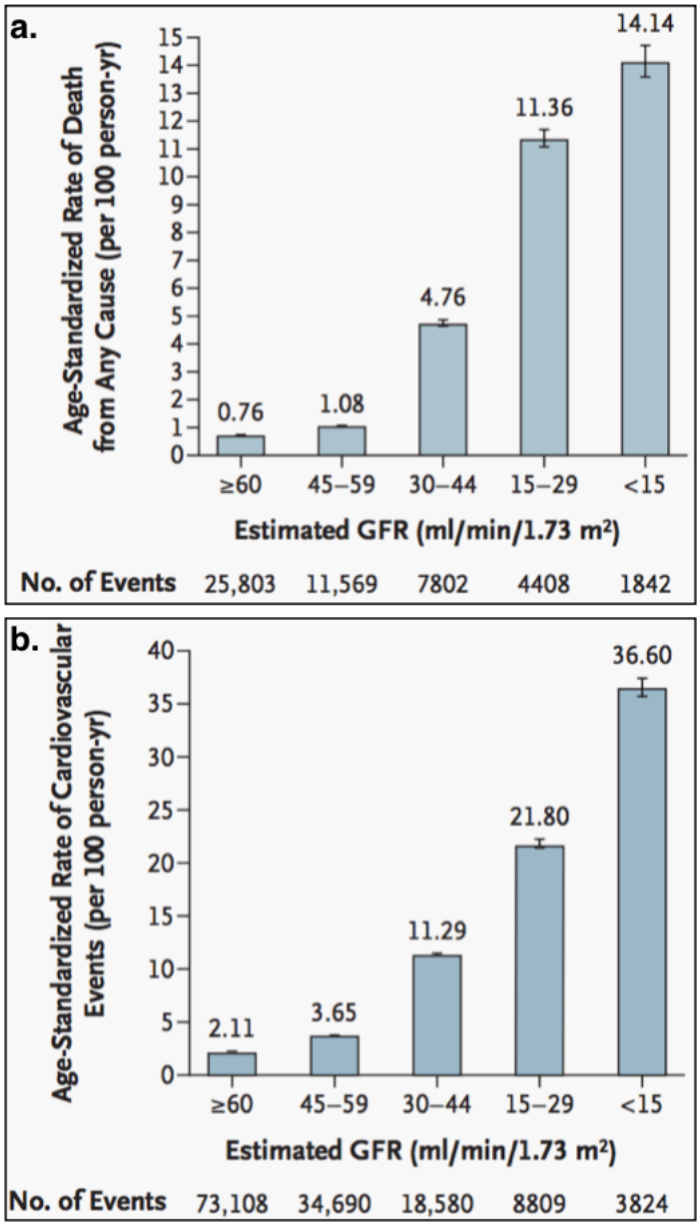

Figure 1.1: Graphs showing (a) age-standardised mortality rate and (b) cardiovascular events. (Reproduced with permission, Go *et al*. (1). Copyright Massachusetts Medical Society).

1.1 Paediatric renal disease

Paediatric CKD represents a unique opportunity to study the independent effects of renal disease on the CV system. Although CV mortality is also a major cause of death in children (4), the diagnosis of CKD is not usually preceded by a long history of traditional CV risk factors, as is commonly the case in adults. This is because the aetiology of paediatric CKD is markedly different to adults. The main causes of renal disease in children are congenital abnormalities of the kidney and urinary tract (CAKUT), glomerulonephritis and hereditary nephropathy (5). These three causes together, account for 72% of the paediatric CKD population (Figure 1.2).

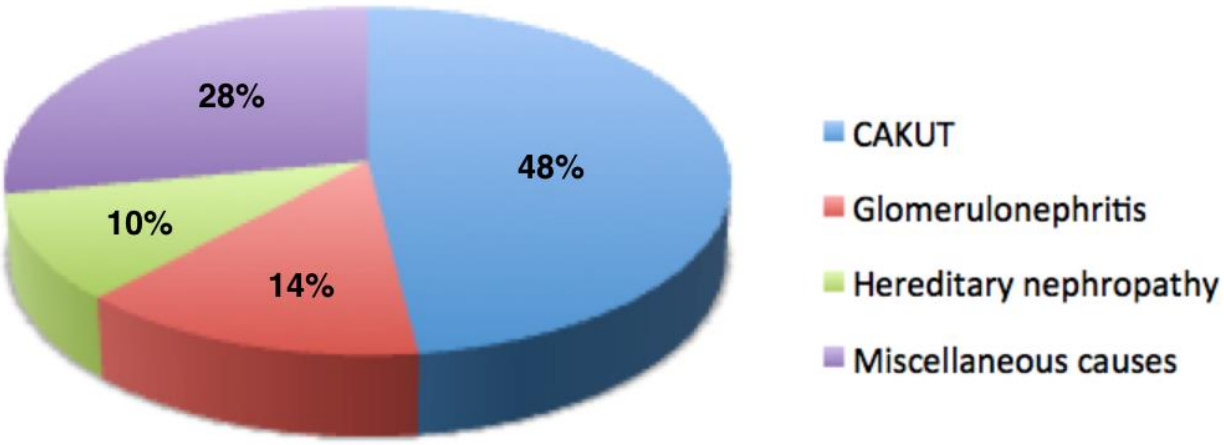

Figure 1.2: Three main causes of chronic renal disease in children (North American Pediatric Renal Transplant Cooperative Study, NAPRTCS, 2008 Annual Report) (5).

Paediatric renal disease may also be associated with CV risk factors. Both hypertension and dyslipidaemia can be found in up to 50% of children with CKD (4). However, unlike adults, the premature development of CV risk in children is likely to be a direct result of the pathological changes to biochemistry, cardiac and vascular function brought on by chronic renal disease itself (6).

Nonetheless, there is seldom a history of chronic exposure to CV risk factors in children. Given that CV risk remains elevated in children, this is further evidence of the independent effect of CKD on the CV system. Indeed, CV abnormalities in children are very similar to that of adults (6). Hence, paediatric CKD may be regarded as a relatively "pure" disease substrate, without the confounding effect of long-standing CV co-morbidities. Studying the CV effects of CKD in children may offer valuable insight into the disease process.

1.2 Mechanisms of cardiorenal syndrome

The complex interaction between kidney and heart involve a multitude of different neurohumoral and immune-mediated pathways. The relationship between heart and renal failure has been categorised into five different types of cardiorenal syndrome. This project is primarily concerned with studying the effects of chronic renal disease on the cardiovascular system, namely cardiorenal syndrome type 4 (Figure 1.3).

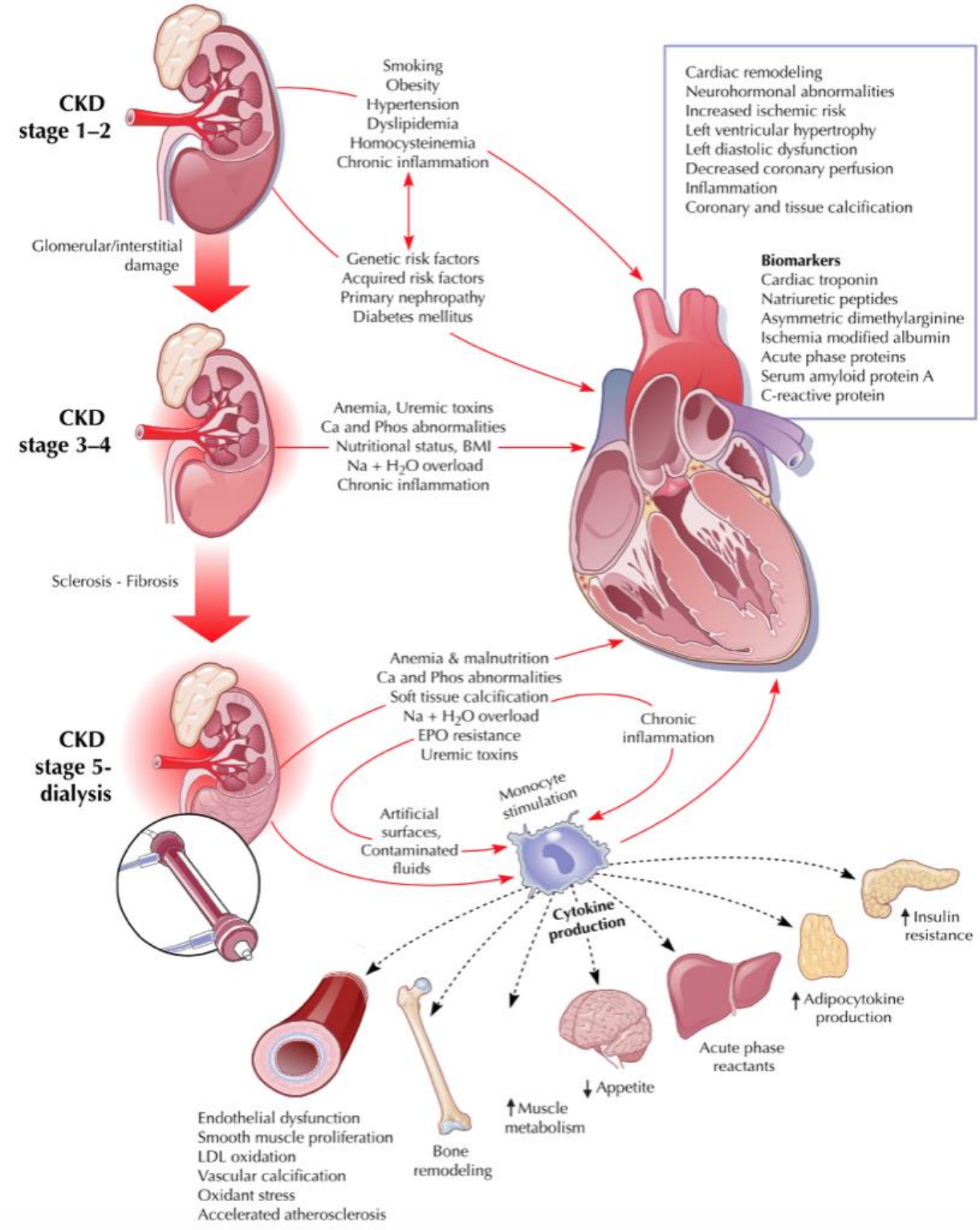

Figure 1.3: Overview of different mechanisms of Cardiorenal Syndrome Type 4 (Reproduced with permission Ronco *et al*. (7))

Chronic kidney disease is associated with structural and functional changes to the myocardium and vasculature (7). These are thought to be primarily due to the adverse effects of progressive renal dysfunction and dialysis. The pathophysiological mechanisms are summarised in Figure 1.3

Renal dysfunction leads to accumulation of the uraemic milieu and fluid and is associated with complications such as mineral bone disease and anaemia. Uraemic toxins contribute to the development of diffuse interstitial fibrosis and microvascular disease in the myocardium (8). Myocardial fibrosis leads to left ventricular diastolic dysfunction and arrhythmias and may be a contributory factor to high rates of sudden cardiac death in end stage renal disease (9). Patients with uraemia related microvascular disease have decreased coronary flow reserve with abnormal coronary vasculature and are at risk of ischaemic myocardial injury (8).

In addition to uraemia, abnormal calcium and phosphate metabolism can also cause atherosclerosis (accelerated coronary atheroma development and associated ischaemic risk) and arteriosclerosis (premature calcification of intima media of aorta leading to increased aortic stiffness and hypertension) (6). Chronic fluid overload and anaemia have neurohumoral effects that lead to adverse cardiac remodelling. Furthermore, dialysis confers additional risks. It is associated with a chronic inflammation state that promotes endothelial dysfunction. Haemodialysis has also been shown to cause repeated episodes of subclinical myocardial ischaemia that eventually lead to heart failure (7).

Regardless of the mechanism, CV abnormalities may be an early indication of increased CV risk. Early intervention may be beneficial in these patients. However, identifying them early is difficult, as the cardiovascular changes in CKD are often subtle.

1.3 Vascular effects of renal dysfunction

Hypertension is common in paediatric CKD and may in part account for the adverse myocardial effects described in the later sections (6). The under diagnosis (10) and under treatment (11) of hypertension that is frequently observed in clinical practice further contributes to CV risk.

Hypertension is present in almost half of all children in pre-dialysis CKD, with increasing prevalence in the later stages of CKD (12). It can be found in up to 75% of the dialysis population (6). Although the cause of hypertension in CKD is multifactorial (13), abnormal vascular structure and function is thought to be an important determinant (Figure 1.4).

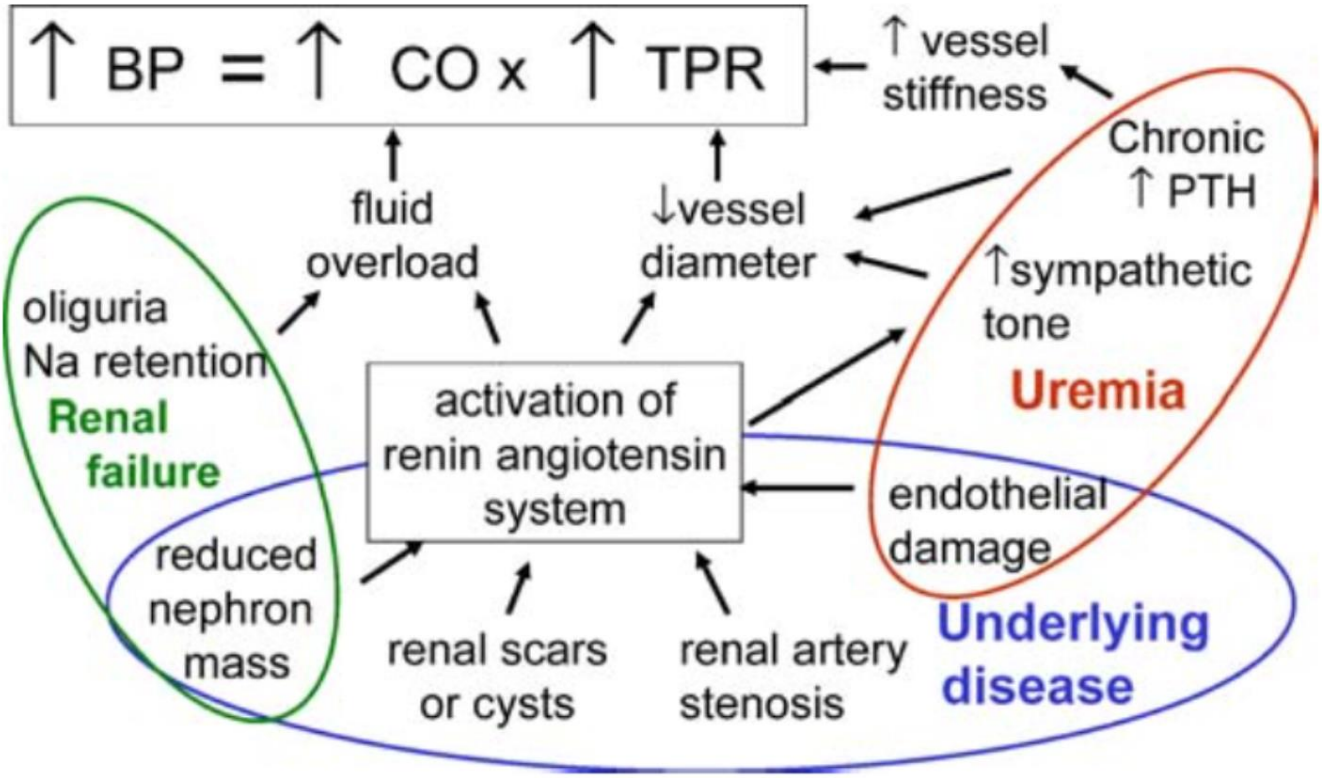

Figure 1.4: Multifactorial causes of hypertension in Chronic Kidney Disease (Reproduced with permission from Hadtstein et al. (13)) Abbreviations: BP= blood pressure, CO= cardiac output, TPR= total peripheral resistance, PTH= parathyroid hormone, Na= sodium.

The key changes to vascular structure in paediatric CKD are atherosclerotic and arteriosclerotic processes, leading to vessel wall remodelling and calcification resulting in arterial wall thickening and stiffness (6). These changes have been documented early in the disease process in mild to moderate CKD with minimal haemodynamic consequence (14). They become markedly abnormal in end-stage renal failure, particularly in the dialysis population. The consequence is significant reduction in arterial compliance and distensibility, which in turn contributes to an increased arterial afterload and high blood pressure (BP) (6).

Pulse wave velocity (PWV) and carotid artery intima-media wall thickness (cIMT), both clinically validated markers of arterial stiffness and vascular structural changes respectively, are commonly used for vascular assessment. However, there are other haemodynamic features in CKD such as elevated circulating volume and vascular resistance that may be physiologically important but are not reflected in either of these indices (Figure 1.4). They require different methods to measure, are difficult to assess accurately and are seldom measured. At present, comprehensive assessment of vascular function will therefore require multiple imaging modalities, which is time-consuming and impractical to perform. Because quantifying components of vascular load and myocardial function simultaneously can be challenging with conventional methods, it is difficult to determine their relative contribution to hypertension and studying its impact on myocardial function.

1.4 Myocardial effects of renal dysfunction

The most common finding in CKD is concentric left ventricular hypertrophy (LVH). It is a maladaptive ventricular response to increased arterial afterload commonly seen in hypertension (15). As hypertension is common in CKD, LVH is also prevalent and can be found in up to 17-50% of pre-dialysis and 80-90% of dialysis children (16). Left ventricular hypertrophy is associated with worse long term outcomes in adults (17) and its presence indicate the need for further BP optimisation (18). Indeed, good BP control may promote regression of LVH in paediatric CKD (19).

In addition, other LV geometric abnormalities such as concentric remodelling and eccentric LVH are commonly seen in paediatric CKD (20) and may also be associated with adverse CV risk (21). However, the reasons for different remodelling responses in this population remain unclear. Furthermore, accurate diagnosis of LVH is challenging due to limitations associated with two-dimensional echocardiography (ECHO), which is the standard method used in clinical practice (22). This will be further discussed in subsequent sections.

Global left ventricular (LV) function as measured by ejection fraction (EF) is frequently preserved in paediatric CKD (23, 24). Despite that, subtle LV abnormalities such as diastolic impairment may be present in children with CKD (25-27). The evidence for systolic impairment is more equivocal. Several small studies have documented a reduction in longitudinal myocardial systolic velocities using tissue Doppler ECHO (26, 28). On the other hand, a larger study found preserved longitudinal systolic strain but impairment in radial and circumferential mechanics (23). Unfortunately, all previous studies have used ECHO (which has well-known methodological limitations, as elaborated later in the chapter) and few have involved large study numbers. Furthermore, no single study has ever undertaken a comprehensive cardiac assessment in this population. This has undoubtedly contributed to the lack of consistency between studies. Consequently, myocardial function in CKD remains poorly defined.

1.5 Cardiovascular effects of renovascular disease

The CV effects outlined above arise from the pathophysiological consequences associated with kidney dysfunction, and are mainly the result of renal parenchymal disease (5). Indeed, parenchymal disease is the final common pathway for end stage renal failure. However, it is by no means the only way that kidney disease can affect the CV system. Disorders affecting renal vasculature can also cause profound CV changes through mechanisms different to those outlined previously.

In adults, atherosclerotic renal artery stenosis is the main cause of renovascular disease. It is also an important cause of renal failure, accounting for up to 14% of dialysis patients over 50 years of age (29). Its prevalence increases with age and is closely associated with other CV co-morbidities such as essential hypertension, diabetes, peripheral vascular disease and coronary artery disease (30). It is also associated with LVH, diastolic dysfunction and heart failure. It is therefore unsurprising that renovascular disease in adults confers an increased CV mortality risk (31).

Renovascular disease is less common in children compared to adults. However, it is important as it accounts for 10% of the paediatric hypertension population (32). The causes of renal artery stenosis in children are markedly different to adults. In children, fibromuscular dysplasia and Takayasu's arteritis are the two most common causes (33). Other causes include syndromic related conditions such as neurofibromatosis type 1 and tuberous sclerosis, other vasculitides e.g. Kawasaki disease and polyarteritis nodosa, and external compression due to tumours like neuroblastoma.

Hypertension is a cardinal feature in children with renal artery stenosis. The CV risk factors typically seen in the adult population are seldom encountered in paediatric renovascular disease (32). Renal artery stenosis in children is almost always treatable and in some instances hypertension may even be completely reversible (33). Because of this, the CV risk is not believed to be

significant. However, there have been no studies on long-term CV effects of paediatric renovascular disease. Thus, CV effects of renal artery stenosis are unknown, as it has never been documented in children.

1.6 Cardiovascular risk assessment in renal disease

While there has been some improvements in mortality over the past decade, it remains significantly elevated in CKD (4). Cardiovascular events continue to be a major contributor to that risk (4). Clearly, any effort to improve mortality and morbidity will require intervention measures targeting CKD children at increased CV risk. However, as previously mentioned, one of the difficulties associated with this approach is the challenge of accurately identifying high-risk patients early on using imaging biomarkers. At present, echocardiography, applanation tonometry or oscillometry and high-resolution ultrasound for cardiac assessment, aortic pulse wave velocity and carotid intimal-media thickness measurement respectively, have been used in the clinical assessment of these children. Although these techniques have been able to detect abnormal changes, they also have significant limitations.

1.7 Limitations of two-dimensional echocardiography

Echocardiography is the standard imaging modality used in the CV assessment of paediatric CKD. The main advantages are that it is widely available, cheap and can be performed quickly. Because ECHO is non-

invasive and does not require any contrast, it is usually well tolerated by children.

Apart from assessment of LV structure and global function, it can also detect subtle changes to cardiac function. Diastolic function is assessed with measures of cardiac timings and mitral inflow such as like isovolumic relaxation time (IRT) and ratio of early (E) to late (A) mitral diastolic flow velocity (E/A). Measurements of myocardial tissue velocity may also be obtained using tissue Doppler (34). Although tissue Doppler can only measure longitudinal function, changes in longitudinal velocities are sensitive markers of myocardial impairment and may precede the deterioration in global function (35).

More recently, the strain imaging via speckle tracking in ECHO has been used to quantify the myocardial systolic strain. It is able to assess the main components of systolic mechanics namely longitudinal, radial and circumferential function and is a sensitive marker of myocardial abnormality (36).

Despite its strengths, ECHO has several important limitations. Two-dimensional ECHO relies on geometrical assumptions to calculate haemodynamic parameters such as cardiac output. These assumptions are often not valid and contribute to inaccuracies in haemodynamic measures (37). Thus, ECHO is seldom used to assess vascular function in clinical practice.

Similarly, ECHO measures of LV mass are not accurate as it is also based on assumptions of LV geometry and is susceptible to high inter- and intra-observer variability (38). Previous studies comparing cardiovascular magnetic resonance (CMR) measurement of LV mass with ECHO assessment, found that ECHO consistently overestimated mass measurements (39). Echocardiography also suffers from poor reproducibility of its measurements (22). This may be due to poor spatial resolution in ECHO, which is further compounded by poor echogenic windows in some individuals. In addition, the intrinsic nature of techniques such as tissue Doppler (e.g. angle dependence) and strain imaging (e.g. reliance on good spatial resolution) are susceptible to inaccurate measurements and high observer variability (40, 41). This may be the reason for inconsistency in tissue Doppler and strain findings between different studies mentioned above (23, 26, 28).

1.8 Limitations of current methods of vascular assessment

Many different non-invasive methods of vascular assessment exist and have been used in research. Of these, pulse wave velocity and carotid intimal media thickness (cIMT) measurements are most widely used in the clinical setting. This is because both methods have been validated with established reference values and been shown to have prognostic significance in adults (42).

Pulse wave velocity is a measure of aortic stiffness. The detection of pulse waves at well-defined sampling sites (carotid and femoral arteries) can be performed using applanation tonometry, oscillometry or ultrasound methods. The distance between the sampling sites is then divided by the transit time (time of travel of the PW from carotid to femoral) to obtain the PWV (43). It has been shown to be increased in CKD children and is associated with reduced aortic compliance (6). However, assessment of PWV in children has several difficulties. The measurements can be inaccurate due to technical difficulty of recording pulse waves with different devices (43). The distance between sampling sites cannot be measured accurately without a CMR scan. Thus, it is often estimated using different methodologies and this further contributes to inaccuracy (42). Pulse wave velocity is also highly dependent on age and body dimensions, which makes it difficult to evaluate and compare in children (44).

Carotid intimal-media thickness is recorded using high-resolution ultrasound and is a measure of the structural changes to the carotid artery (42). Increased cIMT has been found in both pre-dialysis and dialysis CKD children (14, 45). It has also been shown to correlate with a higher risk of mortality and coronary events in dialysis adults (46). Because of its association with high BP and increased LV mass, cIMT is thought to be a marker of arterial stiffness (42). However, it is important to point out that cIMT is merely a surrogate of arterial stiffness. Studies have shown that although cIMT is increased in pre-dialysis children, the arterial compliance and distensibility remains normal (14). This suggests that cIMT poorly reflects the haemodynamic consequence

of vascular remodelling in CKD. Both PWV and cIMT are not ideal indicators of the haemodynamic effects of vascular remodelling. Thus, there is a need for better methods of assessing for vascular and myocardial abnormalities in paediatric CKD.

1.9 CMR – a tool for cardiovascular assessment in CKD

Cardiac magnetic resonance imaging is the reference method for CV assessment. Nonetheless, conventional CMR suffers from a major limitation. It is unable to detect sub-clinical myocardial impairment such as diastolic dysfunction. This is particularly important in the paediatric CKD population where sub-clinical changes to cardiac mechanics precede the deterioration in global function. Undoubtedly, this has been an impediment to the clinical use of CMR as a cardiovascular assessment tool in this population. However, recent innovations in CMR technology may overcome these conventional limitations. This will be further described in chapter 2.

If CMR may detect the subtle CV changes in the paediatric CKD population, its utility as a clinical tool may be considerable. It will avoid the inconvenience and cost of multiple investigations. Indeed, the ability to simultaneously assess cardiac and vascular function is one of the greater strengths of CMR. It may also provide greater insight into the complex relationship between vascular remodelling, myocardial function and renal severity.

2 Application of novel CMR sequences in paediatric renal disease

Cardiovascular magnetic resonance is a valuable clinical tool for the assessment of cardiovascular disease. Measurements of conventional myocardial indices by CMR are superior to two-dimensional ECHO. This is because cardiac magnetic resonance imaging (MRI) does not rely on geometric assumptions for LV mass and volume calculations, unlike ECHO. Myocardial borders are usually clear enough for direct tracing of the LV. Hence, inter- and intra-observer variability is superior in CMR because of better spatial resolution (22).

In addition, cardiac output and stroke volume can be measured accurately and correlates well with invasive measurements (47, 48). Thus, systemic vasculature can be characterised by quantifying the pulsatile and non-pulsatile components of systemic afterload, namely, total arterial compliance (TAC), systemic vascular resistance (SVR) (49) and regional vascular properties such as aortic strain and distensibility indices in the ascending aorta (50). Furthermore, CMR does not involve ionising radiation, is non-invasive and can be performed even without using magnetic resonance contrast. This is important as contrast media is contra-indicated in end-stage renal disease due to the risk of nephrogenic systemic fibrosis (51).

As previously mentioned, the ability to detect subclinical myocardial impairment is essential for early disease detection and intervention. This is especially relevant in the paediatric CKD population where abnormalities are frequently subtle. Thus, in order for CMR to be an effective cardiovascular assessment tool, it must be able to accurately assess conventional cardiovascular indices as well as other indicators of early myocardial dysfunction. It is also important that the CMR study protocol is optimised for these children as this will contribute to improved scan quality by promoting better compliance with the investigation. The novel CMR sequences used in this study were specifically selected to optimise the utility of CMR in this population.

In this chapter, I will give an overview of the novel CMR sequences used to detect sub-clinical abnormalities and how it is used to optimise cardiovascular assessment in paediatric CKD. It is beyond the scope of this thesis to discuss magnetic resonance physics in great detail. However, I will briefly discuss the basic concepts in magnetic resonance physics of image acquisition in order to provide the context to the clinical application of these sequences in this project.

2.1 Basics of CMR image acquisition

Magnetic resonance imaging comprise of signals that arise from the hydrogen nuclei in the body precessing (52). In the presence of a strong MRI magnetic field, the hydrogen protons, which act as multiple individual magnets, “line up” and precess at the Larmor frequency (ω), which is mathematically defined by $\omega = \gamma \times B_0$, where γ=gyromagnetic constant (specific for the nuclei being imaged, normally hydrogen) and B_0=magnetic field strength. The transmission of a radiofrequency (RF) pulse at the Larmor frequency flips the net magnetisation vector into the transverse plane and is the basis of the magnetic resonance (MR) signal. The RF pulse also causes the nuclei to become aligned and as they continue to precess, the net magnetisation induces a small electrical current, which is subsequently detected by the receiver coils. In effect, this is a demonstration of Faraday’s law of induction; voltage in an adjacent conductor can be induced by a changing magnetic field. The MR signal is recorded with receiver coils able to detect magnetic flux in two orthogonal directions. The resulting MR signal is complex in nature and comprises of two parts, namely, a ‘real’ and ‘imaginary’ component. It can also be expressed as a vector with a magnitude and phase component (Figure 2.1).

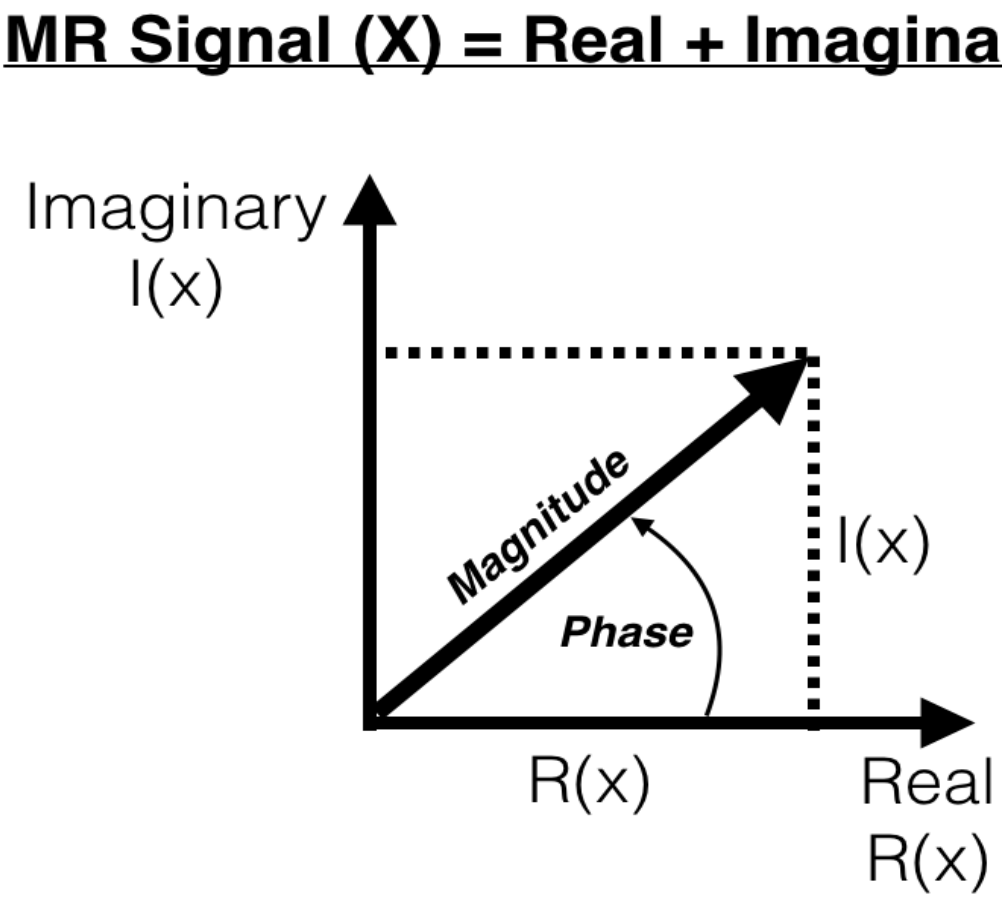

Figure 2.1: Magnetic resonance (MR) signal: Represented as complex numbers consisting of real and imaginary numbers or as magnitude and phase components. X=Total MR signal at a point in K-space, I(X)=Imaginary component of MR signal, and R(X)= Real component of MR signal

2.1.1 Slice selection

The total MR signal detected is a vectoral sum of all individual signals emitted by the hydrogen protons in the body. In order to obtain a meaningful image, a method of localising each individual signal is necessary. By altering the magnetic field, it is possible to vary the magnetic strength according to spatial

position. Applying a magnetic gradient along the length of the subject (z-axis) in turn leads to variation in proton precession frequency across space. Thus, by delivering RF pulse at a resonance frequency that corresponds with the target location, signal acquisition can be restricted to an area of interest (slice).

2.1.2 Spatial localisation

Signal localisation within the selected slice, in the xy-plane, requires resolution of signals in the x- and y- axes. This is performed using frequency and phase encoding. Similar to slice selection, frequency encoding applies an additional magnetic field gradient in one axis (e.g. x-axis) in the xy-plane to create a gradient of precession frequencies corresponding to location. The total MR signal from the slice, like all oscillating signals, is a composite of many sine and cosine waves with different frequencies. Consequently, a complex mathematical method known as Fourier transformation can be used to breakdown the total signal into its constituent frequency components. This is expressed as amplitude for each frequency, which corresponds to intensity at each x-axis position.

Phase encoding involves the manipulation of magnetic gradients in an orthogonal direction (e.g. y-axis) to induce a shift in the phase of the MR signal, such that phase shifts vary along the y-axis. The MR sequence is repeated and signal is measured for many different phase encoding gradients. Each successive phase shift of the signal is identical to successive

measurements of the same signal over time. Thus, the rate of phase shifts is itself a frequency that can also be subjected to Fourier transformation to determine the amplitude associated with each phase shift, in order to obtain intensity for each y-axis position.

Therefore, each pixel of the image slice has a distinct phase and frequency combination and two-dimensional Fourier transformation is used to obtain the image.

2.1.3 Multi-phase acquisition in cine imaging

In cine imaging, an image is obtained for each cardiac phase and all the images (ideally, an image representing a phase in the cardiac cycle) are combined to produce a multi-frame cine that captures cardiac motion. As such, MR signal acquisition needs to be synchronised to the cardiac cycle in a process known as cardiac gating. There are two types of gating, prospective and retrospective.

In prospective gating, the electrocardiographic (ECG) tracing is monitored and R wave detection is used to trigger the beginning of data acquisition. For the purposes of this discussion, ‘acquisition window’ refers to the duration within the R-R interval where data acquisition occurs. This usually ends well before the next R wave begins to allow a time window (trigger window) when the scanner is searching for the next valid R wave. Therefore, trigger windows are a necessary feature to accommodate normal heart rate variability. However, it

means that no data is collected in late diastole, which is a recognised drawback in prospective gating.

Data acquisition is typically completed over several cardiac cycles as one R-R interval is never enough time to acquire all the data required to construct an image for each cardiac phase. In order to create an image for each cardiac phase (i.e. a single frame in a multi-frame cine), the data acquired in the acquisition window can be categorised into groups known as ‘segments’, where a segment represents the data acquired for each particular cardiac phase. Thus, all the data from each segment (acquired over several R-R intervals) are collated together to produce an image for each frame of the cine. All the frames are complied together to produce a multi-frame cine in order to achieve an accurate depiction of cardiac motion.

In retrospective gating, ECG data and MR signal are simultaneously recorded in a continuous fashion, over several heartbeats. Based on the number of cardiac phases required (determined by the operator) for the cine, the data is interpolated at a time point corresponding to each cardiac phase. This is then collated to form a cine. The key advantage is that information is collected from the entire cardiac cycle and retrospective sequences provide a more complete representation of all phases in the cardiac cycle.

Another important advantage of cardiac gating is that it enables the avoidance of cardiac motion related artefacts.

2.1.4 K-space filling and parallel imaging

To briefly summarise, in conventional Cartesian MRI, the sequence of events leading to generation of an MR image is as follows: Transmission of radiofrequency pulse, slice selection gradient applied, frequency encoding gradient applied, phase encoding gradient applied, followed by readout (i.e. measurement of MR signal). This entire sequence is then repeated numerous times with different phase encoding gradients. The multitude of MR signals is collected and stored in a frequency space known as K-space. Each line in K-space represents a phase encoding step. Hence, K-space is an array of raw data from the digitalised MR signals arranged according to spatial frequencies of the actual image.

In theory, the entire K-space must be filled in order to generate a complete image. The most common method of filling K-space is the Cartesian method, which is the rectilinear filling of K-space, i.e. line by line (Figure 2.2). The benefits of the Cartesian method are that it relies on a simple gradient design, data is uniformly sampled and can be reconstructed using fast Fourier transformation, swiftly and easily (53). However, it is relatively time consuming which means that scan time may be prolonged. As such, many different methods have been employed to reduce acquisition time. As it is beyond the scope of this thesis to describe all of them, discussion will be restricted to the two main techniques used in this study, namely, efficient K-space filling methods and parallel imaging.

Non-cartesian methods of K-space filling such as echo-planar, radial or spiral trajectories are more efficient and have been used to increase acquisition speed (Figure 2.2). In particular, the spiral trajectory is thought to be one of the most time efficient ways to fill K-space (53). These methods have been used in the novel sequences in this study and are outlined in later sections.

Parallel imaging is also another technique commonly used to reduce acquisition time (52). The undersampling of K space reduces acquisition time but results in aliasing artefacts, which must be removed for the images to be clinically useful. Parallel imaging is the use of a mathematical algorithm to mitigate these artefacts by utilising additional spatial information provided by the receiver coils. Multiple receiver coils detect the MR signals simultaneously (in ‘parallel’). As each coil has a different distance from the imaged object, there is varying intensity in the detected signals in each coil, which is relative to its distance from the object (stronger signals when closer in proximity). This information is used to help with spatial localisation of the signal. This helps to shorten acquisition time by reducing the number of phase encoding steps required. Sensitivity encoding (SENSE) is one of the most commonly used methods in parallel imaging (54). SENSE is a system of equations that calculate the unaliased pixel data using information from coil sensitivities, gradient encoding, and the acquired aliased pixel. This method has been used in the sequences described below.

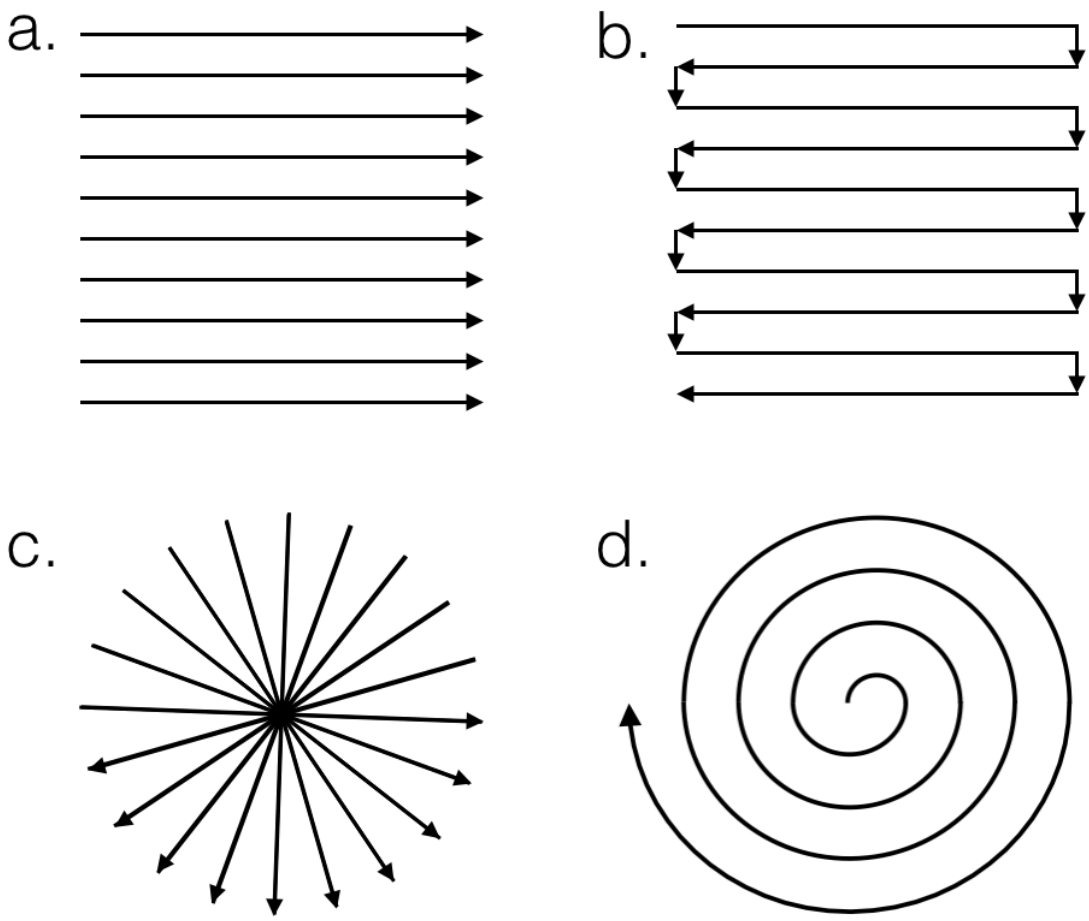

Figure 2.2 Different methods of K-space filling: a. Cartesian or Rectilinear method - line by line filling of K-space, b. Echo-planar method - similar to rectilinear filling except each readout includes multiple lines in K-space, c. Radial trajectory, d. Spiral trajectory.

2.1.5 Phase contrast Imaging

Phase contrast MR (PCMR) imaging is a technique used to measure blood flow (52). When a bipolar gradient is applied to a stationary proton (i.e. a stationary magnetic spin), there is no net change in the phase component of the MR signal (Figure 2.1). However, when such a gradient is applied to a moving hydrogen proton (i.e. moving blood), it will display a net change in its phase that is proportional to the velocity of the proton (Figure 2.3). The use of phase measurements to estimate blood flow velocity is the principle behind PCMR.

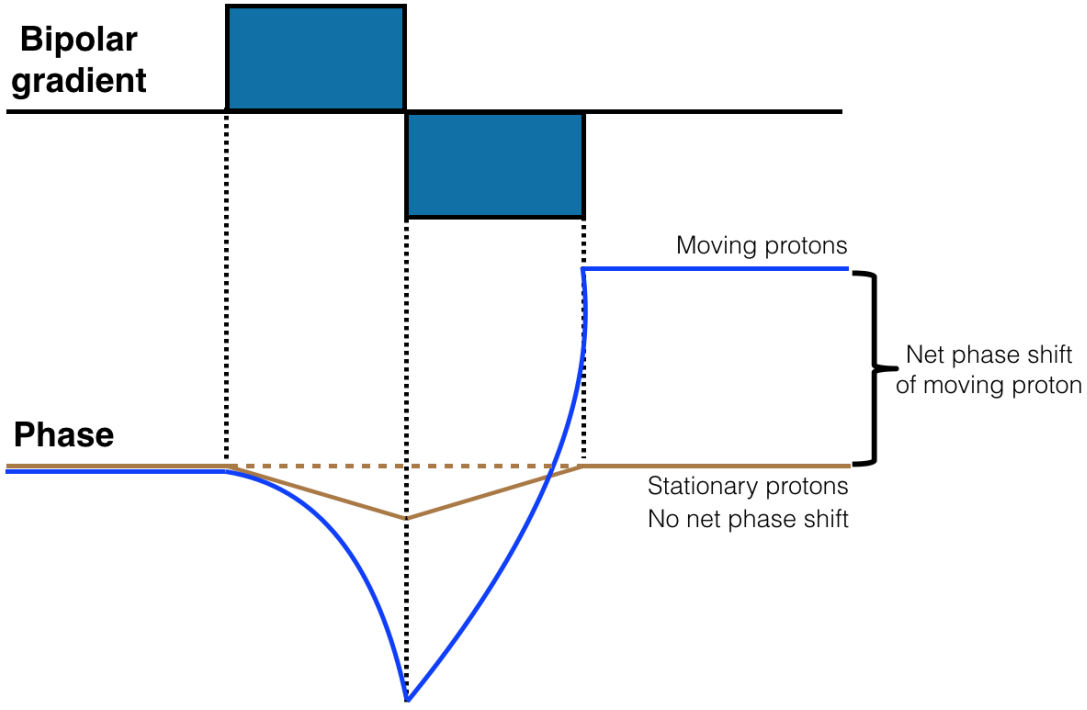

Figure 2.3: Bipolar phase encoding gradient results in a net phase shift in moving protons.

The bipolar gradient strength can be altered to assign a maximum velocity (expected in the vessel of interest) to correspond to a maximum phase shift of 180 degrees. This process is known as velocity encoding (VENC) and is determined by the operator before running the sequence. Typically, each line in K-space is acquired twice with a different VENC; one with velocity-compensated gradients (i.e. with a VENC of zero) and the other with velocity-encoded gradients (i.e. with the expected VENC). The final phase image is formed from the subtraction of the velocity-compensated data from the velocity-encoded data, in order to subtract out these background phase shift. This process is necessary as it allows the cancellation of potential artefacts from background phase shifts arising from magnetic field homogeneities.

Flow is most commonly measured in the through-plane, but can be measured in any direction. The PCMR sequence typically produces a phase image (where blood or tissue velocity is encoded in each voxel) and the corresponding magnitude image (which depicts the anatomical structures). Blood flow velocity is measured by segmentation of the region of interest on the magnitude image (Figure 2.4).

2.2 Optimising cardiac flow assessment in children

The main drawback of conventional (Cartesian) PCMR is the slow speed of acquisition (55). One of the reasons for this is the need to acquire each line in K-space twice with different VENCs, as previously explained. Unsurprisingly, image acquisition using a free breathing sequence is prolonged and this

creates lengthy MRI scans that are poorly tolerated in the paediatric population. Spatial and temporal resolution may be reduced to increase the speed of acquisition such that data can be acquired in a breathold. However, often the breathholds are still greater than 15 seconds and remain too long for children to perform. Furthermore, the reduction in spatiotemporal resolution is not ideal for the clinical assessment in children who have higher heart rates and smaller vascular structures.

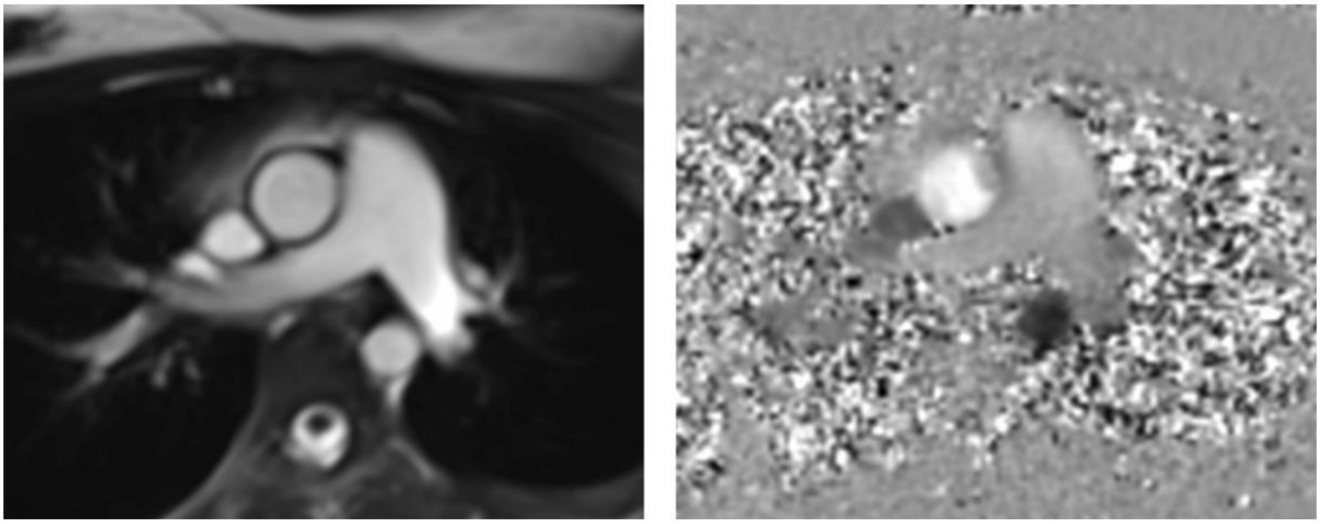

Figure 2.4: Example of Magnitude and Phase images from a PCMR sequence acquired in the proximal ascending aorta

In order to accurately assess flow in children, this department created a novel PCMR sequence with a high spatiotemporal resolution and a short breathold. This was achieved using efficient K-space filling via spiral trajectories and

undersampling combined with SENSE, a parallel imaging reconstruction technique. This technique has been shown to reliably measure flow in children with congenital heart disease (55). This sequence will be used in this study (described further in Chapter 3).

2.3 Optimising ventricular assessment in children

Assessment of cardiac volume and structure involves taking numerous sequential cine images in a stack along the length of the ventricles. Motion artefacts caused by cardiorespiratory movement are mitigated by breathholding during acquisition and electrocardiographic gating. However, as previously mentioned, conventional Cartesian CMR sequences are slow. This results in multiple long breatholds that are poorly tolerated by children and contributes to prolonged scan times and sub-optimal images (56).

Real-time cine imaging is one way to overcome these problems. Conventionally, it uses the echo-planar trajectory (Figure 2.2), which is another efficient K-space filling technique; a rectilinear method of filling K-space similar to Cartesian method, whereby each readout fills several lines in K-space. This is combined with reduction in the number of phase encoding lines in K-space to facilitate rapid acquisition of multiple single shot images to create the cine. Consequently, real time imaging can be performed during free breathing. However, its accuracy may be limited by a significantly lower spatiotemporal resolution.

This department developed a superior real-time cine imaging sequence with good spatiotemporal resolution. This was achieved by combining efficient radial K-space filling, K-space undersampling and a parallel imaging technique known as k-space and time sensitivity encoding (K-T SENSE). The K-T SENSE is a more robust reconstruction algorithm, which uses spatiotemporal correlations in addition to coil sensitivities (compared to SENSE which only uses coil sensitivities). This allows a greater degree of undersampling to be performed and facilitates further acceleration in acquisition. This sequence has been shown to be able to accurately quantify ventricular volumes and functions in children with congenital heart disease (56) and has been used in this study.

2.4 Measuring cardiac timings

The role of CMR as a tool to detect early disease is dependent on its ability to detect subtle cardiac changes. Assessment of diastolic function is important, as diastolic dysfunction may be a feature of early cardiac disease. In echocardiography, the measurement of cardiac timings such as isovolumic relaxation time and early (E wave) and late transmitral flow (A wave) to obtain the E/A ratio, are commonly used indices. Indeed, diastolic indices have been shown to be abnormal in the paediatric CKD population (27). Unfortunately, these indices are not measured in standard clinical CMR studies.

Conventional PCMR may be used to measure cardiac timings and transmitral flow. However, its utility is severely limited by cardiac gating (used in

conventional PCMR sequences) as it results in alterations in ventricular flow patterns flow due to interbeat variability in heart rate and stroke volume (57). This may affect the accuracy of cardiac timing measurements. Furthermore, in order to achieve an adequately high temporal resolution to measure cardiac timings, long acquisition times are required and may not be practical in the clinical setting.

An accelerated real time spiral PCMR sequence may be achieved by combining efficient K-space filling with parallel imaging like SENSE (57). Although this will not require cardiac gating and avoids the aforementioned problem, temporal resolution remains insufficient for a reliable measurement of cardiac timings (which requires high temporal resolution, <15ms).

In order to overcome these challenges, this department developed a highly accelerated PCMR sequence by combining parallel imaging reconstruction algorithm with temporal acceleration to allow a higher degree of undersampling, namely “unaliasing by fourier-encoding the overlaps using the temporal dimension” (UNFOLD) and SENSE techniques. This was also combined with spiral trajectory to achieve a sufficiently high temporal resolution. This sequence has been validated against echocardiography and been shown to accurately measure cardiac timings (57). It will be used in this study to assess diastolic function.

2.5 Alternative methods of myocardial assessment

Sub-clinical changes in myocardial function may be detected using myocardial deformation and velocity assessment. Echocardiography has been used to demonstrate sub-clinical abnormalities in both domains in paediatric CKD. Thus, they may be useful indicators of early cardiac disease. Cardiac MRI may also be used to study these domains.

2.5.1 Alternative methods of myocardial assessment in CMR

Feature tracking has attracted some recent attention due to its ease of application (58). It is a post-processing method that can be applied to routine cine images and does not require additional image acquisition. Displacement of myocardial segments is measured by tracking image features through sequential cardiac phases to obtain longitudinal, circumferential and radial strain. A significant limitation of this technique is the great variability in strain values observed between studies, which will inevitably hamper its widespread use as a clinical tool.

Cardiovascular MR tagging is a method of superimposing magnetic labels on the myocardium using a specific radiofrequency saturation pulse known as spatial modulation of magnetization (SPAMM) (58). These ‘tags’ are tracked throughout the cardiac cycle to obtain myocardial deformation. It is a validated method of measuring strain in CMR. However, its utility is severely limited by low spatiotemporal resolution, long acquisition and post-processing times. It

also does not provide any information in late diastole due to the problem of tag fading (as a result of T1 relaxation).

2.5.2 Measuring myocardial velocity

Magnetic resonance tissue phase mapping (TPM) is a phase contrast MR sequence that can measure myocardial velocity (59). Tissue velocity is acquired in 3 orthogonal directions (x-, y- and z- plane) and at a sufficient spatiotemporal resolution. In a conventional Cartesian TPM sequence, this results in a relatively long acquisition time (about 10 minutes long), which cannot be performed in a single breathold (59). Consequently, respiratory navigation is required to avoid breathing motion artefacts. Respiratory navigation is a technique used to limit data acquisition to a part of the respiratory cycle (usually in the expiratory phase) to mitigate motion artefacts. This is usually done using real-time imaging with a pencil beam excitation to measure diaphragmatic motion (52). Thus, prospective cardiac gating is required to create a period in the cardiac cycle (usually in diastole) where no TPM data acquisition occurs, in order for respiratory navigation to be performed. The main problem with this method is that myocardial velocity in a part of the cardiac cycle cannot be measured. This significantly limits its ability to comprehensively assess diastolic function.

To overcome this limitation, this department implemented a novel self-navigated retrospectively gated spiral TPM sequence. Self-navigation involves reconstructing real-time images from the TPM data collected to create an

image-based navigator. Only spiral interleaves acquired in expiration (identified with the navigator) are then used for reconstruction of the final TPM data. The use of spiral acquisition meant that data acquisition was relatively more time efficient than the conventional Cartesian TPM sequence. The average acquisition time is 8.7 min (compared to 10.5 min in a Cartesian TPM sequence) (59). This sequence produced a magnitude image and 3 phase images (one for x-, y-, and z- directions). Post processing of this data enabled the calculation of the longitudinal, radial and circumferential velocities (further described in Chapter 3). These data have been validated (59) and used to demonstrate subtle abnormalities in diastolic function in pulmonary hypertension (60). It will be used in this study to assess for sub-clinical systolic and diastolic dysfunction.

3 Research objectives

In summary, cardiovascular disease burden is high in children with renal disease. The ability to identify high-risk children who will benefit from early intervention is key to reducing CV mortality. Better methods of assessment are needed to detect CV changes that are often subtle in this population. Cardiovascular magnetic resonance imaging using novel sequences may be a better alternative.

The aim of this MD project is to investigate the utility of CMR in the CV assessment of children with renal disease. As pre-dialysis chronic kidney disease is most commonly encountered in clinical practice, this project will mainly focus on the comprehensive characterisation of the cardiac and vascular phenotype in pre-dialysis paediatric CKD.

In addition, I will also undertake two smaller exploratory studies to investigate the utility of CMR in children on dialysis and with renovascular hypertension, in order to determine its potential applicability in the wider paediatric renal population. These results will form the basis for the conduct of larger studies in paediatric dialysis and renovascular hypertension in the future.

3.1 Study hypotheses

Separate studies were designed to test each of the following three hypotheses:

1. Cardiovascular abnormalities in paediatric renal disease can be detected using CMR and worsens with disease severity.

2. Cardiovascular abnormalities are present in treated paediatric renovascular hypertension and are different to essential hypertension patients.

3. Renal replacement therapy has an incremental adverse cardiovascular effect in paediatric CKD.

Correspondingly, cardiac MRI was performed on three study groups, namely pre-dialysis CKD children, children with renovascular hypertension (without renal impairment) and children receiving dialysis, and compared with control population.

3.2 Thesis Outline

The clinical context of this project, principles behind the novel MRI sequences used, methodology and findings from these three studies are described in the following chapters.

Chapter 1, 2 and 3 outlined the introduction, novel CMR sequences used in this study and research objectives, respectively.

Chapter 4 will describe the methodology employed in all three studies.

Chapter 5 will discuss the vascular findings in pre-dialysis population compared with essential hypertension and healthy control population.

Chapter 6 will discuss the myocardial findings in pre-dialysis population compared with a healthy control population.

Chapter 7 will discuss cardiovascular findings of the renovascular population compared with essential hypertension and healthy control population.

Chapter 8 will discuss cardiovascular findings in the dialysis population compared with pre-dialysis and a healthy control population.

Chapter 9 will summarise the findings and reflect on potential future work.

4 Methodology

In this chapter, I will discuss the methodology, which have been used consistently in all the three studies described in this thesis.

4.1 Personal contribution

For all the studies described in this thesis:

- I wrote the ethics application, presented it to a national ethics committee meeting and successfully got ethics approval at the first sitting
- I undertook all patient recruitment related activities, including patient recruitment and taking assent and consent from all subjects and their parents.
- I reviewed and recorded all relevant details from patients' notes.
- I designed the CMR protocol using existing departmental CMR sequences.
- I personally performed the CMR scan on the majority of subjects.
- I completed the segmentation and data analysis on all study subjects.

4.2 Study population recruitment

Patient recruitment was carried out from June 2015 to September 2016. The CKD, renovascular and essential hypertension patients were recruited from the renal clinic and paediatric hypertension clinics at Great Ormond Street Hospital (GOSH) respectively. The exclusion criteria for each of the three studies are

described in detail in the respective chapters. The medical notes were reviewed in all recruited subjects to ensure that they did not fulfil any exclusion criteria. Medical history and current medications were recorded and confirmed with parents and patients on the day of the study.

Healthy subjects were recruited by advertisements within the hospital. A detailed history was taken from the parents of healthy children to ensure there was no significant medical history and they were not on any current medications.

4.3 Medical ethics and consent

This study was approved by UK national research ethics service (NRES Committee London, London Bridge, REC reference: 15/LO/0213). Suitable patients were identified by their clinicians and given initial information about the study. Subjects who were interested were subsequently contacted with a telephone call and received an information sheet (via email or post) containing all the required information. Ample opportunity was provided to patients to ask questions before consenting. All subjects were given more than 24 hours to consider the study information before consenting to taking part. Informed parental consent and patient assent was obtained from all participants.

4.4 Protocol

The entire study population underwent the same research protocol. This consisted of non-invasive BP measurements and CMR characterisation of cardiovascular phenotype as further described in the below section.

4.4.1 Blood pressure measurement

Casual brachial systolic, diastolic and mean arterial blood pressures (SBP, DBP, MBP) were measured using a CMR compatible oscillometric sphygmomanometer (Datex Ohmeda; General Electric, Boston, USA) in the CMR scanner bore. Two BP measurements were taken after the subject had been lying in the scanner for at least 10 minutes using an appropriate sized arm cuff according to current guidelines (61). The first BP measurement was discarded. The second blood pressure measurement was acquired simultaneously with CMR assessment of aortic flow. This enabled optimum combination of BP and flow data for calculation of vascular indices. Pulse pressure (PP) was the difference between SBP and DBP.

The age and sex specific centiles of the BP measurements were recorded using the second measurement (61). Subjects with systolic and diastolic BP readings $<90^{th}$ percentile were regarded as normotensive while systolic or diastolic BP $\geq 90^{th}$ and $<95^{th}$ percentile were pre-hypertensive and $\geq 95^{th}$ percentile were hypertensive, as previously defined (61). Controlled and uncontrolled BP was defined as prior diagnosis of hypertension (HTN), current use of anti-

hypertensive medication and (systolic or diastolic) BP <90th percentile or BP ≥90th percentile respectively.

4.4.2 CMR protocol and image analysis

Imaging was performed on a 1.5T CMR system (Avanto; Siemens Medical Solutions, Erlangen, Germany) with vector cardiographic gating. All CMR images were processed using in-house plug-ins developed for open-source DICOM software OsiriX (62) (the Osirix Foundation, Geneva, Switzerland). All images were analyzed by myself, who is a CMR trained cardiologist with 5 years of CMR experience. No gadolinium contrast was given.

4.4.3 Left ventricular volumes and mass

Left ventricular volumes were assessed using short axis (SAX) multi-slice free-breathing real-time radial k-t SENSE steady state free precision sequence (56). Scan parameters - FOV: ≈350 mm, matrix: 128×128, voxel size: ≈2.7×2.7×8 mm, TE/TR: ≈1.1/ ≈2.2 msec, Flip angle: 40°, acceleration factor: 8, temporal resolution: ≈36 msec. Endocardial borders of LV were traced manually at end-diastole and end-systole to evaluate end-diastolic volume (EDV) and end-systolic volume (ESV). Stroke volume (SV) was obtained by subtracting ESV from EDV. All ventricular volumes were indexed to body surface area (BSA). Left ventricular function was assessed by ejection fraction (EF = (SV/LVEDV) × 100).

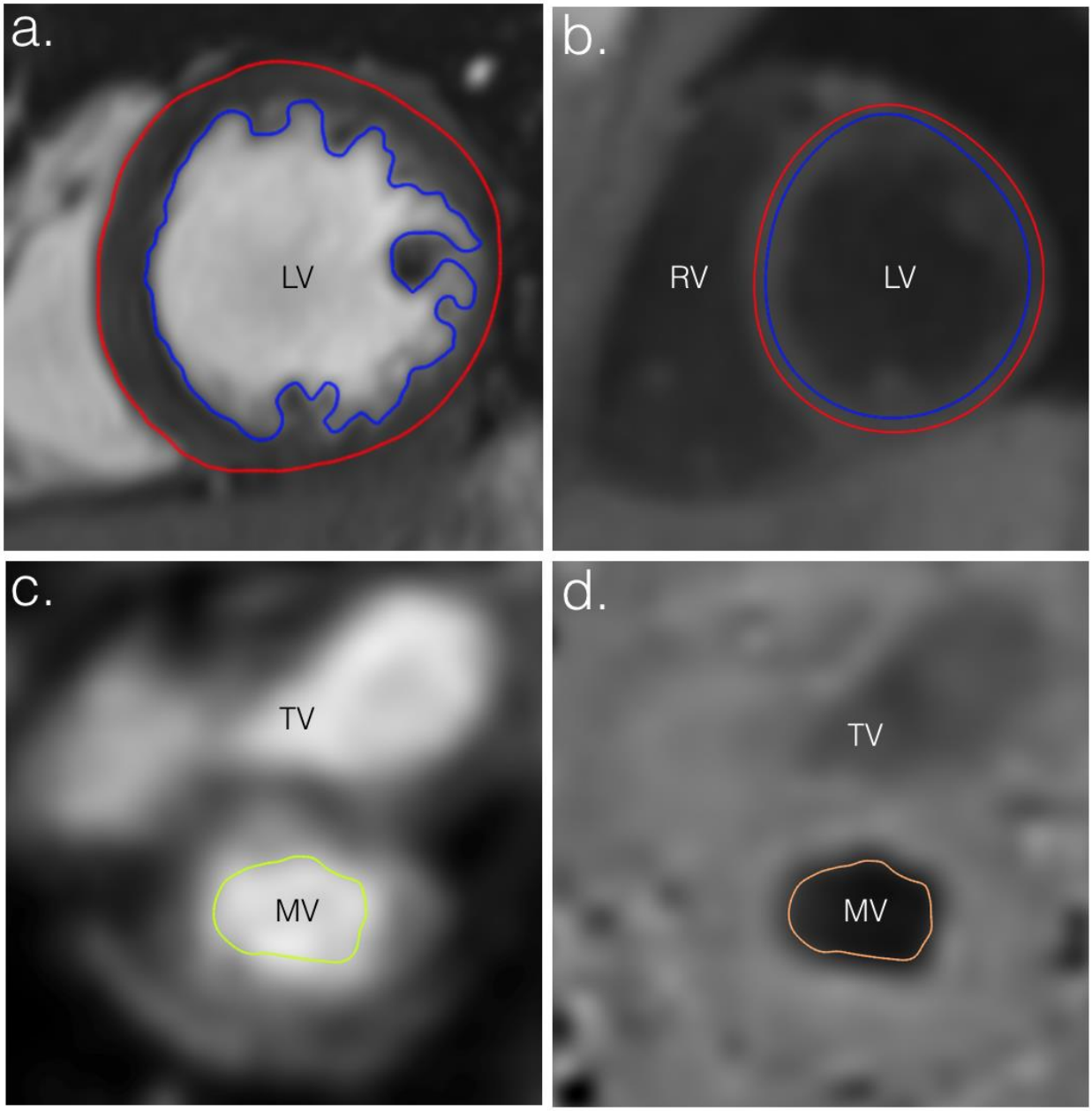

Figure 4.1: Segmentation of (a) LV volumes, (b) tissue phase mapping - segmentation on magnitude image, and (c-d) spiral PCMR for LV inflow velocity - segmentation on magnitude image. Abbreviations: LV=left ventricle, RV=right ventricle, TV=tricuspid valve, MV=mitral valve.

Epicardial borders were traced in end-diastole and combined with endocardial borders (excluding papillary muscles) to obtain LV mass (LVM) (Figure 4.1). The effect of body size on LV mass was controlled in two ways by: i) Indexing to height to the power of 2.7 ($LVMht^{2.7}$) (63) and ii) Dividing LVM by EDV to calculate mass volume ratio (MVR) (64).

The right and left atrial areas (RAA & LAA, respectively) were measured by tracing the end-diastolic border of the right and left atrium from the 4-chamber view (using the same sequence) and indexed to BSA.

4.4.4 Cardiac timing and inflow velocities

Left ventricular outflow tract (LVOT) and mitral inflow velocities were assessed with a free-breathing high temporal resolution real-time UNFOLD-SENSE spiral phase contrast magnetic resonance sequence. This sequence has previously been validated against Doppler ECHO (57). Scan parameters - FOV: ≈450 mm, matrix: 128×128, voxel size: ≈3.5×3.5×7 mm, TE/TR: ≈1.97/ ≈7.41 msec, flip angle: 20°, VENC: 150m/s, acceleration factor: 10, temporal resolution: ≈15ms. The imaging plane was positioned so that both the mitral inflow and LVOT were imaged in the short axis (Figure 4.2).

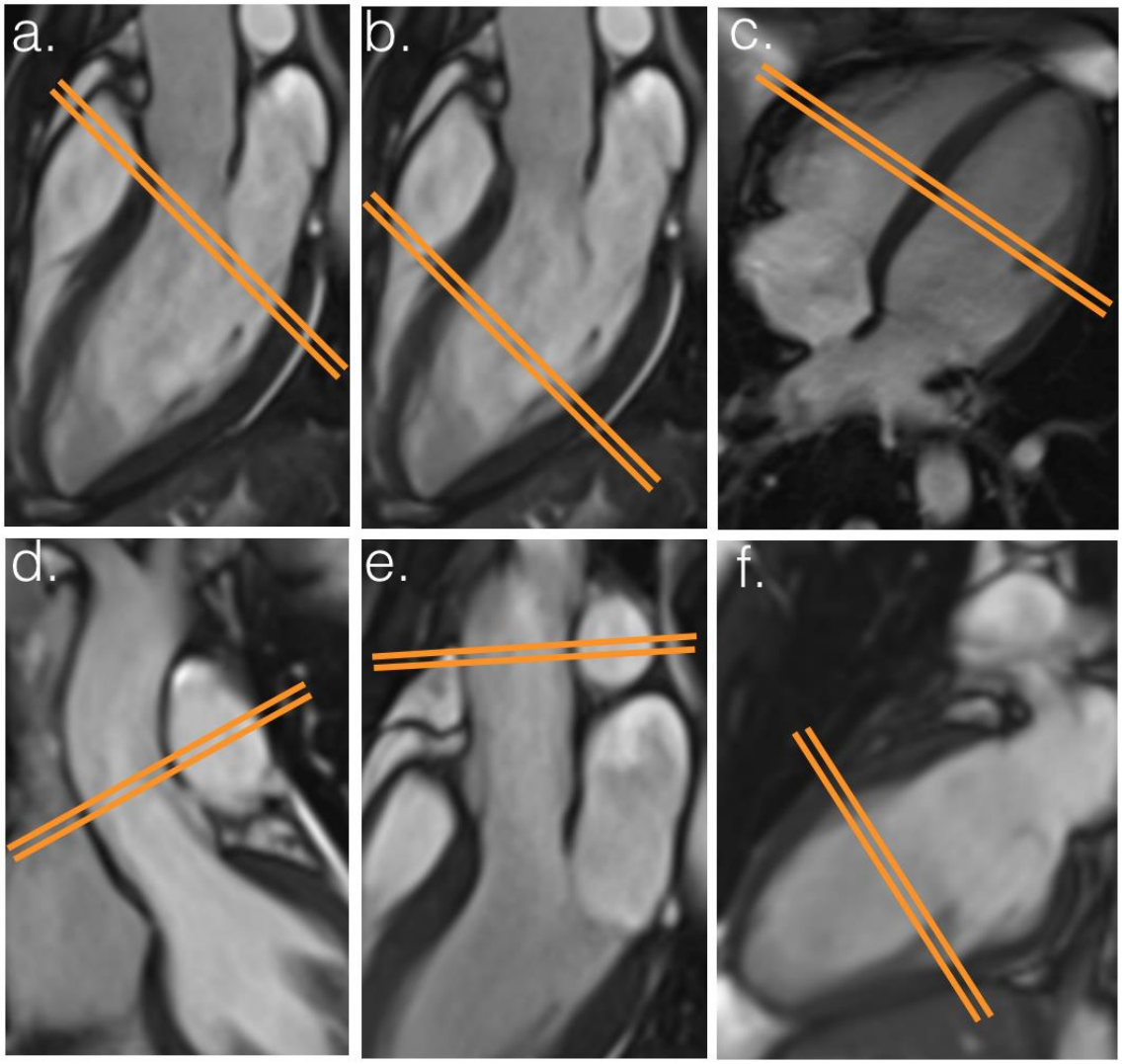

Figure 4.2: Acquisition views of difference sequences: (a) Cardiac timings and inflow velocities measurement acquired in basal LV SAX view. (b-c,f) Myocardial velocities measurement acquired in mid LV SAX view. (d-e) Aortic flow measurement acquired above sinotubular junction in ascending aorta. Abbreviations: LV=left ventricle, SAX=short axis view.

The mitral valve orifice and LVOT were manually segmented to form the resultant inflow and outflow curves (Figure 4.1). The velocity curves were interpolated to ≈1ms temporal resolution. The mitral inflow mean velocity curve consists of an early (E wave) and late diastolic wave (A wave) and were used to obtain the peak E and A diastolic velocities. The LV outflow tract velocity curve consists of a systolic ejection wave (S wave). The start and end of the S wave, the start of the E wave, and the end of the A wave are delineated by the horizontal axis intercepts of tangent lines drawn on the ascending and descending slopes of the respective waves (57). These are then used to calculate the isovolumic relaxation time (IRT), isovolumic contraction time (ICT), and ejection time (ET), as seen in Figure 4.3. Myocardial performance index (Tei) was calculated as the sum of ICT and IRT divided by ET.

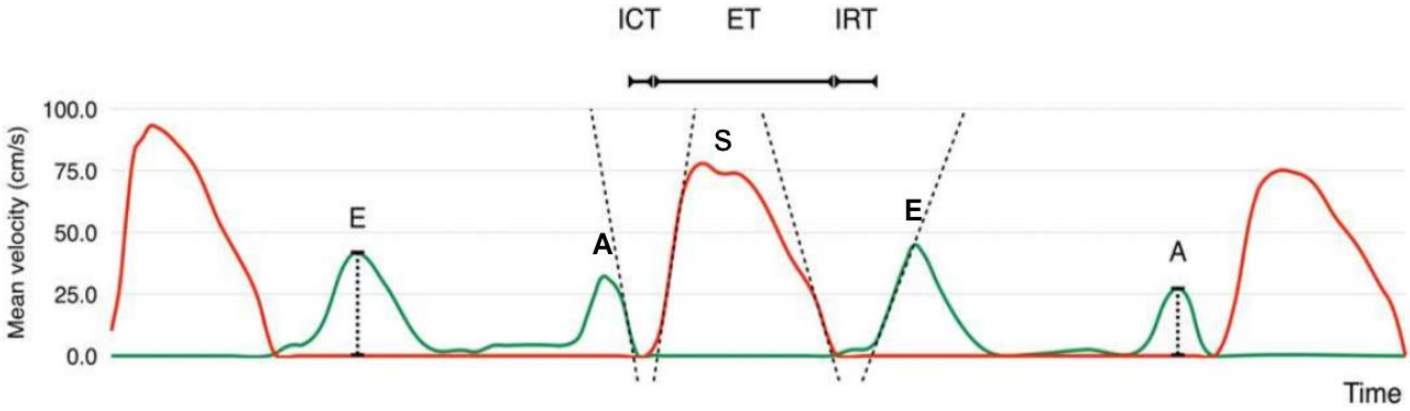

Figure 4.3: Left ventricular outflow tract (red line) and mitral valve inflow (green line) velocity curves against time. (Reproduced with permission from Kowalik et al. (6)). Abbreviations: IRT=isovolumic relaxation time, ICT=isovolumic contraction time, ET=ejection time, E=Early diastolic wave, A=late diastolic wave, and S=systolic wave.

4.4.5 Myocardial velocities

Left ventricular myocardial velocities were measured using a free breathing self-navigated golden-angle spiral tissue phase mapping (TPM) sequence planned in the mid LV SAX view (Figure 4.2) (60). Scan parameters - FOV: ≈400 mm, matrix: 192×192, voxel size: ≈2.1×2.1×8mm, TE/TR: ≈3.51/ ≈11.7 msec, flip angle: 15°, respiratory navigation efficiency: 30%, scan time: ≈7-8min, temporal resolution: ≈23 msec.

The epi- and endocardial borders were manually segmented for all phases of the cardiac cycle (Figure 4.1). Radial (Rad) velocity was calculated by transforming the x and y-direction velocities to an internal polar coordinate system using the LV center of mass as a reference point (60). The longitudinal (Long) velocity was taken as the z-direction velocity. The ventricular region of interest (ROI) was further split into six segments: anterior, anterolateral, inferolateral, inferior, inferoseptal, anteroseptal and anterior. Regional velocities were calculated by averaging the velocities of each segment within the ventricular ROI for each frame. Global radial and longitudinal LV velocities were calculated by averaging velocities across the LV for a given direction. The magnitude of the peak systolic (S'), early diastolic (E') and late diastolic (A') velocities was measured from the velocity-time curves (Figure 4.4). E'/A' ratio was the ratio of E' over A' velocity for a given direction, radial or longitudinal. The longitudinal E/E' ratio was obtained by dividing E wave mitral E velocity by longitudinal peak early diastolic velocity.

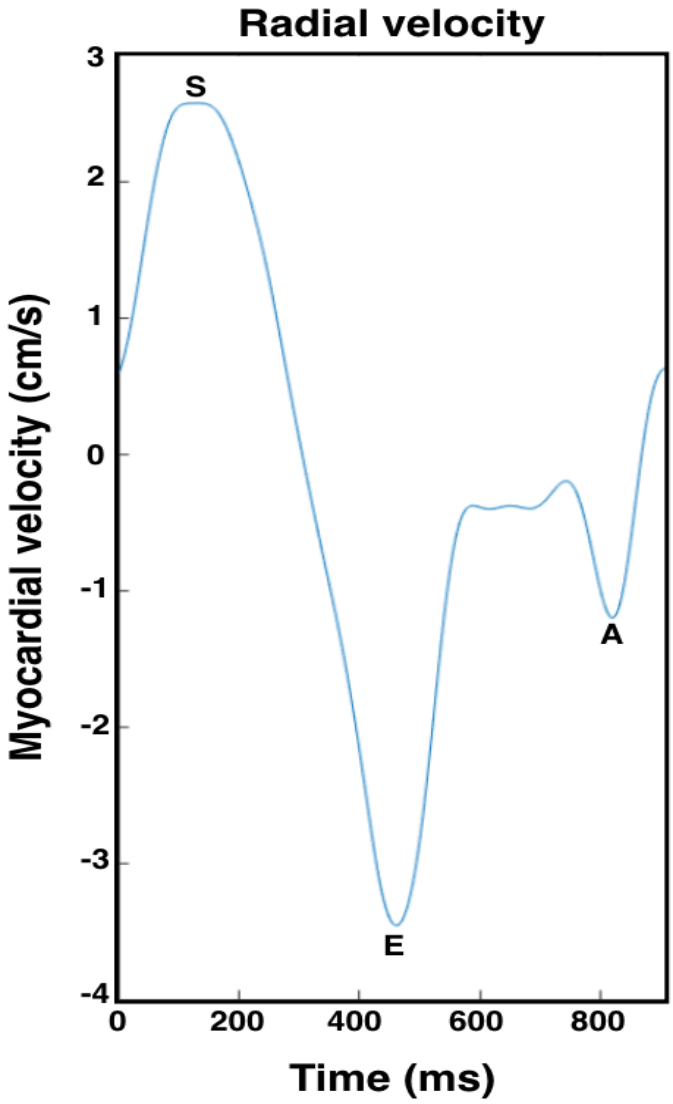

Figure 4.4: Example of a radial velocity-time curve in a renal patient. Peak systolic (S'), early diastolic (E') and late diastolic (A') velocities were measured from the curve.

4.4.6 Aortic flow and measures of vascular characteristics

Aortic flow assessment was performed using a breath held retrospectively gated, spiral SENSE PCMR just above the sinotubular junction (Figure 4.2) (55). Scan parameters - FOV: ≈400 mm, matrix: 256×256, voxel size: ≈1.6×1.6×5 mm, TE/TR: ≈2.1/≈8.0 msec, flip angle: 25°, acceleration factor: 3, breath hold time: 4-8sec, temporal resolution: ≈32.0 msec.

The aorta was segmented using a semi-automatic vessel edge detection algorithm with manual operator correction. The stroke volume was derived from the area under the flow curve and multiplied by heart rate (HR) to calculate cardiac output (CO). The maximum (AoMax) and minimum (AoMin) cross-sectional areas of the ascending aorta over the cardiac cycle were also recorded.

Local arterial stiffness was assessed by calculating ascending aortic compliance (AoC) = (AoMax – AoMin)/pulse pressure (65). Ascending aortic strain (AoS) was calculated as (AoMax – AoMin)/AoMin.

Total systemic vascular resistance (SVR) was calculated by dividing MBP by CO (66). Total arterial compliance (TAC) was calculated using a two-element Windkessel model as described below (66).

The Windkessel effect refers to the buffering function of the aorta due to its elastic properties. It enables continuous peripheral blood flow despite the pulsatility of the heart. The two-element Windkessel model describes the exponential decay of pressure in diastole in relation to resistance and compliance. It is mathematically defined by the following equation:

$$Q(t) = P(t)/R + C.dP(t)/dt$$

Where Q(t) is the flow curve over time, P is pressure, C is total arterial compliance, and R is systemic vascular resistance.

Briefly, aortic flow curves from the MR flow data and measured SVR were inputted into the model. Values of C between 0.1 and 5.0ml/mmHg in increments of 0.01 were inputted to obtain a series of modeled pressure curves (P). The pressure curves were used to calculate the modeled pulse pressure. The compliance was taken as the value that produced the best match with the non-invasive measured pulse pressure (Figure 4.5).

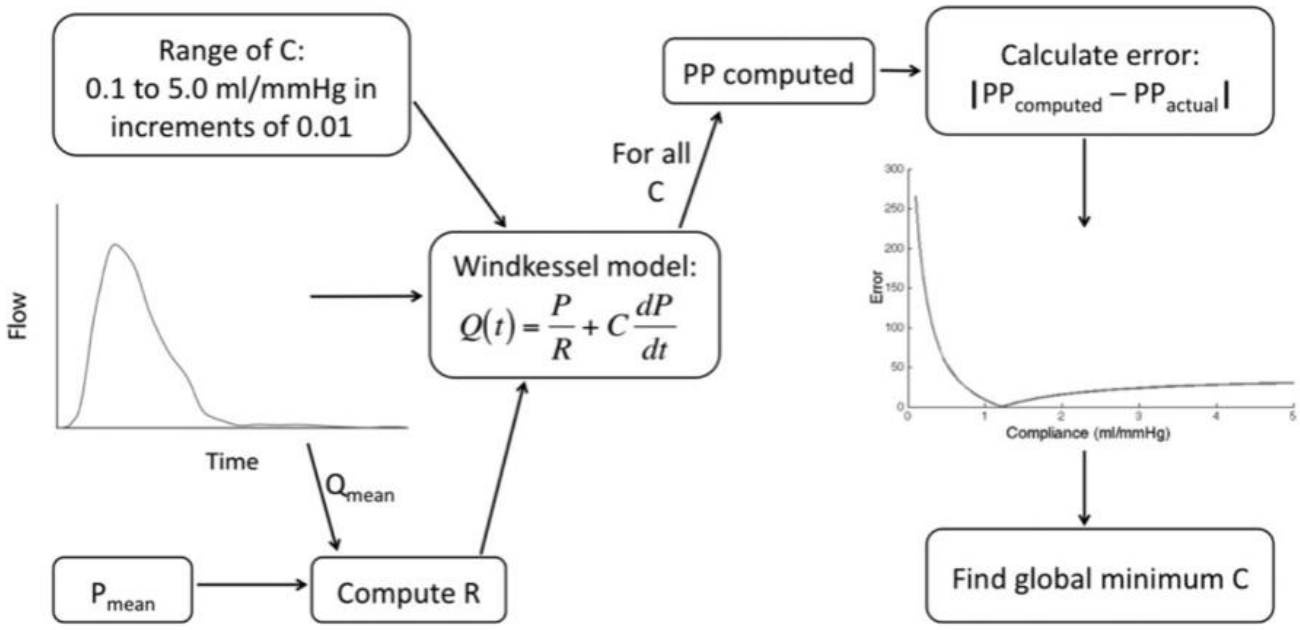

Figure 4.5: Figure showing calculation of compliance (Reproduced with permission from Steeden et al. (66)). Abbreviations: C=total arterial compliance, Q=flow, t=time, Q(t)=flow over time, P=pressure, R=resistance, and PP=pulse pressure.

4.5 Statistics

The statistical analyses were slightly different for each sub-study. They will be described in the respective chapters.

4.6 Adapting the protocol for paediatric renal patients.

There were unique challenges with the recruitment of paediatric renal patients that required protocol modifications and special provisions to be made. The

diagnosis of chronic kidney disease is associated with a high level of psychosocial burden for patients and their families. The main issues the patients and family faced as a result of their diagnosis were frequent hospital appointments resulting in missed school days, difficulties with arranging hospital visits around parental work schedule, impact of lost work days on family income and expensive transport costs. Furthermore, as the subjects were children, compliance with research protocol was more challenging than with an adult.

All the CMR sequences used had been created for quick acquisition and were non-breathhold. Only one sequence (spiral SENSE PCMR for Aortic flow assessment) required a breath-hold. This breath-hold maneuver was practiced with the patient before the scan in order to minimise breathing artifacts and repeat acquisitions. In addition, sequence parameters were optimised for a child's body size and to further reduce the acquisition time where possible. The total scan time was around 15 minutes.

I undertook numerous measures to prevent and manage any potential anxiety the children might have felt about the scan. Child friendly leaflets were sent to the patients before the scan. On arrival for their appointment, I gave ample time to explain the procedure and answer any questions they may have. I also emphasised that they could stop the scan anytime if they felt afraid to continue, in order to give them a sense of being in control. Children who were apprehensive were shown round the scanner beforehand and had a 'practice run' of lying in the scanner. Parents were also encouraged to accompany the patient into the scan room during the scan to assuage their anxiety.

A DVD viewer facility was provided, which allowed them to watch a DVD while having the scan (Figure 4.6). This was one of the most effective measures in helping the patients tolerate the scan through distraction. Consequently, none of the children required sedation for the scan.

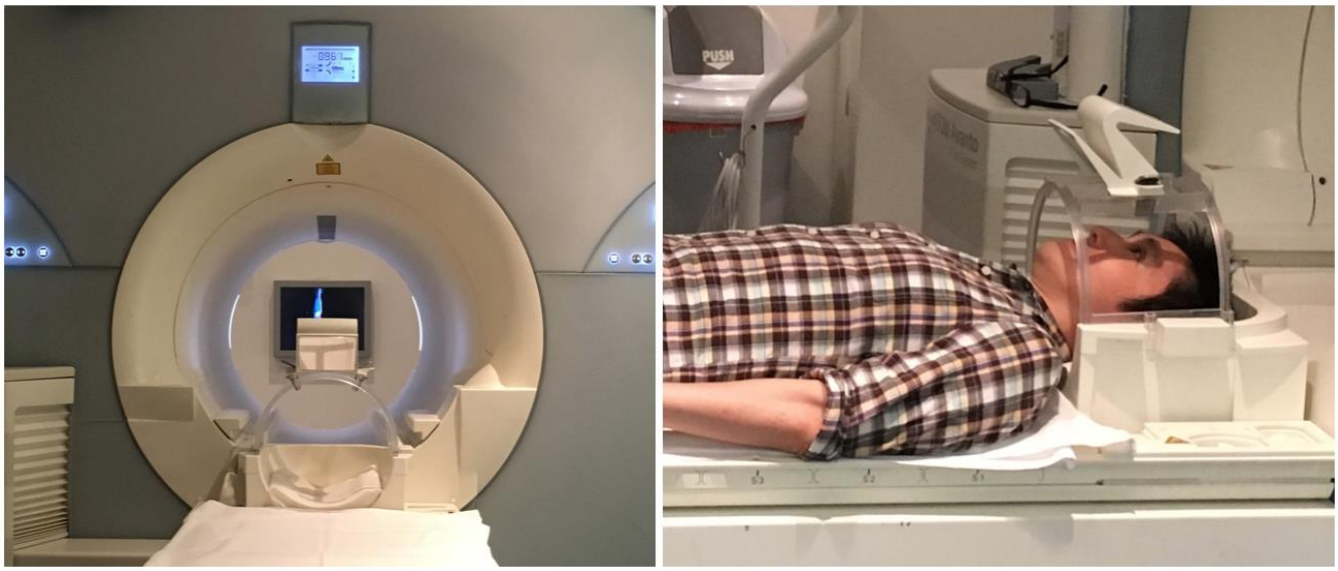

Figure 4.6: DVD viewer facility consisting of mirror headset and TV behind the scanner.

In order to make it as pleasant an experience as possible, the study protocol was designed to not include blood tests or require intravenous cannulation (Gadolinium administration was not required while blood tests results were obtained from their most recent clinic visit). Much effort was made to be as flexible and accommodating as possible when making logistical arrangements.

Appointments were scheduled to coincide with hospital appointments. When this was not possible, out of hours and weekend (including Sundays) appointments were offered. Reimbursements were also offered for transport costs to and from the hospital for the patient and any accompanying family members to cover any excess costs that they may have incurred as a result of the study.

All of these measures together were helpful in ensuring that the scan was well tolerated by all patients who took part in the study. Based on the verbal feedback I received, their experience had been overwhelmingly positive, as the children felt empowered throughout the process. Many of the parents commented that participating in the research encouraged their children to better engage with their condition. Finally, the well-designed protocol and flexible logistic arrangements allowed the successful recruitment of large numbers of patients, which was important for the success of this study.

5 Comprehensive characterization of vascular phenotype in pre-dialysis chronic kidney disease

In this chapter, I will describe the comprehensive evaluation of the vascular phenotype in children with CKD and determine its relationship with CKD severity.

5.1 Personal contribution

For the study described in this chapter:

- I completed the ethics application process.
- I recruited all subjects.
- I acquired, collated, and tabulated the relevant clinical data.
- I completed the segmentation and data analysis on all study subjects.
- I performed statistical analysis on the study dataset.
- I wrote up the findings from this study into a research article and have submitted it to Journal of Cardiovascular Magnetic Resonance. It is currently under review.

5.2 Introduction

Children with chronic kidney disease have an excess of cardiovascular mortality (67), possibly due to associated arterial hypertension (12). In adult CKD, one of the main causes of HTN is thought to be increased arterial stiffness secondary to vessel wall calcification (68). These phenomena are also thought to play an important part in the development of HTN in children with CKD (14, 69-71). However, although several studies have demonstrated increased pulse wave velocity (72-74) in paediatric CKD, others have shown no difference compared to controls (75, 76) This conflicting evidence suggests that global arterial stiffness alone may not explain the increased prevalence of HTN in paediatric CKD (12). In fact, children with CKD also have other abnormalities that may predispose towards HTN (13). These include higher systemic vascular resistance, increased cardiac output and fluid overload (13). Unfortunately, few studies have investigated all these mechanisms together and this has made it difficult to determine their relative importance.

Cardiovascular magnetic resonance is a reference standard method of assessing blood flow (77). It is routinely used in the paediatric population to assess cardiac output and valvar regurgitation. Importantly, CMR derived flow data can also be combined with simultaneous BP measurements to calculate SVR and total aortic compliance (78). Thus, CMR is the ideal method of comprehensively and non-invasively assessing the components of afterload in paediatric CKD.

The aim of this study was to use simultaneous CMR and blood pressure measurements to determine the vascular phenotype in pre-dialysis paediatric CKD. This was achieved by comparing pre-dialysis paediatric CKD patients with healthy (negative controls) and essential hypertensive (positive controls) subjects.

5.3 Methods

5.3.1 Study Population

The study population consisted of 150 children: 110 with confirmed CKD, 20 with primary essential hypertension (eHTN) and 20 healthy volunteers. All patients were recruited from the CKD and hypertension clinics at Great Ormond Street Hospital. Healthy subjects were recruited through hospital advertisements and a clinical history was taken to confirm there was no significant medical history or medications. Study exclusion criteria: i) age <7 or >18 years, ii) congenital structural heart disease or primary myocardial disease, iii) active vasculitis iv) cardiac arrhythmia, v) secondary causes of hypertension (79), vi) medical devices that preclude CMR and vii) on-going renal replacement therapy or previous renal transplants, vii) patients with acute deterioration in renal function (only CKD patients with stable renal function were recruited).

Results of standard clinical blood and urine tests performed as part of routine clinical care within 3 months of the study were collected in CKD patients.

These included; full blood count, urea, creatinine, electrolytes, serum calcium, phosphate, intact parathyroid hormone, and urine albumin to creatinine ratio measurements. The modified Schwartz formula was used to estimate glomerular filtration rate (eGFR) and CKD stage (eGFR = 36.2 x height in cm / serum creatinine in μmol/L). Blood and urine tests were not performed for the eHTN or healthy cohort, as this was not part of their on-going routine evaluation.

5.3.2 Study protocol

The study protocol has been previously outlined in detail in Chapter 4. In summary, I performed non-invasive blood pressure measurements, assessment of left ventricle (SAX LV stack acquisition using KT-SENSE sequence) and aortic flow (acquired in ascending aorta using retrospective-gated, spiral SENSE PCMR sequence). This was used to calculate LV mass and volume and aortic flow and vascular characteristics as described below.

Blood pressure measurements at the time of CMR were also used to divide the CKD patients into 2 groups. Children with SBP or DBP ≥95th percentile (61), or a previous clinical diagnosis of HTN irrespective of BP were considered to have hypertensive chronic kidney disease (H-CKD). All other children were considered to have normotensive chronic kidney disease (N-CKD).

5.3.3 Statistics

Statistical analyses were performed using Stata 13 (StataCorp, College Station, Texas, USA). Data were examined for normality using Shapiro-Wilk normality test and non-normally distributed data was transformed using a zero-skewness log transform to ensure normal distribution prior to analysis. Descriptive statistics were expressed as mean (± standard deviation) or geometric mean (± geometric standard deviation) if data was log transformed. To assess the effect of BP in CKD, comparisons were made between the H-CKD, N-CKD, eHTN and healthy controls (HC). Between group differences were assessed using analysis of variance (ANOVA). Levene's test was used to assess for homogeneity of variances across the groups and Welch's correction was applied for non-homogeneous variance. To further interrogate differences between each group, a post-hoc pairwise comparison was performed on parameters significantly different on ANOVA testing. The Bonferroni method was employed to adjust for potential Type 1 errors in the post-hoc pairwise comparisons (build into post-hoc comparison method in Stata). Adjustments for sex, age and use of anti-hypertensive medication (including angiotensin converting enzyme (ACE) inhibitor, angiotensin-2 receptor (AT2) inhibitor, calcium channel blocker (CCB) and or beta blockers (BB)) were made to examine for confounder effect where appropriate. Chi-squared test was used to determine if sex distribution between groups were different. Pearson's correlation (r coefficient) was used to assess the relationship between SBP and LVM or MVR. Spearman's correlation (rho

coefficient) was used to interrogate the relationship between renal severity (eGFR and CKD stage) with BP and vascular indices. A p value < 0.05 was considered statistically significant. Indices not statistically different to healthy controls have been described as ‘normal’.

5.4 Results

5.4.1 Study Population

The eHTN group was slightly older with higher BMI and a greater male preponderance, reflecting the typical demographics of these children (80) (Table 5.1). However, there were no demographic differences between the CKD and healthy control groups. Of the 110 CKD patients, the majority had congenital abnormalities of the kidney and urinary tract (n=65, 59%) or renal dysplasia (n=12, 10%). All other causes represented <10% of the population and are fully described in Table 5.2. The distribution of CKD severity was: Stage 1 - 4 (4%), Stage 2 - 36 (33%), Stage 3 - 49 (45%), Stage 4 - 16 (14%), Stage 5 - 5 (4%). The mean eGFR in the CKD cohort was 54±24 ml/min/1.73 m^2. None of the children had previous renal transplantation or were on renal replacement therapy. Eight children had undergone a previous nephrectomy.

Table 5.1: Demographics and baseline characteristics of study population

	HC N=20	N-CKD N=67	H-CKD N=43	eHTN N=20	p-value
Age (years)*	11±1.3	11±1.3§	12±1.3	14±1.2	0.01††
Sex (% male)§§	60%	78%	53%	75%	0.05
Height (cm)	158±19	149±20§	151±17	164±13	0.003††
Weight (kg)*	48±1.4	42±1.5§	44±1.4‖	66±1.4	<0.001
BMI (kg/m^2)*	20±1.1	19±1.2§	19±1.2‖	25±1.3#	0 .002††
BSA (m^2)	1.5±0.32	1.4±0.37§	1.4±0.29‖	1.8±0.33	<0.001
Recent blood test ‡‡					
Hemoglobin (g/L)		130±15	131±12		0.74
Hematocrit (L/L)		0.38±0.042	0.38± 0.029		0.98†
Mean Corpuscular Volume (fL)		82±4.7	81±3.8		0.19
Platelet count (x10^9/L)*		250±1.3	263±1.3		0.44
White Cell Count (x10^9/L)*		6.3±1.4	6.8±1.4		0.43

Sodium (mmol/L)	143±3	143±2.4	0.71
Potassium (mmol/L)*	4±1.2	4.3±1.1	0.025
Bicarbonate (mmol/L)	26±2.6	24±2.6	0.013
Urea (mmol/L)*	9.6±1.6	8.2±1.7	0.26
Creatinine (umol/L)*	134±1.7	125±2	0.65
eGFR (ml/min/1.73 m^2)	46±20	54±31	0.847†
Magnesium (mmol/L)	0.85± 0.16	0.89± 0.1	0.20
Chloride (mmol/L)	101±3.6	104±2.8	<0.001
Alkaline phosphatase (U/L)	202±78	179±101	0.29
Alanine transaminase (U/L)*	26±1.7	15±1.9	0.024
Serum Albumin (g/L)*	43±1.1	42±1.2	0.48
Calcium (mmol/L)*	2.4±1.1	2.4±1.1	0.61
Phosphate (mmol/L)	1.4±0.17	1.5±0.24	0.045
Calcium-Phosphate product ($mmol^2/L^2$)	3.3±0.43	3.5±0.51	0.068
Ionised Calcium (mmol/L)	1.2±0.064	1.2±0.064	0.43
Ionised Calcium pH corrected (mmol/L)	1.2±0.058	1.2±0.058	0.55
Intact PTH (pmol/L)*	4.5±2.7	6.1±2.5	0.25

Recent urine test ‡‡				
Urine Albumin (mg/L)*	112±6.1	112±10		0.99
Urine Creatinine (mmol/L)*	4.9±2.3	4.5±2.3		0.76
Urine Albumin/ Creatinine Ratio* (mg/mmol)	23±6.6	25±10		0.91
Medications (%)				
ACE or AT2 Inhibitor	18%	47%	55%	-
Calcium Channel Blocker	0%	26%	50%	-
Beta-Blocker	0%	19%	15%	-
Aldosterone antagonist (Spironolactone)	1%	0%	5%	-

Data presented as mean ± standard deviation. ⋆- Logarithmic transformation was applied. †- P-value <0.05 when N-CKD compared with HC. ‡ - P-value <0.05 when H-CKD compared with HC. §- P-value <0.05 when N-CKD compared to eHTN. ||- P-value <0.05 when H-CKD compared to eHTN. #- P-value <0.05 when eHTN compared with HC. ⋆⋆– P-value <0.05 when H-CKD compared to N-CKD. ††– ANOVA Welch (W) test was used. ‡‡ - Recent (within 3 months of CMR scan) blood test were only available in 68 CKD patients. §§-Chi-squared test was performed. Abbreviations: HC=Healthy control, N-CKD=Non hypertensive CKD, H-CKD=Hypertensive CKD, eHTN=Essential hypertension, BMI=Body mass index, BSA=Body surface area. eGFR=estimated glomerular filtration rate, PTH=Parathyroid hormone, ACE=angiotensin converting enzyme, AT2=angiotensin receptor 2.

Table 5.2: Proportion of CKD patients with other causes of primary renal disease.

Type of Renal Disease	N (% of total population)
Renal cystic disease	6 (5%)
Previous history of Haemolytic Uraemic syndrome	4 (4%)
Previous history of acute tubular necrosis	4 (4%)
Previous history of glomerulonephritis	3 (3%)
Bartter syndrome	2 (2%)
Chronic Tubule Interstitial Disease	2 (2%)
Focal Segmental Glomerular Sclerosis	2 (2%)
Cystinosis	2 (2%)
Miscellaneous causes (comprised of hypercalciuric syndrome, nephrocalcinosis, Alport syndrome, previous Henoch Schonlein nephritis, renal ischaemic damage, cortical necrosis, Branchio-Oto-Renal syndrome and Lowe syndrome)	8 (7%)

All 26 CKD children with a previous diagnosis of hypertension were treated with anti-hypertensive medications (Table 5.1), apart from one whose medication was temporarily stopped while awaiting further investigations. A further 15 normotensive CKD children were treated with angiotensin converting enzyme inhibitors or angiotensin-2 receptor antagonists for proteinuria. A significant proportion of CKD patients were also receiving

additional treatments for CKD related complications (See Table 5.3 and Table 5.4). Routine blood and urine tests, which had been performed within three months of the study, were available in 68 patients (Table 5.1).

Table 5.3: Proportion of CKD patients with complications associated with CKD.

Renal associated complications	N (% of total population)	Relevant Blood or Urine tests*
Normocytic anemia	17 (15%)	Hemoglobin: 112±10g/L Mean Corpuscular Volume: 81.9±3.8fL
CKD Mineral Bone Disease	40 (36%)	Intact Parathyroid Hormone: 11.9±8.4pmol/L
Elevated Urine albumin/creatinine ratio (UACR)	62 (56%)	UACR: 140±261mg/mmol

*- Blood and Urine test results presented as mean ± standard deviation.

All eHTN patients had a diagnosis of primary hypertension and were receiving anti-hypertensive medication except for one child who was recruited before commencement of therapy. Six patients were on two or more anti-hypertensive medications.

Table 5.4: Proportion of patients on treatment for complications associated with CKD

	N (% of total population)
Treatment for Anaemia	
Oral iron supplements	40 (36%)
Erythropoietin (or analog)	16 (15%)
Treatment for CKD Mineral Bone Disease	
Calcium supplements	42 (38%)
Vitamin D supplements	75 (68%)
Treatment for proteinuria	
ACE inhibitors	15 (14%)

5.4.2 Blood pressure differences between groups

Sixty-seven (61%) CKD patients were assigned to the N-CKD group. Nevertheless, MBP, DBP and DBP percentiles were still significantly higher (Table 5.5) in these children compared to healthy controls ($p \leq 0.04$).

Table 5.5: Comparison of blood pressure between groups.

	HC N=20	N-CKD N=67	H-CKD N=43	eHTN N=20	p-value
SBP (mmhg)	105±11	108±8.6	124±12‡**	127±12#§	<0.001
DBP (mmhg)	53±6.8	60±6.8†	72±11‡**	65±12#‖	<0.001††
MBP (mmhg)	75±7	81±5.7†	93±9.5‡**	90±10#§	<0.001††
PP (mmhg)	52±12	48±9.6	51±11	62±8.7#§‖	<0.001
SBP percentile*	31±2.1	47±1.9	80±1.6‡**	78±1.4#§	<0.001††
DBP percentile*	18±2.2	37±1.9†	68±1.5‡**	36±2.4#‖	<0.001††
Heart Rate (BPM)*	74±1.2	74±1.2	75±1.2	80±1.2	0.45

Data presented as mean ± standard deviation. *- Logarithmic transformation was applied. †- P-value <0.05 when N-CKD compared with HC. ‡ - P-value <0.05 when H-CKD compared with HC §- P-value <0.05 when N-CKD compared to eHTN. ‖- P-value <0.05 when H-CKD compared to eHTN. #- P-value <0.05 when eHTN compared with HC. **– P-value <0.05 when H-CKD compared to N-CKD. ††– ANOVA Welch (W) test was used. Abbreviations: HC=Healthy control, N-CKD=Non hypertensive CKD, H-CKD=Hypertensive CKD, eHTN=Essential hypertension, SBP=Systolic blood pressure, DBP=Diastolic blood pressure, MBP=Mean blood pressure, PP=Pulse pressure.

Forty-three (39%) CKD patients were assigned to the H-CKD group. Of these, 26 had a previous diagnosis of HTN (12 controlled and 14 uncontrolled) and 17 were hypertensive during the CMR exam. Absolute SBP, MBP and DBP, as well as BP percentiles (Table 5.5), were significantly higher in H-CKD compared to both healthy controls and N-CKD patients ($p<0.001$). There were no significant differences in PP between healthy controls, and either CKD sub-groups.

In eHTN patients, SBP, SBP percentile and MBP were elevated compared to the healthy controls and N-CKD patients ($p<0.001$) and similar ($p=1.0$) to H-CKD patients (Table 5.5). The DBP and DBP percentile were higher compared to healthy subjects ($p<0.001$), similar to N-CKD ($p\geq0.30$) and lower than in H-CKD ($p\leq0.01$). Pulse pressure was also significantly elevated ($p\leq0.02$) in eHTN patients compared to healthy controls and both CKD groups.

The between group differences remained after adjustment for age, sex and anti-HTN medication use.

5.4.3 Components of blood pressure between the groups

There was no significant difference in TAC between healthy controls and either of the CKD sub-groups ($p>0.50$ - Table 5.6). However, the eHTN group had significantly lower TAC compared to healthy controls and both CKD sub-groups ($p<0.04$), as seen in Figure 5.1. The between groups differences remained after adjustment for age, sex and anti-HTN medication use. Although AoC was lower in eHTN compared to N-CKD ($p=0.011$), this was no longer significant after correction for age, sex and anti-HTN medication use. There were no other significant differences in AOC between the groups.

Compared to healthy controls (Table 5.6), SVR was significantly higher in the H-CKD group ($p<0.001$), and trended towards higher in the N-CKD group ($p=0.06$), as can be seen in Figure 5.2. In addition, SVR was higher in the H-CKD patients compared to N-CKD patients ($p=0.03$). There was a trend towards greater SVR in the eHTN patients compared to controls ($p=0.10$), but there were no differences compared to the CKD sub-groups. Between group differences remained after adjustment for age, sex and anti-HTN medication use.

There were no significant differences (Table 5.6) in RA size, IVC size or CO between the three groups with and without adjustment for age, sex and anti-HTN medication use.

Table 5.6: Determinants of blood pressure and indices of ascending aortic stiffness between groups.

	HC N=20	N-CKD N=67	H-CKD N=43	eHTN N=20	p-value
SVR ($WU.m^2$)*	20±1.2	23±1.2	26±1.2‡**	24±1.2	<0.001
TAC ($ml/mmHg.\ m^2$)*	0.54±1.3	0.58±0.3	0.54± 1.2	0.45±1.2#§||	<0.001
CO ($l/min/m^2$)*	3.7±1.2	3.5±1.2	3.6±1.2	3.8±1.2	0.26
RAA (cm^2/m^2)	12±1.8	11±2	12±2.3	11±1.4	0.16
IVCA (cm^2/m^2)*	2.4±1.2	2.3±1.3	2.3±1.2	2.1±1.4	0.51
AoS (%)*	47±1.6	54±1.6	52±1.6	51±1.7	0.73
AoC ($cm^2.mmHg^{-1}.10^{-2}$)*	2.8±1.6	3.1±1.5§	2.9±1.4	2.2± 1.5	0.02

Data presented as mean ± standard deviation. *- Logarithmic transformation was applied. †- P-value <0.05 when N-CKD compared with HC. ‡- P-value <0.05 when H-CKD compared with HC §- P-value <0.05 when N-CKD compared to eHTN. ||- P-value <0.05 when H-CKD compared to eHTN. #- P-value <0.05 when eHTN compared with HC. **– P-value <0.05 when H-CKD compared to N-CKD. ††– ANOVA Welch (W) test was used. Abbreviations: HC=Healthy control, N-CKD=Non hypertensive CKD, H-CKD=Hypertensive CKD, eHTN=Essential hypertension, SVR=Systemic vascular resistance, TAC=Total arterial compliance, CO=Cardiac output, RAA=Right atrial area, IVCA=Inferior vena cava area, AoS=Ascending aortic strain, AoC=Ascending aortic compliance.

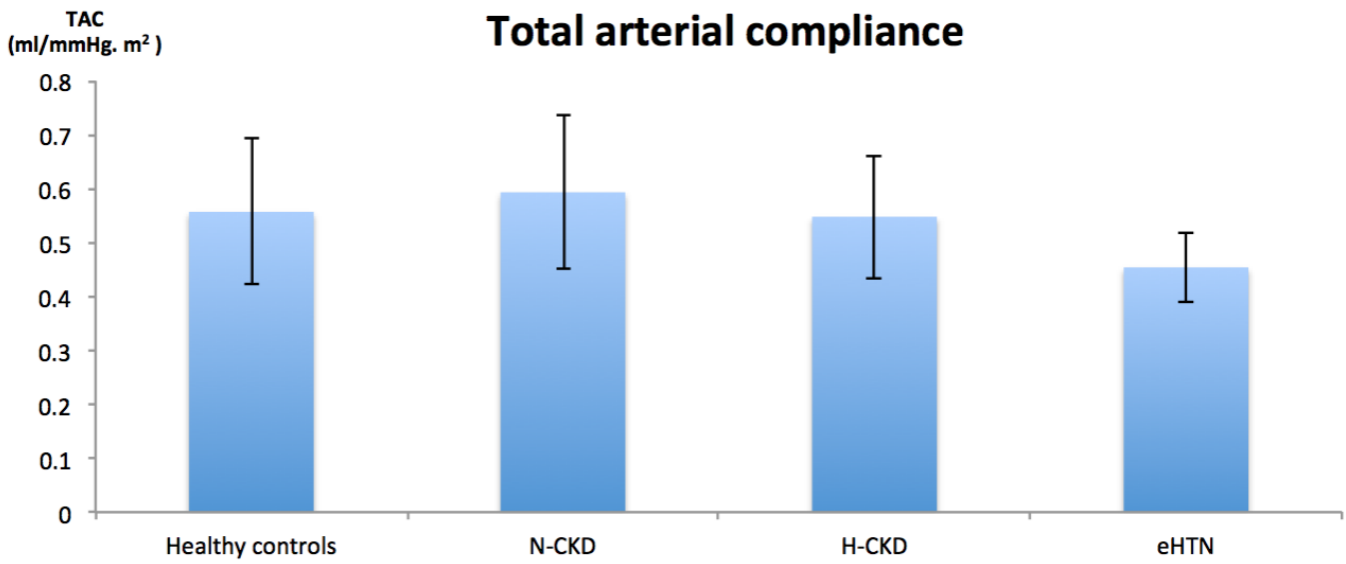

Figure 5.1: Bar chart showing differences in TAC between groups: TAC is significantly ($p<0.05$) lower in eHTN compared to all the other groups. Abbreviations: TAC=total arterial compliance, N-CKD=non-hypertensive chronic kidney disease group, H-CKD=hypertensive chronic kidney disease group, eHTN=essential hypertension group.

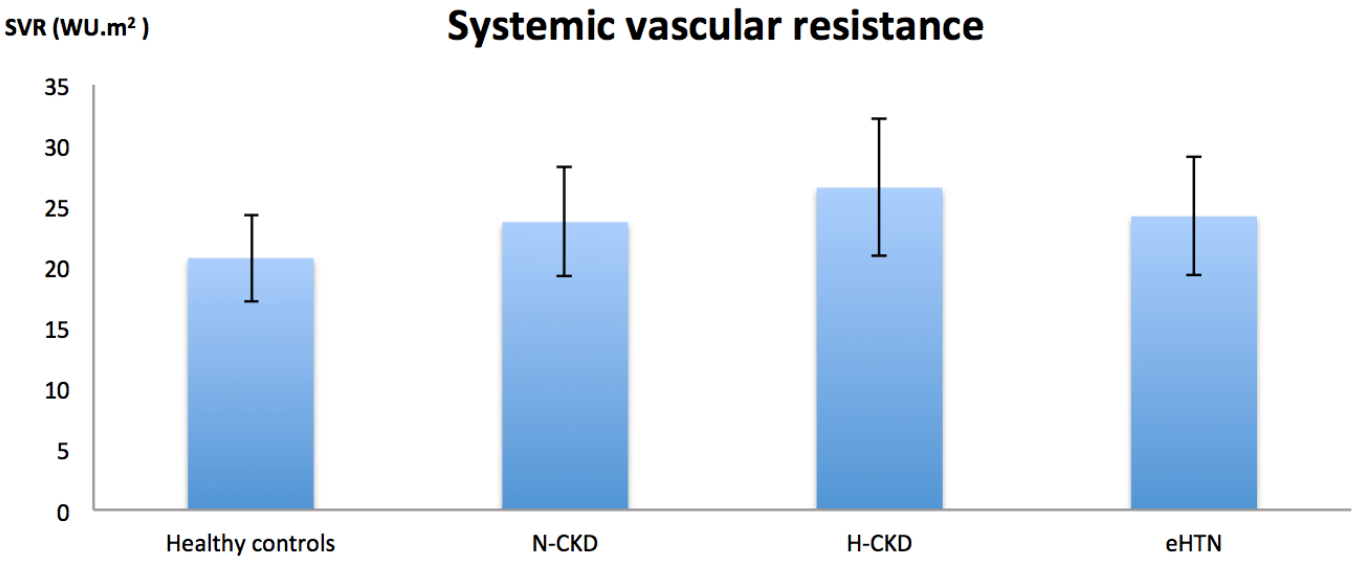

Figure 5.2: Bar chart showing differences in SVR between groups: SVR is significantly ($p<0.05$) higher in H-CKD compared to healthy controls and N-CKD. Abbreviations: SVR=systemic vascular resistance, N-CKD=non-hypertensive chronic kidney disease group, H-CKD=hypertensive chronic kidney disease group, eHTN=essential hypertension group.

5.4.4 Assessment of Left Ventricular indices

Systolic blood pressure was significantly correlated with LVM (r=0.40, p<0.0001) and MVR (r=0.40, p<0.0001) when the population was considered as a whole.

There was no difference in $LVMht^{2.7}$ between the CKD groups compared to healthy children but was higher in eHTN (Table 5.7). Conversely, MVR was significantly different between the groups (p=0.004). Both H-CKD and eHTN trended towards a higher MVR when compared to controls (p=0.054 and 0.061, respectively).

5.4.5 Relationship between Blood Pressure, Vascular Indices and Renal Severity

In CKD patients, higher MBP and DBP were significantly associated with lower eGFR and higher CKD stage (Table 5.8). For SBP, these associations were only a trend (p = 0.055 and 0.083 respectively). There was also a trend between higher SVR and CKD stage, but not with eGFR (Table 5.8). There were no associations between TAC and either CKD stage or eGFR. There were no associations between blood and urine based biomarkers of complications associated with CKD (calcium phosphate product, parathyroid hormone level, and urine albumin to creatinine ratio) with BP, SVR and TAC.

Table 5.7: Conventional indices of left ventricular assessment.

	HC N=20	N-CKD N=67	H-CKD N=43	eHTN N=20	p-value
LVEDV (ml/m^2)	72±10	67±9.5	67±10	69±9.6	0.20
LVESV (ml/m^2)*	23±1.3	20±1.3	19±1.3	21±1.3	0.21
LVSV (ml/m^2)	50±6.5	47±6.1	48±8.2	48±6.6	0.56
EF (%)	68±4.5	69±5.8	70±6.7	69±4.2	0.78††
LVMht$^{2.7}$ (g/$m^{2.7}$)	21±3.6	22±4.9§	24±5.9	26±6.5#	0.008
MVR (g/ml)	0.68±0.095	0.72±0.16	0.79±0.18	0.81±0.14	0.004††

Data presented as mean ± standard deviation. ⋆- Logarithmic transformation was applied. †- P-value <0.05 when N-CKD compared with HC. ‡ - P-value <0.05 when H-CKD compared with HC §- P-value <0.05 when N-CKD compared to eHTN. ||- P-value <0.05 when H-CKD compared to eHTN. #- P-value <0.05 when eHTN compared with HC. ⋆⋆– P-value <0.05 when H-CKD compared to N-CKD. ††– ANOVA Welch (W) test was used. Abbreviations: HC=Healthy control, N-CKD=Non hypertensive CKD, H-CKD=Hypertensive CKD, eHTN=Essential hypertension, LVEDV=Left ventricular end-diastolic volume, LVESV=Left ventricular end-systolic volume, LVSV=Left ventricular stroke volume, EF=Ejection fraction, LVMht(2.7)= Left ventricular mass indexed to height to the power of 2.7, MVR= Left ventricular mass volume ratio.

Table 5.8: Relationship between blood pressure, vascular indices and renal severity.

	CKD cohort with recent bloods, N=68			
	eGFR* Rho	p-value	CKD Stage* Rho	p-value
SBP (mmhg)	-0.23	0.055	0.21	0.083
MBP (mmhg)	-0.29	0.015	0.31	0.011
DBP (mmhg)	-0.27	0.028	0.29	0.015
SVR ($WU.m^2$)	-0.15	0.23	0.21	0.093
TAC ($ml/mmHg.\ m^2$)	-0.01	0.92	0.04	0.77

Data presented as mean ± standard deviation. ⁎-Spearman's correlation was applied. Abbreviations: CKD=Chronic kidney disease, eGFR=Estimated glomerular filtration rate, Rho=Spearman Correlation Coefficient, SBP=Systolic blood pressure, DBP=Diastolic blood pressure, MBP=Mean blood pressure, SVR=Systemic vascular resistance, TAC=Total arterial compliance.

5.5 Discussion

In this study, I used CMR to investigate vascular phenotype in paediatric CKD. The main finding was that SVR was significantly elevated in hypertensive and non-hypertensive CKD patients, but TAC was normal.

5.5.1 Hypertension in CKD

I have shown that the vascular phenotype of paediatric CKD is different from both healthy children (negative controls) and eHTN patients (positive controls). In eHTN, there were signs of arterial stiffening (reduced TAC) and BP characteristics consistent with stiffening being the cause of HTN (predominantly raised SBP and PP). In contrast, compliance was normal in CKD and the changes in BP (high SBP, DBP and MBP with normal PP) were in keeping with the raised SVR. This goes against the assumption that increased arterial stiffness is the main cause of hypertension in paediatric CKD (81).

The role of arterial stiffness in the aetiology of paediatric CKD related HTN has been inferred from 2 important findings. The first is the demonstration of raised pulse wave velocity (PWV), as recently shown in the 4C's study (74). However, raised PWV is not a universal finding and even in positive studies, PWV is only mildly raised (i.e. in the 4C's study the PWV z-score was 0.33

(74)). Furthermore, pulse pressure is normal in larger paediatric CKD studies (75), suggesting that global arterial stiffness is not increased in the population. The second finding is the observation of arterial wall calcification in children with CKD. Calcification does increase wall stiffness (82). However, it appears limited to muscular arteries (14, 69-71, 83) (e.g. the mesenteric and carotid arteries). There may be aortic sparing in pre-dialysis children due to the limited expression of vascular smooth muscle cells (implicated in calcification) in the media (83, 84). The aorta is the main repository of arterial compliance (85) (~80%). Therefore, it is possible to have stiff muscular arteries with normal total arterial compliance. Thus, my results are not inconsistent with the published data in pre-dialysis children.

The main difference between CKD patients and healthy controls was significantly higher SVR. In addition, SVR was higher in H-CKD patients compared to N-CKD patients and trended towards being higher with increasing CKD stage. This mirrors the BP associations seen in these patients, which was not the case for total arterial compliance. These findings suggest that SVR does play a role in the development of HTN, although my data does not prove causation. There are several possible explanations for increased SVR in CKD. They include salt retention and abnormal renin-angiotensin stimulation (86), and sympathetic overdrive (87).

Renin-angiotensin-aldosterone system (RAAS) activation is the hallmark of renal disease. Renal impairment begins with nephron injury and loss of glomeruli, which can be triggered by any pathological process. This causes

hyperfiltration and glomerular capillary hypertension, resulting in progressive glomerular injury and pressure induced capillary stretch. This leads to subsequent activation of intra-renal RAAS. The increased local production of angiotensin 2 creates a vicious cycle of glomerular damage by exacerbating efferent arteriolar vasoconstriction. It also promotes proteinuria and renal fibrosis, which in turn result in further renal injury and RAAS activation. Increased RAAS activity is associated with systemic vasoconstriction (88).

Sympathetic overactivity is another feature of CKD. Renal injury or ischaemia is thought to trigger several potential mechanisms including impaired reflex control of autonomic activity, stimulation of renin-angiotensin-aldosterone system and activation of renal afferent signals. The resultant increase in sympathetic activity promotes vasoconstriction, accelerated atherosclerosis and left ventricular hypertrophy (89).

Salt retention is a direct consequence of CKD and worsens with renal dysfunction (90). In renal failure, the salt and water accumulation leads to increase circulating blood volume. In healthy individuals, fluid retention secondary to increased oral salt intake (mediated via vasopressin), causes small increases in intraglomerular pressure that result in higher clearance of sodium. This is a normal mechanism for salt clearance and is known as pressure natriuresis. In CKD, this process is dysfunctional (86), which further exacerbates sodium retention. Furthermore, sodium causes an increase in SVR through direct effects on the vascular endothelium (causing peripheral

vasoconstriction) and indirect effects mediated via other mechanisms such as altered sympathetic activity (91).

Determination of the exact mechanism by which SVR is elevated in paediatric CKD was not the main purpose of this study, but would be an important next step.

Other possible causes of hypertension in CKD are fluid overload or high cardiac output. Although fluid overload is difficult to assess, I did show that RAA (a marker of fluid overload) was normal in this cohort. Furthermore, I also demonstrated that CO was not increased in CKD. Therefore, it is unlikely that these factors are important in the pathogenesis of HTN in early CKD.

In this study, I also showed a trend towards LV hypertrophy in eHTN and H-CKD patients when assessed using LV mass volume ratio. However, there was no statistically significant difference in indexed LV mass between the CKD and healthy control groups. Nevertheless, there was still a strong association between BP and both LVM and MVR.

5.5.2 Vascular phenotyping methodology

Most studies in paediatric CKD use PWV measurements to determine vascular phenotype, specifically arterial stiffness. However, PWV does not directly reflect the total buffering capacity of the arterial bed and can be difficult to assess accurately in children. Furthermore, PWV does not provide

any information about SVR, which is the main component of afterload. Therefore, in this study, I simultaneously assessed flow and BP to calculate both SVR and TAC, which allows more robust determination of vascular phenotype. Importantly, phase contrast MR provides more accurate assessment of flow compared to other techniques such as impedance cardiography or echocardiography. Nevertheless, there are some important points that should be addressed regarding this technique. Firstly, it is possible that TAC is a poor measure of stiffness and my findings in CKD are falsely negative. To guard against this, I included eHTN patients as positive controls and as expected (92) these children did have reduced TAC. Thus, I believe this method is valid and sufficiently sensitive for evaluating global arterial stiffness. Secondly, I did not include RA pressure in my calculation of SVR and if raised this could cause SVR to appear falsely elevated. However, the RA pressure would have to be extremely high (almost 20mmHg greater than normal in H-CKD patients) to explain these results. The fact that RA size was normal and there were no other signs of severe fluid overload suggests that this method of measuring SVR is valid in these children.

5.6 Limitations

The main limitation of this study was the fact that the eHTN population were older and had a male preponderance. This problem was overcome for SBP and DBP by using blood pressure percentiles for age and gender. However, percentiles are not readily available for other parameters such as SVR and TAC and BSA indexing may not be sufficient.

Another limitation of the study comes from the fact that most CKD patients were already on antihypertensive medications at the time of the study and this may have biased the results. Because of this, adjustments for the potential confounding effect of sex, age and use of anti-HTN medications were additionally undertaken to interrogate the influence of these factors. The exact pubertal status of patients was not assessed and this is a limitation as pubertal status can affect hemodynamic parameters. The control group were relatively small in sample size. However, the numbers were sufficiently powered to detect the differences.

Blood pressure measurements were carried out using an oscillometric sphygmomanometer, which may be less accurate than using manual sphygmomanometer (93). This was because it was essential for BP measurement to be acquired simultaneously during PCMR flow acquisition for accurate assessment of vascular measures. Unfortunately, this could not be performed manually in the CMR scanner during flows acquisitions. However, BP measurement was taken with a standardized protocol for all subjects using the same machine. This meant that the measurements were comparable across the cohort. Therefore, I believe that the group wise differences noted are a reflection of real differences.

Finally, calculation of compliance using central aortic PP, instead of brachial PP, may provide a more accurate assessment of arterial stiffness. This is because brachial PP is believed to be a surrogate of central aortic PP due to the amplification phenomenon (65). There are methods to estimate central aortic PP from brachial PP such as the reconstruction of central aortic pressure waveforms by applying a Generalised Transfer Factor to the peripheral blood pressure waveform (94). However, as these methods may not be accurate, the direct measurement of central PP for arterial stiffness assessment would be ideal. Unfortunately, this is challenging to perform non-invasively during a CMR scan and was not done. Despite that, I was able to demonstrate a significant difference between groups in compliance calculated using brachial PP. Future studies should consider assessing central aortic pressure in these patient groups to determine if it differs with my findings.

5.7 Conclusion

In this study, I have shown that systemic vascular resistance, not aortic stiffness, is increased in paediatric CKD. My data suggests elevated BP in CKD is associated with increased resistance rather than reduced compliance. This novel finding may be important in determining the optimum antihypertensive therapy for these children. Hopefully, improved directed treatment will reduce cardiovascular risk in paediatric CKD.

6 Comprehensive characterization of cardiac phenotype in pre-dialysis chronic kidney disease

In this chapter, I will describe the comprehensive evaluation of the cardiac phenotype in children with CKD and determine its relationship with CKD severity.

6.1 Personal contribution

For the study described in this chapter:

- I completed the ethics application process.
- I recruited all subjects.
- I acquired, collated, and tabulated the relevant clinical data.
- I completed the segmentation and data analysis on all study subjects.
- I performed statistical analysis on the study dataset.
- I wrote up the findings from this study into a research article and have submitted it to Journal of Cardiovascular Magnetic Resonance. It is currently under review.

6.2 Introduction

Cardiovascular events are a leading cause of death in paediatric chronic kidney disease (95). Unfortunately, reducing mortality in this group remains challenging, partly due to difficulties in identifying children at risk.

Two-dimensional echocardiography is conventionally used to assess the heart in children with CKD. Several ECHO markers have been used as indicators of increased risk including left ventricle hypertrophy and left ventricular global dysfunction (i.e. reduced ejection fraction) (96, 97). More recently, there has been increasing interest in advanced ECHO techniques like tissue Doppler and speckle tracking, which have demonstrated sub-clinically impaired diastolic and systolic function in paediatric CKD. However, the utility of ECHO is significantly limited by inaccurate measurement of volumes and mass, limited reproducibility and operator dependence (22).

Cardiovascular magnetic resonance imaging is the reference standard method of assessing LV volumes, ejection fraction and mass (77). Robust evaluation of the left ventricle by CMR is vital as the LV represents a possible pathophysiological link between increased mortality and co-morbidities such as hypertension. Of particular note is LV mass, which is an independent risk factor for sudden cardiac death in adult CKD (98).

New CMR techniques are also being developed that could provide more sophisticated evaluation of cardiac function. These include tissue phase

mapping to assess myocardial velocities (59) and high temporal resolution phase contrast MR to measure mitral inflow velocities and cardiac timing intervals, as previously discussed in Chapter 2. Thus, CMR may be a useful technique to comprehensively assess myocardial phenotype in paediatric CKD.

The objectives of this study were to i) perform comprehensive cardiac phenotyping of children with CKD, and ii) determine the relationship between phenotype and CKD severity. To accomplish this, CMR was performed in a large cohort of pre-dialysis CKD children and findings were compared with healthy subjects.

6.3 Methods

6.3.1 Study Population

The study population consisted of 120 children: 100 with confirmed CKD (stages 1-5) and 20 healthy volunteers. Exclusion criteria were: i) age <7 or >18 years, ii) congenital structural heart disease or primary myocardial disease, iii) primary renovascular disease, iv) active vasculitis v) cardiac arrhythmia, vi) medical devices precluding CMR, vii) history of current or previous renal replacement therapy and viii) acutely deteriorating renal function.

The data presented in this chapter was collected together (at the same sitting) as the vascular data presented in Chapter 5. Ten children from the original pre-dialysis CKD cohort (n=110) had the vascular assessment protocol but did not manage to complete the myocardial assessment protocol for logistic reasons (e.g. needed to leave the hospital early due to time pressures) and were excluded from this analysis.

All CKD participants had blood and urine tests as part of their outpatient care including: haemoglobin (HB), urea, creatinine, electrolytes, calcium, phosphate, intact parathyroid hormone level (PTH), and urine albumin to creatinine ratio measurements. Estimated glomerular filtration rate was estimated by modified Schwartz formula. All medical notes were also reviewed specifically looking for previous renal function to confirm that the documented renal function results is stable and there is no clinical suspicion of renal deterioration. Neither blood nor urine tests were performed for healthy controls.

6.3.2 Study protocol

The study protocol has been previously outlined in detail in Chapter 4. In summary, I performed non-invasive blood pressure measurements, and assessment of left ventricle (SAX LV stack acquisition using KT-SENSE sequence), aortic flow (acquired in ascending aorta using retrospective-gated, spiral SENSE PCMR sequence), cardiac timing (acquired at the LV inflow/outflow SAX position using real-time UNFOLD-SENSE spiral PCMR

sequence) and myocardial velocity (acquired in Mid LV SAX position using self-navigated golden-angle spiral TPM sequence). This was used to calculate LV mass and volume, aortic flow, cardiac timing and myocardial velocity measures as described below.

6.3.3 Statistics

Statistical analyses were performed using Stata 13 (StataCorp, College Station, Texas, USA). Data were examined for normality using Shapiro-Wilk test and non-normally distributed data was transformed using a zero-skewness log transform prior to analysis. Descriptive statistics were expressed as mean (± standard deviation) or geometric mean (± geometric standard deviation) if data was log transformed.

To assess the CKD group, the patients were divided into 3 CKD groups – stages 1–2, stage 3a–3b and stage 4–5 and compared to healthy controls. Between group differences were assessed using analysis of variance (ANOVA). The ANOVA models were adjusted for confounders like age, sex, where indicated. Levene's test was used to assess for homogeneity of variances across the groups and Welch's correction was applied for non-homogeneous variance. To further interrogate differences between each group, a post-hoc pairwise comparison was performed on CV parameters significantly different on ANOVA testing. The Bonferroni method was employed to adjust for potential Type 1 errors in the post-hoc pairwise comparisons (build into post-hoc comparison method in Stata).

Spearman's correlation coefficient (rho) was used to determine the relationship between continuous variables as further described in the results section. Chi-square test was used to determine differences in sex distribution and the proportion of anti-hypertension medication use between the groups.

Separate multi-variable ANOVA models were also constructed to examine the independent effect of CKD group and other significant correlates on various CV characteristics, namely: i) the effect of CKD and SBP on LV remodeling, ii) effect of CKD and MVR on IRT, and iii) effect of CKD and DBP on radial S' velocity. All models were adjusted for the influence of age and sex.

Finally, multi-variable linear regression was also used to determine if significant CV indices (MVR, IRT, S', E', E'/A', E/E') were related to eGFR or other markers of CKD severity i.e. anaemia (HB) and CKD-mineral bone disease (PTH). Adjusted R^2 was used to assess for goodness of fit. The beta coefficient (β) was used to evaluate the relationship between the dependent variable and the independent factors in the regression model. Only patients with recent blood tests (within 3 months of CMR scan) were included into models involving blood indices. A p value <0.05 was considered statistically significant. Indices not statistically different to healthy subjects have been described as 'normal'.

6.4 Results

6.4.1 Demographics

The CKD cohort (n=100) consisted of 40 children in stage 1-2 (group 1: mean eGFR: 78.6±8.8 ml/min/1.73 m^2), 40 children in stage 3 (group 2: 48.3±8.4 ml/min/1.73 m^2) and 20 children in stage 4-5 (group 3: 19.2±6.5 ml/min/1.73 m^2). Twenty-five (25%) children (group 1: 10, group 2: 9 and group 3: 6) had a prior diagnosis of HTN and were on treatment (Table 6.1). The two most common causes of CKD were congenital abnormalities of the kidney and urinary tract (CAKUT, n=60, 60%) and renal dysplasia (n=11, 11%). All other causes represented <10% of the population. Eight CKD children had undergone a previous nephrectomy. No children had previously received or were currently receiving renal replacement therapy as per exclusion criteria. None of the healthy subjects (n=20) had any significant past medical history nor were taking any medications. There were no differences in age, BSA or sex distribution between groups (Table 6.1). Recent blood and urine test were available in 62 patients (group1: n=16, group 2: n=28, group 3: n=18) and are summarised in Table 6.1.

Both DBP and MBP were significantly elevated in CKD as seen in Table 6.1. In addition, DBP centile was higher in CKD ($p<0.001$). There were no group differences in SBP and PP ($p\geq0.13$), although there was a trend towards a higher SBP centile in CKD ($p=0.08$).

Table 6.1: Demographics and baseline characteristics of study population.

	Healthy Controls (n=20)	Group 1 CKD (n=40)	Group 2 CKD (n=40)	Group 3 CKD (n=20)	p-value
Age (years)*	12±1.3	11±1.3	12±1.3	13±1.3	0.12
Sex (% male)	40%	38%	23%	45%	0.42
Height (cm)	162±18	150±17	152±18	151±18	0.075
Weight (kg)*	53±1.4	43±1.5	45±1.5	44±1.4	0.22
Body Mass Index (kg/m^2)*	20±1.1	19±1.2	20±1.2	20±1.1	0.77
Body Surface Area (m^2)	1.6±0.32	1.4±0 .33	1.4±0.35	1.4±0.3	0.16
Systolic BP (mmhg)*	109±1.1	113±1.1	116±1.1	116±1.1	0.14
SBP percentile*	33±2.5	58±1.7	61±1.8	64±1.7	0.08††
Diastolic BP (mmhg)*	53±1.2	63±1.2†	65±1.2‡	69±1.2§	<0.001
DBP percentile*	17±2.3	45±1.9†	48±1.8‡	60±1.6§	<0.001††
Mean BP (mmhg)	78±7.8	84±8.8†	87±9.9‡	89±8.8§	<0.001
Pulse Pressure (mmhg)	55±13	50±10	51±9.5	48± 12	0.13
Heart Rate (BPM)*	72±1.2	75±1.2	72±1.2	74±1.2	0.75

Relevant blood results‡‡					
Haemoglobin (g/L)	-	132±13	133±16	128±11	0.57
Urea (mmol/L)	-	5.4±1.2	8.6±2.5||	18.0±5.2#**	<0.001††
Creatinine (umol/L)*	-	68±1.2	117±1.2||	305±1.4#**	<0.001††
eGFR (ml/min/1.73 m^2)	-	79±8.8	48±8.4||	19±6.5#**	<0.001
Calcium-Phosphate product ($mmol^2/L^2$)	-	3.4±0.45	3.4±0.39	3.5±0.56	0.40
Intact parathyroid hormone (pmol/L)*	-	3.5±3.2	3.7±2.4	8.5±2.4**	0.011
Urine Albumin/ Creatinine Ratio (mg/mmol)	-	4.7±3.7	22±6.2	261±2.5#**	<0.001
Medications§§					
Angiotensin converting enzyme inhibitor	-	28%	40%	15%	0.13
Calcium Channel Blocker	-	5%	13%	15%	0.38
Beta-Blocker	-	5%	5%	20%	0.09
Aldosterone antagonist (Spironolactone)	-	3%	0%	0%	0.47

Data presented as mean ± standard deviation. *- Logarithmic transformation was applied. †- P-value <0.05 when group 1 compared with controls. ‡ - P-value <0.05 when group 2 compared with controls. §- P-value <0.05 when group 3 compared with controls. ||- P-value <0.05 when group 2 compared with group 1. #- P-value <0.05 when group 3 compared with group 1. **– P-value <0.05 when group 3 compared with group 2. ††– ANOVA Welch (W) test was used. ‡‡ - Recent (within 3 months of CMR scan) blood test were available in 62 CKD patients. §§-Chi-squared test was performed. 10% of CKD patients were on 2 or more anti-hypertensive agents. Abbreviations: CKD= chronic kidney disease, eGFR=Estimated glomerular filtration rate.

6.4.2 Cardiac geometry and global function

Mass volume ratio (a marker of LV remodeling) was elevated in CKD, with the highest MVR observed in group 3 (Table 6.2). This finding remained significant after adjusting for age and sex (p=0.009). Mass volume ratio correlated with all measures of blood pressure (SBP: rho=0.29, p=0.001; MBP: rho=0.26, p=0.004; and DBP: rho=0.19, p=0.04) as seen in Figure 6.1. When a model was created to study the combined effect of blood pressure and renal disease severity on LV remodeling, both SBP (BP with highest univariate correlation) and CKD group were independent predictors of MVR (p=0.003, p=0.02 respectively).

Although $LVMht^{2.7}$ did appear higher in CKD, this did not reach statistical significance (p=0.12).

There were no differences in ESV, SV, EF, RAA or LAA between the groups. However, LV EDV was slightly smaller in CKD groups compared to controls (p=0.03).

Table 6.2: Cardiac structure and global function in CKD.

	Healthy Controls (n=20)	Group 1 CKD (n=40)	Group 2 CKD (n=40)	Group 3 CKD (n=20)	p-value
LVEDV (ml/m^2)	74±11	68±9.1†	68±10	65±9.7§	0.03
LVESV (ml/m^2)*	23±1.3	21±1.3	20±1.3	19±1.3	0.13
LVSV (ml/m^2)*	50±1.1	46±1.1	47±1.2	46±1.2	0.18
CO* (l/min/m^2)	3.6±1.2	3.5±1.2	3.4±1.2	3.4±1.2	0.61
EF (%)	68±4.6	68±6.1	69±6.7	70±5.8	0.72
$LVMht^{2.7}$ (g/$m^{2.7}$)*	21±1.2	21±1.3	22±1.2	25±1.2	0.12
MVR (g/ml)	0.7±0.1	0.72±0.16	0.75±0.16	0.87±0.17§#**	0.003
RAA (cm^2/m^2)	12±1.8	12±1.9	11±2.5	11±2	0.69
LAA (cm^2/m^2)*	12±1.3	12±1.2	11±1.2	11±1.2	0.38

Data presented as mean ± standard deviation. *- Logarithmic transformation was applied. †- P-value <0.05 when group 1 compared with controls. ‡ - P-value <0.05 when group 2 compared with controls. §- P-value <0.05 when group 3 compared with controls. ||- P-value <0.05 when group 2 compared with group 1. #- P-value <0.05 when group 3 compared with group 1. **– P-value <0.05 when group 3 compared with group 2. ††– ANOVA Welch (W) test was used. Abbreviations: CKD=Chronic kidney disease, LVEDV=Left ventricular end-diastolic volume, LVESV=Left ventricular end-systolic volume, LVSV=Left ventricular stroke volume, LVMht(2.7)=Left ventricular mass indexed to height to the power of 2.7, MVR=Left ventricular mass to volume ratio, R/LAA =Right / left atrial area, EF=Ejection fraction, CO =Cardiac output.

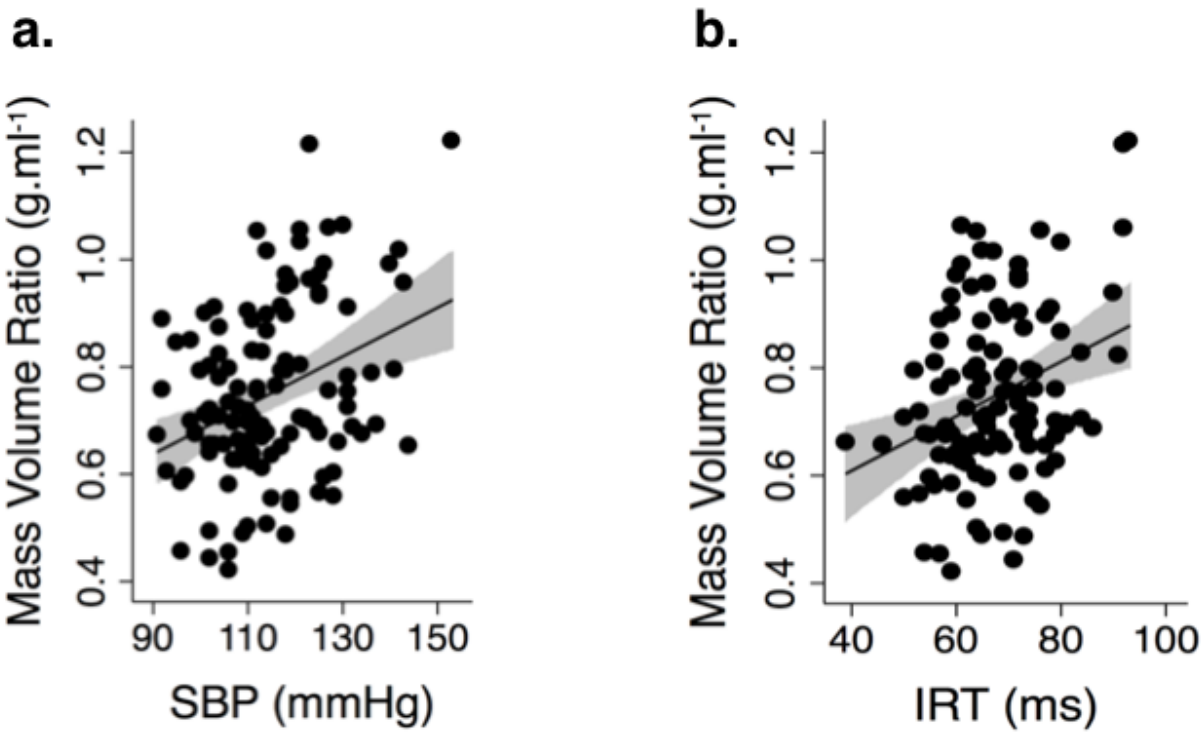

Figure 6.1: Relationship between mass volume ratio (MVR) and cardiovascular characteristics: (a) MVR versus systolic blood pressure (SBP), (b) MVR versus isovolumic relaxation time (IRT). The 95% confidence interval of the predicted mean is illustrated by grey zone.

6.4.3 Inflow velocities and cardiac timing intervals

Isovolumic relaxation time (a marker of active myocardial relaxation (99)) was prolonged in CKD and significantly increased in CKD groups 2 and 3 (Table 6.3). This remained significant after adjustments for age and sex and heart rate. There was a significant association between IRT and MVR (rho=0.25, p=0.008) as seen in Figure 6.1.

Table 6.3: Cardiac timings and mitral inflow velocities in CKD

	Healthy Controls (n=20)	Group 1 CKD (n=40)	Group 2 CKD (n=40)	Group 3 CKD (n=20)	p-value
IRT (ms)*	61±1.2	64±1.1	70±1.1‡	72±1.1§	<0.001
ICT (ms)*	44±1.6	36±1.6	33±1.8	37±1.8	0.24
ET (ms)	277±21	275±16	274±19	276±15	0.92
Tei*	0.39±1.3	0.37±1.2	0.38±1.2	0.41±1.3	0.56
E (mls)	47±9.8	49±11	50±11	49±9.7	0.87
A (mls)	19±4.3	20±6.7	21±6.8	22±5.6	0.36
E/A ratio*	2.6±1.2	2.6±1.4	2.5±1.5	2.3±1.3	0.63

Data presented as mean ± standard deviation. *- Logarithmic transformation was applied. †- P-value <0.05 when group 1 compared with controls. ‡ - P-value <0.05 when group 2 compared with controls. §- P-value <0.05 when group 3 compared with controls. ||- P-value <0.05 when group 2 compared with group 1. #- P-value <0.05 when group 3 compared with group 1. **– P-value <0.05 when group 3 compared with group 2. ††– ANOVA Welch (W) test was used. Abbreviations: CKD=Chronic kidney disease, IRT=Isovolumic relaxation time, ICT=Isovolumic contraction time, E=Early transmitral mean velocity, A=Late transmitral mean velocity, E/A ratio=E to A ratio. ET=Ejection time, Tei=Myocardial performance index.

Table 6.4: Tissue phase mapping in CKD

	Healthy Controls (n=20)	Group 1 CKD (n=40)	Group 2 CKD (n=40)	Group 3 CKD (n=20)	p-value
Rad S' (cm/s)	2.7±0.31	2.6±0.24	2.5±0.38‡	2.4±0.31§	0.003
Rad E' (cm/s)	4.2±0.59	3.6±0.62†	3.4±0.78‡	3.3±0.53§	<0.001
Rad A' (cm/s)	1.3±0.35	1.1±0.34	1.2±0.31	1.2±0.28	0.30
Long S' (cm/s)	4.6±1.6	3.9±1.1	3.4±1.3‡	3.6±1.3	0.009
Long E' (cm/s)	7.9±1.5	7.5± 2.0	6.7±1.8	6.8±1.4	0.046
Long A' (cm/s)	2.3±0.71	2.5±1.1	2.7±0.85	2.5±0.64	0.61
Long E'/A' ratio*	3.4±1.3	3.2±1.6	2.6±1.4‖	2.8±1.3	0.003††
Long E/E' ratio*	6±1.2	6.7±1.3	7.5±1.4‡	7.3±1.4	0.03

Data presented as mean ± standard deviation. *- Logarithmic transformation was applied. †- P-value <0.05 when group 1 compared with controls. ‡ - P-value <0.05 when group 2 compared with controls. §- P-value <0.05 when group 3 compared with controls. ||- P-value <0.05 when group 2 compared with group 1. #- P-value <0.05 when group 3 compared with group 1. **– P-value <0.05 when group 3 compared with group 2. ††– ANOVA Welch (W) test was used. Abbreviations: CKD=Chronic kidney disease, Rad=Radial, Long=Longitudinal, S'=Systolic myocardial velocity, E'=Early diastolic myocardial velocity, A'=Late diastolic myocardial velocity, E'/A'=E' over A' ratio, E/E'=E over E' ratio.

However, both MVR and CKD group were independent predictors of IRT in a multi-variable ANOVA model, after adjusting for age and sex (p=0.007 and 0.005 respectively). There were no differences in ICT, ET or Tei index between the groups. Mitral E and A velocities and E/A ratio were also normal in CKD.

6.4.4 Tissue phase mapping

Radial and longitudinal S' velocities (markers of systolic contraction) were reduced in CKD (Table 6.4). Radial S' negatively correlated with MBP (rho=-0.22, p=0.016) and DBP (rho=-0.37, p<0.0001 – Figure 6.2), but not SBP (p=0.52). Conversely, longitudinal S' did not significantly correlate with any blood pressures.

A multivariate ANOVA model was created to study the effects of blood pressure and CKD on radial systolic velocities. In this model, both DBP (BP with highest univariate correlation) and CKD group were independent predictors of radial S' (p=0.02 and 0.01 respectively). Radial S' also significantly correlated with LVEF (rho=0.24, p=0.009 - Figure 6.2), but there was no association between LVEF and longitudinal S' (p=0.24).

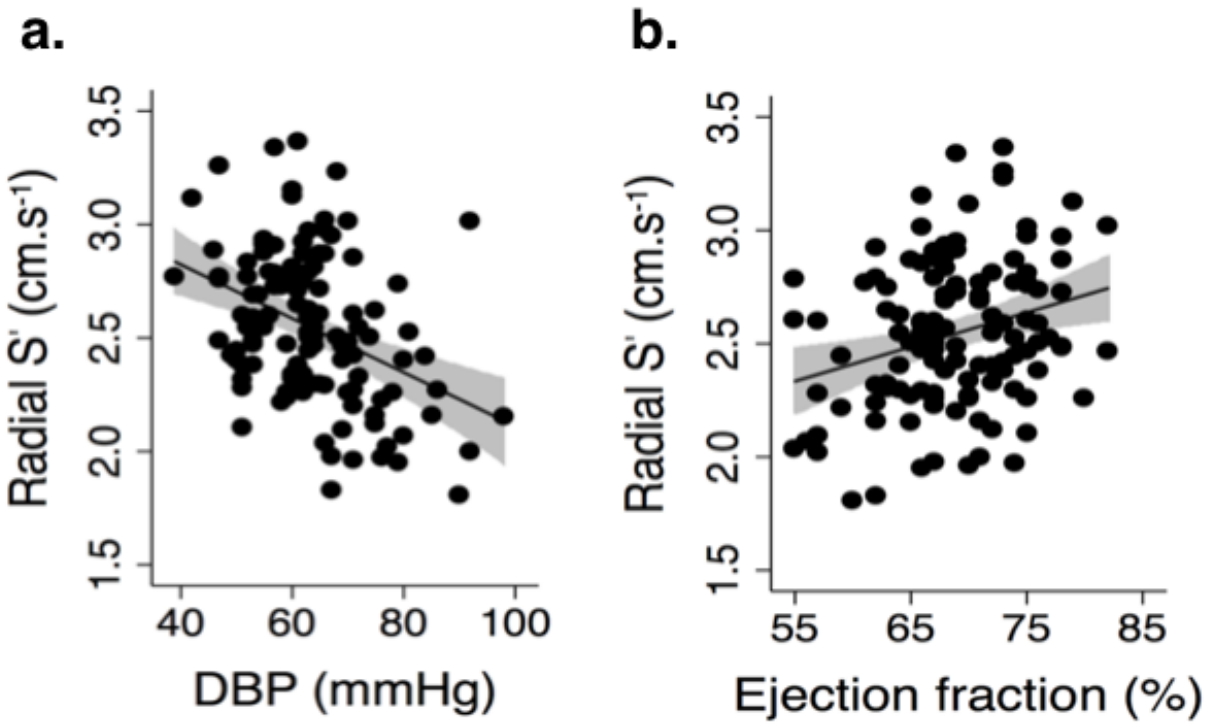

Figure 6.2: Relationship between tissue phase mapping indices and conventional measures of cardiac function: (a) Radial systolic myocardial velocity (Rad S') versus diastolic blood pressure (DBP), (b) Rad S' versus ejection fraction. The 95% confidence interval of the predicted mean is illustrated by the grey zone.

Radial and longitudinal E' velocities (markers of LV relaxation and stiffness) were also reduced in CKD. This difference remained significant after adjustment for age and sex. Radial and longitudinal E' correlated negatively with IRT (rho=-0.28, p=0.003 & rho=-0.24, p<0.01 respectively). Unlike IRT, neither was associated with MVR (p>0.3). In addition, E'/A' was reduced and E/E' was raised in CKD (p≤0.046). There were no group differences in radial and longitudinal A' velocities.

6.4.5 Association between renal and cardiovascular biomarkers

Worsening eGFR was independently associated with MVR (eGFR β=-0.30, p=0.02, R^2= 0.14). In addition, anaemia was associated with a reduced radial function (Rad S': Hb β=0.29, p=0.02, R^2=0.17, Rad E': Hb β=0.34, p=0.01, R^2=0.12). All models were adjusted for age, sex, and use of anti-HTN medications. These relationships remained significant after adjusting for the effect of afterload (SBP, DBP or MBP). There were no other significant relationships between eGFR, PTH and HB with other CV parameters.

6.5 Discussion

In this study, I have investigated the cardiac phenotype in pre-dialysis paediatric CKD using CMR. The main findings were that children with CKD had: i) Elevated blood pressure (primarily MBP and DBP), ii) Higher LV mass volume ratio independent of blood pressure, iii) Abnormalities of diastolic function suggestive of reduced active relaxation and increased chamber stiffness and iv) Reduced systolic velocities with preserved global systolic function.

6.5.1 LV remodelling in CKD

I demonstrated that paediatric CKD was associated with concentric remodelling as evidenced by increased LV mass volume ratio. Height indexed LV mass was not statistically different in this population, unlike previous echocardiographic studies. This may be due to the well-recognized overestimation of LV mass using echocardiography, particularly in patients with renal disease (39).

Ventricular remodelling in these children is partly explained by their hypertensive phenotype. However, CKD still remains a predictor of MVR after controlling for BP, implying that uraemia-related processes are involved. This is important as LVH confers significantly increased cardiovascular risk (96). Anaemia and hyperparathyroidism have been suggested as possible causes of hypertrophy in CKD (100). Chronic anaemia is associated with increased cardiac stress through tachycardia and increased stroke volume, resulting in LVH (101). Parathyroid hormone is thought to have a direct trophic effect on cardiac myocytes (102). Identification of the exact stimulus may provide new targets for therapeutic intervention.

6.5.2 Diastolic function in CKD

In this study, conventional mitral inflow E/A was normal in children with CKD. However, both IRT and E' were abnormal, pointing towards subtle diastolic dysfunction in these patients. Isovolumic relaxation time is a marker of active

myocardial relaxation and correlates with invasively measured isovolumic relaxation constant (99). Previous studies in adults have shown that active relaxation is associated LV mass (103) and my findings are in keeping with this. However, even after controlling for MVR, CKD remains a predictor of IRT. Thus, CKD must exert an independent effect possibly mediated through abnormal energy or calcium handling. This could be due to relative oxygen deficit in the myocardium arising from a mismatch between myocyte and capillary as demonstrated in animal models (104). Blood capillary supply is thought to be insufficient in hypertrophied hearts and this contributes to risk of myocardial ischaemia, which may result in impaired relaxation.

Early diastolic peak velocity is a marker of both active relaxation and ventricular compliance (105). My demonstration of lower E' measured using TPM is in keeping with a previous small study in paediatric CKD (106). In this study, E' did not correlate with MVR or $LVMht^{2.7}$. Thus, reduced early filling cannot simply be explained by LV hypertrophy. One explanation for reduced ventricular compliance is myocardial fibrosis, which has been demonstrated in several animal models (107). Unfortunately, it is not possible to perform post contrast T1 mapping in these patients due to the risk of nephrogenic systemic fibrosis (108). Nevertheless, non-contrast methods such as native T1 mapping are now available (108) and these could be useful to quantify fibrosis in CKD in future studies.

6.5.3 Systolic function in CKD

Global systolic function was preserved in CKD patients with normal LVEF. However, both radial and longitudinal S' were reduced implying some element of systolic dysfunction. These findings are in keeping with previous tissue Doppler imaging and echocardiographic strain studies and illustrate the importance of assessing systolic function in a more sophisticated manner (23, 28). The most obvious explanation for reduced S' is that increased blood pressure limits contraction through the force velocity relationship. However, only radial S' negatively correlated with blood pressure and CKD was still a predictor of radial S' after controlling for BP. Thus, CKD specific factors must also be involved, which is consistent with the idea of 'uraemic' cardiomyopathy. Possible biochemical causes include: uraemia induced coronary microvascular disease (109) and renal hyperparathyroidism causing cardiac fibrosis (110). Importantly, the ability to detect subtle systolic dysfunction may allow better risk stratification for these patients.

6.5.4 Renal and cardiovascular biomarkers

I was not able to demonstrate a relationship between eGFR and CV indices (apart from MVR), which may be due to the limited number of subjects with recent blood tests. Despite that, CKD severity and anaemia (a complication of renal disease) were clearly associated with CV abnormalities. Hence, this may suggest that CV impairment is mainly conferred by the diagnosis of CKD

(and anaemia) rather than renal deterioration. Future large studies are needed to confirm this.

6.5.5 The use of CMR for cardiac assessment in CKD

I have demonstrated that children with CKD exhibit a specific, but subtle cardiac phenotype. To evaluate the cardiac phenotype, cardiac timing intervals, myocardial velocities and LV mass must be measured. This is possible using echocardiography, which has been successfully performed in several previous studies (27, 28). However, echocardiography has several limitations including overestimation of LV mass (39) and an inability to measure myocardial velocities throughout the ventricle. Cardiovascular MR does not suffer from these limitations and could have an important role to play in phenotyping these patients. Furthermore, new fast imaging techniques enable volumetric analysis, inflow assessment and measurement of myocardial velocities to be performed quickly and without long breath holds. In addition, CMR provides reference standard assessment of aortic flow and this allows the vascular phenotype to also be evaluated. Thus, CMR represents a clinically feasible method of comprehensively phenotyping children with CKD.

6.6 Limitations

The main limitation of this study is the lack of patient numbers in each of the CKD stages. Despite this, I was able to demonstrate a worsening CV impairment with increasing renal dysfunction. Future larger studies with greater sampling of patients in each CKD stage will be useful to determine if a linear relationship exists between renal severity and CV impairment. Finally, performing an echocardiogram in tandem may also have been informative for the comparison of CMR findings with an established standard clinical investigation. Unfortunately, this was not carried out in order to minimise disruption and inconvenience to these patients.

Circumferential myocardial velocities were not examined in this study. This is because this parameter has not been validated using the present TPM sequence - only radial and longitudinal velocities have been validated (59). Assessment of circumferential function and LV torsion may be informative in this population where myocardial impairment is subtle. Future studies should consider evaluating circumferential motion in addition to radial and longitudinal function for a more comprehensive evaluation of myocardial function.

6.7 Conclusion

In this study, I have shown that CMR can be used to comprehensively evaluate cardiac phenotype in children with CKD. Paediatric CKD is associated with subtle systolic and diastolic impairment. The novel CMR indices used in this study may be useful for identifying high-risk paediatric CKD patients. However, more work is needed to determine normative values. Future prospective studies will also be required to correlate these markers with prognosis in order to predict cardiovascular risk.

7 Cardiovascular effects of renovascular hypertension

In this chapter, I will describe the comprehensive evaluation of the cardiovascular phenotype in children with renovascular hypertension and determination of how that may differ in essential hypertension.

7.1 Personal contribution

For the study described in this chapter:

- I completed the ethics application process.
- I recruited all subjects.
- I acquired, collated, and tabulated the relevant clinical data.
- I completed the segmentation and data analysis on all study subjects.
- I performed statistical analysis on the study dataset.

7.2 Introduction

Renovascular hypertension (RH) is associated with high cardiovascular mortality in adults (31). This is because adult renal artery stenosis (RAS) is typically atherosclerotic in origin and associated with conventional CV risk

factors (33). In contrast, the long-term CV risk of RAS in children is unknown. The CV effects of RAS have never been characterized in children.

Any CV abnormalities that arise are thought to be mainly due to the effect of hypertension as paediatric RAS is seldom associated with other CV risk factors. Thus, the main therapeutic goal in paediatric RH is to normalize blood pressure using aggressive pharmacological treatment, renal artery angioplasty, or surgical revascularization (33). Good BP control is frequently achieved and complete resolution of hypertension is sometimes possible (111, 112). Because of this, paediatric RH is widely regarded as “reversible” compared to idiopathic essential hypertension (eHTN). However, it is not known if CV effects persist after successful treatment of RH in children.

Two-dimensional echocardiography is conventionally used to assess for CV changes associated with hypertension. However, as previously mentioned, ECHO has known limitations such as inaccurate left ventricular (LV) mass measurements and poor reproducibility (22), particularly in patients with poor acoustic windows (113).

Cardiac magnetic resonance imaging is the reference standard method for quantification of ventricular mass and volume mass and is thus ideal for assessment of hypertensive changes in paediatric RH (77). Measurement of cardiac timings, mitral diastolic flow and longitudinal and radial myocardial velocity is also now possible due to recent CMR technological advancements

(57, 59). Thus, subtle changes to myocardial structure and function such as diastolic dysfunction may now be reliably assessed using CMR (57).

The objective of this study was to characterize cardiovascular structure and function in a cohort of optimally treated paediatric RAS, using CMR. The findings in RAS will be compared with a cohort of treated idiopathic hypertension patients and healthy controls.

7.3 Methods

7.3.1 Study Population

The study population consisted of 45 children in total: 15 children with a diagnosis of renovascular hypertension, 15 children with idiopathic essential hypertension and 15 healthy controls.

A diagnosis of RAS was confirmed with a combination of non-invasive and invasive investigations including renal vessel Doppler ultrasound scan, renal scintigraphy, renal vein renin sampling or renal angiography (33). The optimal treatment plan of all RH children was recommended following discussion at the GOSH renal artery stenosis multidisciplinary team (MDT) meeting comprising of paediatric nephrologists, surgeons and interventional radiologists. Only patients with stable optimally treated RH after completing recommended treatment were recruited.

The eHTN patients were clinically evaluated according to published recommendations to exclude secondary causes of HTN (79). Exclusion criteria were: i) age <7 or >18 years, ii) congenital structural heart disease or primary myocardial disease, iii) chronic kidney disease greater than stage 2 or deteriorating renal function, iv) active vasculitis v) cardiac arrhythmia, vi) medical devices precluding CMR, vii) presence of an alternative diagnosis for hypertension apart from RH (in the RH cohort), and viii) current or previous renal replacement therapy.

The last available blood test (full blood count, urea, creatinine, electrolytes) performed as part of their outpatient care was retrieved for the RAS and eHTN participants. Renal function was estimated by the modified Schwartz formula to obtain the estimated glomerular filtration rate (eGFR) and CKD stage. The medical notes were also reviewed specifically to confirm that the current documented renal function is stable and there is no clinical suspicion of renal deterioration.

7.3.2 Study protocol

The study protocol has been previously outlined in detail in Chapter 4. In summary, I performed non-invasive blood pressure measurements, and assessment of left ventricle (SAX LV stack acquisition using KT-SENSE sequence), aortic flow (acquired in ascending aorta using retrospective-gated, spiral SENSE PCMR sequence), cardiac timing (acquired at the LV inflow/outflow SAX position using real-time UNFOLD-SENSE spiral PCMR

sequence) and myocardial velocity (acquired in Mid LV SAX position using self-navigated golden-angle spiral TPM sequence). This was used to calculate LV mass and volume, aortic flow, cardiac timing and myocardial velocity measures as described below.

7.3.3 Statistics

Statistical analyses were performed using Stata 13 (StataCorp, College Station, Texas, USA). Data were examined for normality using Shapiro-Wilk normality test and non-normally distributed data was transformed using a zero-skewness log transform to ensure normal distribution prior to analysis. Descriptive statistics were expressed as mean (± standard deviation) or geometric mean (± geometric standard deviation) if data was log transformed. Chi-squared test was used to determine if sex distribution between groups were different. To assess for CV changes in RH patients, comparisons between RH, eHTN and healthy controls were made. Between group differences were assessed using analysis of variance (ANOVA). Levene's test was used to assess for homogeneity of variances across the groups and Welch's correction was applied for non-homogeneous variance. To interrogate differences between each group, a post-hoc pairwise comparison was performed on parameters significantly different on ANOVA testing. The Bonferroni method was used to adjust for potential Type 1 errors in the pairwise comparisons. To determine if potential confounders may explain the significant differences, indexed SVR/TAC and MVR models were adjusted for sex, while diastolic indices, were adjusted for age and sex. A p value < 0.05

was considered statistically significant. Indices not statistically different to healthy subjects have been described as ‘normal’.

7.4 Results

7.4.1 Demographics

The CMR scan was well tolerated by all the children. All subjects had sufficient image quality and none were excluded. Blood results were available in all except in two eHTN subjects (Table 7.1). Some patients (n=12) had blood tests performed greater than 12 months from the CMR scan. However, as clinical status and renal function were stable in all patients, the blood results were deemed reflective of their baseline function. All subjects had eGFR>90 ml/min/1.73 $m^{2,}$ apart from 5 RAS and 3 eHTN patients who had eGFR >74 ml/min/1.73 m^2.

Table 7.1: Demographics and baseline characteristics of study population.

	Controls n=15	RH n=15	eHTN n=15	P-value
Age (years)*	12±1.3	12±1.3	14±1.3	0.11
Sex (% male)	53%	73%	80%	0.26
Height (cm)	156±14	156±18	164±14	0.31
Weight (kg)*	50±1.3	48±1.4	64±1.4§	0.029
Body Mass Index (kg/m^2)	21±2.3	20±3.6	25±5.5	0.07‖
Body Surface Area (m^2)	1.5±0.24	1.5±0.35	1.7±0.34	0.045
Hemoglobin (g/L)	-	129±9.7	141±14	0.017
Hematocrit (L/L)	-	0.37±0.031	0.41±0.04	0.012
Mean Corpuscular Volume (fL)	-	81±3.6	78±8.4	0.77‖
Platelet count ($x10^9/L$)	-	279±76	246±51	0.23
White Cell Count ($x10^9/L$)	-	7.4±2.5	6.9±1.7	0.55

Sodium (mmol/L)	-	143±1.8	142±2.3	0.86
Potassium (mmol/L)*	-	4.2±1.1	4±1.1	0.24
Urea (mmol/L)	-	4.8±0.99	4.3±0.89	0.25
Creatinine (umol/L)	-	51±18	61±14	0.12
Medications (%)				
ACE or AT2 Inhibitor	-	20%	53%	-
Beta-Blocker	-	33%	13%	-
Calcium Channel Blocker	-	40%	53%	-

Data presented as mean ± standard deviation. ⁎- Logarithmic transformation was applied. †- P-value <0.05 when RH compared with controls. ‡ - P-value <0.05 when eHTN compared with controls. §- P-value <0.05 when RH compared to eHTN. ||- ANOVA Welch (W) test was used. Abbreviations: RH=Renovascular hypertension group, eHTN=Essential hypertension group, ACE=Angiotensin converting enzyme, AT2=Angiotensin 2 receptor.

All RH patients had objective evidence of RAS, while 6 had bilateral RAS. Optimal treatment recommended by the MDT had been completed at the time of the CMR scan and none were awaiting any further invasive treatment. All had been treated with angioplasty (7 patients underwent two or more angioplasty attempts), except for 4 who were either medically managed (n=2) or had a unilateral nephrectomy (n=2). In addition, one patient received ethanol embolization of a small branch of the renal artery (RA).

Three patients underwent surgical revascularization; one was successful on the second surgical attempt while two had sub-optimal surgical results and required a nephrectomy (n=1) or optimal medical therapy (n=1). They continued to be followed up either at GOSH or at their local hospital. Prior to recruitment, all patients had been deemed by their clinicians (at the last clinical consultation) to have optimally controlled hypertension with clinically stable BP.

At the time of the CMR, 6 RAS children were no longer on anti-HTN therapy. Of the 9 who received anti-HTN medication, 5 were taking two or more drugs. Other significant medical history is listed in Table 7.2. Of note, two patients had mild mid-aortic syndrome, which was deemed not clinically significant and managed conservatively.

Table 7.2: Associated co-morbidities of study population.

	Associated co-morbidities	No. of patients / (%)
Renovascular Hypertension	Fibromuscular dysplasia	1 (7%)
	Previous embolic stroke	2 (13%)
	Mild mid-aortic arch syndrome	2 (13%)
	Asthma	3 (20%)
	Neurofibromatosis	3 (20%)
	Coeliac disease	1 (7%)
Essential Hypertension	Previous intracerebral bleed	1 (7%)
	C6 complement deficiency	1 (7%)
	Asthma	2 (13%)
	Neurofibromatosis	1 (7%)
	G6PD deficiency	1 (7%)
	Epilepsy	1 (7%)

All eHTN patients had a diagnosis of idiopathic hypertension and received anti-HTN medication, apart for one child whose medication was temporarily stopped for 2 weeks while awaiting an investigation. Five patients were on 2 anti-HTN medications. All eHTN patients (apart from the child awaiting investigation) were deemed to have optimally controlled BP when last reviewed in the outpatient clinic. The healthy subjects had no significant past medical history and were not on any medications.

There was no difference in sex, age or BSA between RAS and controls (Table 7.1). However, weight was significantly greater in the eHTN compared to RAS patients, reflecting the slight preponderance for older boys in primary hypertension.

7.4.2 Vascular function

Systolic and diastolic BP (including SBP and DBP centiles) were significantly elevated in RAS ($p \leq 0.02$) and eHTN ($p \leq 0.003$) compared to controls (Table 7.3). Nevertheless, there was no difference in SBP, DBP and MBP (including BP centiles) between eHTN and RAS ($p > 0.19$).

Table 7.3: Vascular phenotype of study population.

	Controls n=15	RH n=15	eHTN n=15	P-value
SBP (mmhg)	103±11	122±8.4†	129±12‡	<0.001
DBP (mmhg)	52±6.6	63±12†	68±11‡	<0.001
MBP (mmhg)	74±5.9	88±8.6†	93±10‡	<0.001
PP (mmhg)	51±12	59±13	61±9.2	0.058
SBP percentile*	25±2.5	80±1.3†	83±1.3‡	<0.001‖
DBP percentile	22±14	50±31†	56±30‡	<0.001‖
CO (l/min/m^2)*	3.7±1.2	3.6±1.2	4±1.2	0.30
SVR (WU.m^2)*	20±1.2	25±1.3†	23±1.2	0.018
TAC (ml/mmHg. m^2.10^2)	59±14	50±11	45±5.4‡	0.004‖
AoS (%)*	50±1.7	36±1.9	45±1.7	0.30
AoC (cm^2.$mmHg^{-1}$.10^{-2})*	3.2±1.5	1.7±1.5†	2.2±1.5‡	<0.001

Data presented as mean ± standard deviation. *- Logarithmic transformation was applied. †- P-value <0.05 when RH compared with controls. ‡ - P-value <0.05 when eHTN compared with controls. §- P-value <0.05 when RH compared to eHTN. ‖- ANOVA Welch (W) test was used. Abbreviations: RH=Renovascular hypertension group, eHTN=Essential hypertension group, SBP=Systolic blood pressure, DBP=Diastolic blood pressure, MBP=Mean blood pressure, PP=pulse pressure, CO=Cardiac Output, SVR=Systemic vascular resistance, TAC=Total arterial compliance, AoS=Ascending aortic strain, AoC=Ascending aortic compliance.

Systemic vascular resistance was significantly elevated in RAS compared to controls (p≤0.02), as can be seen in Figure 7.1. Total arterial compliance was also mildly reduced compared to controls, although this did not reach statistical significance (p=0.06).

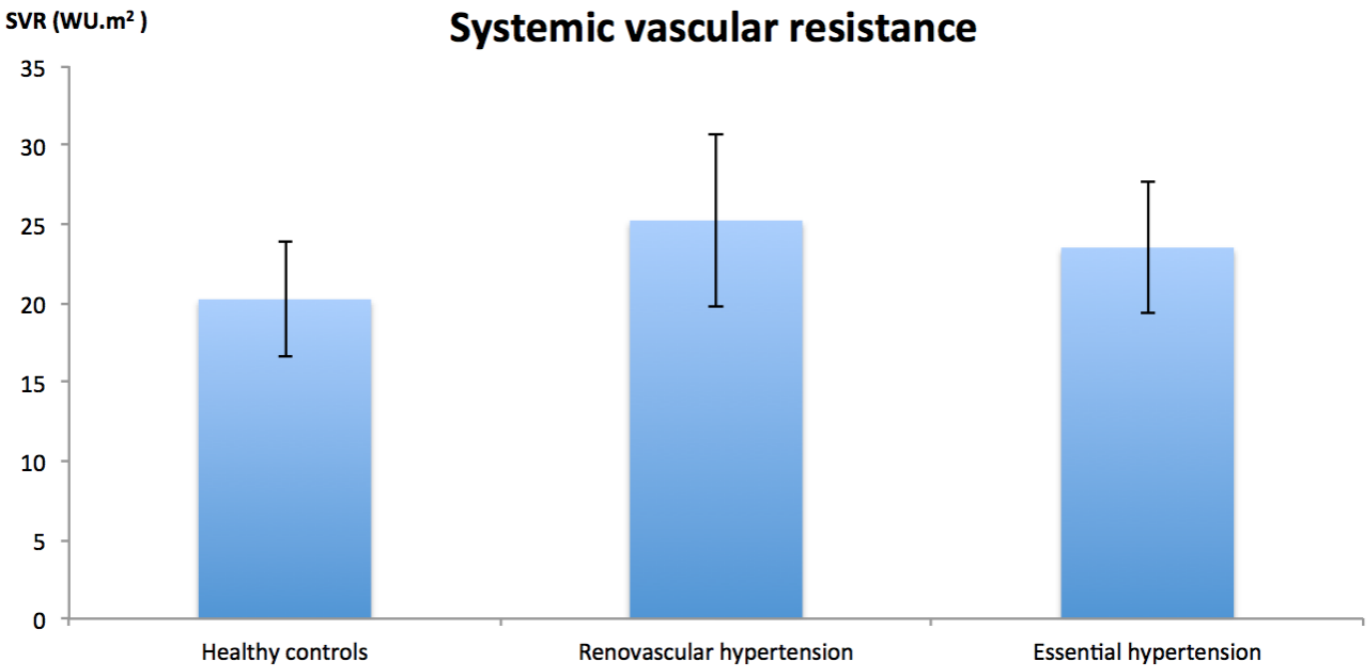

Figure 7.1: Bar chart showing differences in SVR between groups: SVR is significantly (p<0.05) higher in Renovascular hypertension compared to healthy controls. Abbreviations: SVR=systemic vascular resistance.

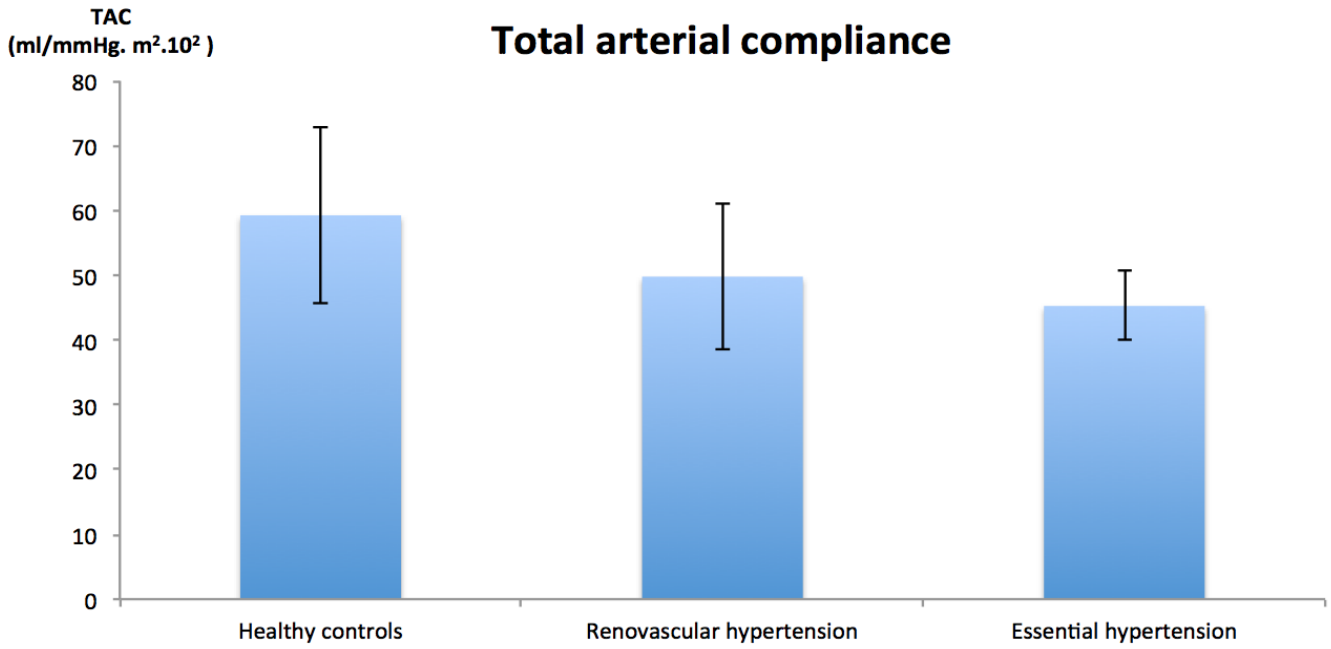

Figure 7.2: Bar chart showing differences in TAC between groups: TAC is significantly ($p<0.05$) lower in eHTN compared to healthy controls. Abbreviations: TAC=total arterial compliance.

Conversely, the eHTN cohort had a significantly lower TAC compared to controls ($p=0.003$), as seen in Figure 7.2. Despite that, there was no statistical difference in TAC or SVR between RAS and eHTN ($p=0.76$, $p=1.00$ respectively). In addition, AoC was significantly lower in RAS and eHTN compared to controls. There were no significant differences in CO, SV or AoS between all groups.

The SVR, TAC and AoC relationships remained significant even after correcting for sex and age.

7.4.3 Cardiac structure and global function

Left ventricular MVR, a marker of LV remodeling, was significantly elevated in RAS and eHTN compared to controls (p=0.04). However, there was no difference between RAS and eHTN (Table 7.4). Although some significance was lost after adjustment for sex, there was still a trend for elevated MVR in the RAS group (p=0.078). Although $LVMHT^{2.7}$ appeared elevated in RAS and eHTN, they did not reach statistical significance (p=0.82, p=0.09) when compared with controls. There were also no differences in EDV and ESV between all groups.

Table 7.4: Left ventricular assessment.

	Controls n=15	RH n=15	eHTN n=15	P-value
LVEDV (ml/m^2)	74±9.4	69±9.3	70±9.3	0.28
LVESV (ml/m^2)	23±4.2	19±7.8	22±5.4	0.14
LVSV (ml/m^2)	51±6.3	49±7.9	48±5.4	0.40
Heart Rate (BPM)	74±13	73±11	85±15§	0.02
$LVMht^{2.7}$ ($g/m^{2.7}$)	23±2.9	25±5.4	27±6.6	0.09
MVR (g/ml)	0.69±0.091	0.81±0.15†	0.83±0.14‡	0.008

Data presented as mean ± standard deviation. ⁎- Logarithmic transformation was applied. †- P-value <0.05 when RH compared with controls. ‡ - P-value <0.05 when eHTN compared with controls. §- P-value <0.05 when RH compared to eHTN. Abbreviations: RH=Renovascular hypertension group, eHTN=Essential hypertension group, LVEDV=Left ventricular end-diastolic volume, LVESV=Left ventricular end-systolic volume, LVSV=Left ventricular stroke volume, LVMHT(2.7)=Left ventricular mass corrected by height to the power of 2.7. MVR=Left ventricular mass volume ratio.

Table 7.5: Left ventricular global systolic and diastolic function assessment.

	Controls n=15	RH n=15	eHTN n=15	P-value
EF (%)	69±3.4	73±9.1	69±4.4	0.46‖
IRT (ms)	64±11	67±11	68±14	0.58
ICT (ms)	47±15	54±27	47±22	0.8‖
Mitral E flow (mls)	47±9.6	57±11†	48±10	0.02861
Mitral A flow (mls)	19±4.2	25±6.6†	23±5.5	0.037
E/A ratio*	2.5±1.2	2.3±1.4	2.1±1.3	0.38
ET (ms)	278±19	276±22	266±15	0.18
Tei	0.4±0.081	0.44±0.13	0.43±0.11	0.54

Data presented as mean ± standard deviation. ⋆- Logarithmic transformation was applied. †- P-value <0.05 when RH compared with controls. ‡ - P-value <0.05 when eHTN compared with controls. §- P-value <0.05 when RH compared to eHTN. ‖- ANOVA Welch (W) test was used. Abbreviations: RH=Renovascular hypertension group, eHTN=Essential hypertension group, EF=Ejection fraction, IRT=Isovolumic relaxation time, ICT=Isovolumic contraction time, E=Early transmitral mean velocity, A=Late transmitral mean velocity, E/A ratio=E to A ratio, ET=Ejection time, Tei=Myocardial performance index.

Global systolic and diastolic function was preserved in RAS and eHTN patients. Left ventricular EF, E/A ratio, isovolumic relaxation time and myocardial performance index were all normal in both groups (Table 7.5).

7.4.4 Myocardial mechanics

There was impairment of longitudinal relaxation in RAS and eHTN (Table 7.6). Longitudinal E'/A' were both similarly reduced in RAS and eHTN ($p \leq 0.035$). In addition, there was a trend towards an elevated E/E' in the RAS group compared to controls ($p=0.098$). The E/E' ratio was significantly lower in eHTN compared to RAS patients ($p<0.001$). There was no impairment of longitudinal systolic function or radial mechanics in the RAS cohort. These differences remained significant even after adjusting for sex and age.

Table 7.6: Myocardial velocity assessment.

	Controls n=15	RH n=15	eHTN n=15	P-value
Rad S' (cm/s)	2.7±0.41	2.6±0.27	2.9±0.27§	0.04
Rad E' (cm/s)	4±0.85	4±0.7	3.8±0.5	0.77
Rad A' (cm/s)	1.3±0.39	1.2±0.4	1.3±0.31	0.68
Long S' (cm/s)*	4.1±1.4	3.3±1.5	3.8±1.2	0.17
Long E' (cm/s)	7.6±1.9	7.3±1.9	9.5±1.7‡§	0.004
Long A' (cm/s)	2.2±0.49	2.7±0.87	3.6±0.76‡§	<0.001
Long E'/A' ratio	3.5±0.7	2.8±0.67†	2.7±0.66‡	0.006
Long E/E' ratio	6.6±2	8.2±2.3	5.3±1.3§	<0.001

Data presented as mean ± standard deviation. ⁎- Logarithmic transformation was applied. †- P-value <0.05 when RH compared with controls. ‡ - P-value <0.05 when eHTN compared with controls. §- P-value <0.05 when RH compared to eHTN. Abbreviations: RH=Renovascular hypertension group, eHTN=Essential hypertension group, Rad=Radial, Long=Longitudinal, S'=Systolic myocardial velocity, E'=Early diastolic myocardial velocity, A'=Late diastolic myocardial velocity, E'/A'=E' over A' ratio, E/E'=E over E' ratio.

7.5 Discussion

In this study, I assessed the cardiovascular effects in optimally treated renovascular hypertension in children. The key findings were: i) The vascular phenotype in paediatric RH was principally defined by an elevated SVR, while essential hypertension was characterized by reduced TAC, ii) Left ventricular remodelling and diastolic impairment was evident in the RAS cohort despite having received optimal treatment, and iii) Left ventricular changes were no different between treated RAS and eHTN children.

It is increasingly recognised that differences in the pattern of HTN is associated with differential mortality risk (114). Systolic and diastolic HTN in young adults, which is associated with an elevated systemic vascular resistance, has been shown to be associated with the highest risk when compared to other patterns of HTN such as isolated systolic HTN (114). Indeed, the pattern of HTN is closely related to the vascular phenotype (115). I found that an elevated SVR was the primary haemodynamic abnormality in renal artery stenosis. In addition, RAS patients were euvolaemic as CO and EDV, surrogates of volume status, were both normal.

Thus, abnormal vascular function is likely to be the main mechanism for elevated BP in RAS. This is consistent with current understanding (116). Renal artery stenosis results in renal ischaemia, which in turn lead to wide ranging maladaptive neurohumoral and vascular responses. Vasoconstriction is primarily mediated through renin-angiotensin-aldosterone axis activation and increased sympathetic activity in renovascular hypertension (116, 117).

An elevated SVR leads to increase in mean intraluminal pressure (i.e. high MBP). Given the viscoelastic properties of the aortic wall, an increase in intraluminal pressure results in aortic wall stiffening (115). This may explain the finding of mildly reduced local aortic compliance (reduced AoC) in the RAS group. Nonetheless, it was not sufficient to cause any discernible effect on TAC. This study demonstrates that vascular phenotype in RAS is different to essential hypertension where increased aortic wall stiffness appears to be the principal feature.

The finding that SVR is high in RAS children despite having received optimal treatment is significant for two reasons. Firstly, it shows that although renovascular hypertension is eminently treatable, it is not completely “reversible”. Given that elevated systolic and diastolic pressures are a predictor of increased CV risk (114), the systolic and diastolic hypertension in RAS suggests that these children may have increased mortality risk. This will need to be investigated in future studies.

Secondly, although treatment of renal artery stenosis removes the most obvious causes of neurohumoral activation, these results indicate that peripheral vasoconstriction persists in treated patients. In most cases, this is likely due to the presence of residual renal lesions not amenable to further invasive procedures, causing persistent neurohumoral activation. However, it is also possible that the vascular remodelling or dysfunction that was present pre-treatment failed to normalize post-treatment. Nevertheless, optimal treatment of RH may require more aggressive use of vasodilators to counteract the elevated SVR.

Finally, the presence of myocardial involvement in RH and eHTN children is important. Although BP was adequately treated (below 90^{th} centile), it remained significantly elevated compared to healthy controls. Consequently, LV remodelling and sub-clinical diastolic impairment were present in both groups and are early markers of hypertensive heart disease (118). This suggests that while current RAS therapies may be effective at reducing BP, it may only mitigate from the worse effects of hypertension. Therefore, these children continue to be at risk of hypertensive heart disease despite receiving treatment. This study provides evidence that children with renovascular hypertension need to be continually followed up and may require more aggressive treatment to achieve a lower target blood pressure.

7.6 Limitations

The main limitation of this study is the limited number of RAS patients. Renal artery stenosis is a relatively rare condition and commonly associated with significant renal impairment and other comorbidities. As renal impairment and other conditions such as significant mid-aortic syndrome were potential confounders, it was important that only a “pure” population of RAS were included into the study. Hence, it was not possible to recruit a large number of RAS children from a single-centre. However, in spite of that, I was able to demonstrate a significant difference in cardiovascular structure and function between RAS and healthy controls. Future studies will need to consider multi-centre recruitment to increase the study population.

7.7 Conclusion

In this study, I have shown that SVR remains a key feature in optimally treated renovascular hypertension in contrast to treated essential hypertension where aortic stiffness is dominant. In addition, these treated children continue to display evidence of diastolic impairment. Future studies are needed to determine if this difference in vascular phenotype may confer a greater CV risk in the long term.

8 The effect of dialysis on cardiovascular function

In this chapter, I will describe the exploratory study I undertook to investigate the potential utility of CMR for the CV assessment of children on dialysis. This involved the comprehensive evaluation of the cardiovascular phenotype in children receiving dialysis and determination of how that may relate with different dialysis modalities.

8.1 Personal contribution

For the study described in this chapter:

- I completed the ethics application process.
- I recruited all subjects.
- I acquired, collated, and tabulated the relevant clinical data.
- I completed the segmentation and data analysis on all study subjects.
- I performed statistical analysis on the study dataset.

8.2 Introduction

Children on dialysis have a high cardiovascular disease burden (119). Cardiovascular mortality is a major cause of death in paediatric end stage renal failure (ESRF). The highest mortality rates are observed in children on maintenance dialysis (4, 120). Unfortunately, there has been minimal

improvement over the past decades (8). This is partly because the CV disease in paediatric ESRF is difficult to identify. One of the obstacles to improving CV outcomes in this population is the lack of good imaging biomarkers to identify early CV impairment and guide treatment.

Conventional measures of global cardiac function such as left ventricular ejection fraction have limited utility as a biomarker as it is frequently normal in dialysis patients (9, 121). Nonetheless, like the pre-dialysis population, dialysis patients also have left ventricular hypertrophy and abnormal systolic and diastolic function (24, 27, 122). Vascular abnormalities such as arterial calcification and stiffness are thought to be particularly marked in dialysis (14, 69, 123). This in turn leads to an increase in afterload causing hypertension (124) and related myocardial effects (125). Thus, accurate measurement of these abnormalities and determining the relationship between vascular and myocardial dysfunction may be especially important in this population.

Two-dimensional echocardiography is used for the cardiac assessment of renal patients. As previously mentioned, ECHO has limitations such as high inter- and intra-observer variability (22) and is unable to perform vascular assessment. Vascular function may be assessed with pulse wave velocity measurement. As such, comprehensive cardiovascular assessment will require multi-modality imaging which is expensive and time-consuming. Furthermore, non-simultaneous acquisition of myocardial and vascular data makes it challenging to investigate the interaction between vascular and myocardial abnormalities.

Cardiac MRI offers significant advantages over ECHO (22), not least the ability to provide simultaneous assessment of vascular and myocardial function. In addition, CMR measures of arterial stiffness such as total arterial compliance also have prognostic value (126). As demonstrated in the pre-dialysis population, new sequences like tissue phase mapping are also able to detect subtle abnormalities. Hence, using CMR to characterise the CV phenotype in the two main forms of dialysis may offer a better insight into the disease process and even yield new potential biomarkers.

The aims of this study are to:

1. Define the cardiovascular characteristic in haemodialysis and peritoneal dialysis population using CMR and,
2. Determine how specific vascular characteristics associated with dialysis may affect myocardial function.

8.3 Methods

8.3.1 Study Population

The study population consisted of four groups of children, patients receiving in-centre haemodialysis (HD) or automated peritoneal dialysis (PD), pre-dialysis end-stage renal failure children and healthy controls. All patients were recruited from Great Ormond Street Hospital renal outpatient clinics, while

healthy children were recruited through hospital advertisements. Recruitment was carried out from June 2015 to October 2016. Exclusion criteria were: i) age <7 or >18 years, ii) congenital structural heart disease or primary myocardial disease, iii) active vasculitis iv) cardiac arrhythmia, v) intercurrent illness, vi) clinical symptoms of heart failure and viii) medical devices precluding CMR.

Medical history and current medications were obtained from medical notes and checked with parents and subjects on the day of the study. The last available blood test (full blood count, urea, creatinine, electrolytes) performed was retrieved for all CKD participants. Renal function was estimated by the modified Schwartz formula to obtain the estimated glomerular filtration rate (eGFR) and CKD stage. To confirm that the healthy controls had no significant medical history, a clinical history (including drug history) was taken from the parents of the healthy children. No blood tests were performed in the healthy cohort.

Haemodialysis patients were treated three times a week, with standard sodium bicarbonate dialysis (Na 138, HCO3 34, K 1.5, Ca 1.25mmol/L) and 0.6-1.4m^2 dialysers, (using either high or medium flux synthetic dialysers). All HD patients underwent CMR between 1-2 hours after their dialysis sessions.

All peritoneal dialysis patients were treated with automated cyclical PD consisting of ten 1-1.5L automated PD exchanges overnight (fill volume between 1.1-1.3L/m^2 using a standard dialysate containing glucose) and a

daytime dwell (dwell volume between 0.6-1.0L/m^2 using a icodextrin (7.5%) dialysis solution), apart from one who was receiving tidal peritoneal dialysis. All PD patients had their CMR scan more than 3 hours after instillation of the daytime dwell fluid.

8.3.2 Study protocol

The study protocol has been previously outlined in detail in Chapter 4. In summary, I performed non-invasive blood pressure measurements, and assessment of left ventricle (SAX LV stack acquisition using KT-SENSE sequence), aortic flow (acquired in ascending aorta using retrospective-gated, spiral SENSE PCMR sequence), cardiac timing (acquired at the LV inflow/outflow SAX position using real-time UNFOLD-SENSE spiral PCMR sequence) and myocardial velocity (acquired in Mid LV SAX position using self-navigated golden-angle spiral TPM sequence). This was used to calculate LV mass and volume, aortic flow, cardiac timing and myocardial velocity measures as described below.

8.3.3 Statistics

Statistical analyses were performed using Stata 13 (StataCorp, College Station, Texas, USA). Data were examined for normality using Shapiro-Wilk normality test and non-normally distributed data was transformed using a zero-skewness log transform to ensure normal distribution prior to analysis. Descriptive statistics were expressed as mean (± standard deviation) or

geometric mean (± geometric standard deviation) if data was log transformed. Chi-squared test was used to determine if sex distribution between groups were different. To assess for CV changes in dialysis patients, comparisons were made with pre-dialysis and healthy subjects. Between group differences were assessed using analysis of variance (ANOVA). Levene's test was used to assess for homogeneity of variances across the groups and Welch's correction was applied for non-homogeneous variance. To determine if potential confounders may explain the significant differences, all significant indices (on ANOVA testing) were adjusted for age and sex. A post-hoc pairwise comparison was not performed, as patient numbers in each group were not sufficient to detect intergroup differences.

Finally, multiple linear regression analysis was undertaken to interrogate the relationship between the significant myocardial mechanics indices (on ANOVA testing) and BP. The models were adjusted for age and sex. Adjusted r^2 statistic was used to assess the goodness of fit. The beta coefficient (β) was used to evaluate the relationship between the dependent variable and the independent factors in the regression model. A p value < 0.05 was considered statistically significant. Indices not statistically different to healthy subjects have been described as 'normal'.

8.4 Results

8.4.1 Demographics

A total of thirty-seven children were recruited: 9 haemodialysis, 8 peritoneal dialysis, 10 pre-dialysis end-stage renal failure patients and 10 healthy controls. There was no difference in sex, age or BSA between the groups (Table 8.1). Of the 9 HD patients, 5 were dialysed via tunneled line and 4 via AV fistula. One patient was awaiting treatment for an AV fistula stenosis and received dialysis via a tunneled line.

At the time of the CMR scan, the HD patients were receiving three sessions of in-centre conventional haemodialysis a week while PD patients received automated cyclical peritoneal dialysis regimen, which consisted of multiple cycles of exchanges overnight and a daytime dwell of (mean dwell volume 938±400mls) instilled from the end of the nocturnal PD session in the morning (The presence of peritoneal dwell volume was confirmed on the scout images taken at the beginning of the CMR scan). All dialysis patients had been on dialysis for greater than 3 months, apart from one HD patient who had only been on HD for a month.

Table 8.1: Demographics and baseline characteristics of study population.

	Controls n=10	CKD stage 5 n=10	HD n=9	PD n=8	P-value
Age (years)	12±2.4	13±3.7	11±3	12±3.8	0.73
Sex (% male)	60%	50%	56%	38%	0.81
Height (cm)	159±12	145±21	137±18	142±27	0.11
Weight (kg)*	49±1.3	41±1.5	33±1.3	35±1.6	0.086
Body Mass Index (kg/m^2)	19±2.3	20±2.9	18±3	18±1.7	0.28
Body Surface Area (m^2) *	1.5±1.2	1.3±1.3	1.1±1.2	1.2±1.4	0.092
Hemoglobin (g/L)	-	127±11	115±21	119±15	0.29
Hematocrit (L/L)	-	0.37±0.03	0.34±0.06	0.35±0.04	0.39
Mean Corpuscular Volume (fL)	-	84±4	84±11	85± 6.5	0.90
Platelet count ($x10^9/L$)	-	248±64	225±51	247±53	0.64
White Cell Count ($x10^9/L$)	-	8.4±2.4	5.7±2.1	7.4±2.3	0.051

Sodium (mmol/L)	-	142±2.7	138±7.2	139±2.7	0.20
Potassium (mmol/L)	-	4.3± 0.4	4.7±1.2	4.2± 0.49	0.83†
Urea (mmol/L)	-	21±4	15±10	13±2	<0.001†
Creatinine (umol/L)	-	387±109	553±350	643±328	0.26†
Medications (%)					
ACE or AT2 Inhibitor	-	10%	0%	25%	-
Beta-Blocker	-	30%	0%	13%	-
Calcium Channel Blocker	-	20%	0%	13%	-

Data presented as mean ± standard deviation. ⁎- Logarithmic transformation was applied. †-ANOVA Welch (W) test was used. Abbreviations: CKD=Chronic kidney disease, HD= Haemodialysis group, PD=Peritoneal dialysis group, ACE=Angiotensin converting enzyme, AT2=Angiotensin 2 receptor.

The duration of current treatment with renal replacement therapy was an average of 30 months (30±27months) in HD and average of 9 months (9±5months) in PD. All PD patients did not receive any previous RRT prior to current PD apart from 2 patients (1 had a previous failed renal transplant and 1 received 5 months of HD prior to starting current PD). In contrast, the majority of HD patients (n=6) had previous failed renal transplants and also received either HD or PD prior to their transplant. Only two did not have any renal replacement therapy (RRT) prior to current HD regimen, while one received PD for 1 month prior to commencing HD.

All pre-dialysis CKD patients had eGFR ≤20ml/min/1.73 m^2. The renal disease aetiology (or reason for dialysis) and significant co-morbidities in the groups are summarised in Table 8.2. None of the healthy controls had any significant past medical history and were not on any medications.

The CMR scan was well tolerated by all the children. All subjects had sufficient image quality and none were excluded apart from mitral inflow velocity data in a PD patient where EA merging due to tachycardia meant that EA velocity could not be accurately assessed. Blood results were available in all subjects apart from the healthy controls. These are summarised in Table 8.1.

Table 8.2: Summary of renal diagnosis and co-morbidities in the study population.

	Renal diagnosis/ Reason for dialysis	No. of patients / (%)	Co-morbidities	No. of patients / (%)
Haemodialysis	Previous transplant failure	6(67%)	Asthma	1(11%)
			Human immunodeficiency virus	1(11%)
	Miscellaneous causes	3 (33%)	Ventriculo-peritoneal shunt	1(11%)
			Previous hyperthyroidism	1(11%)
Peritoneal dialysis	CAKUT	2(25%)	Nil	
	Renal dysplasia	2(25%)		
	Focal segmental glomerulosclerosis	3(38%)		
	Nephrolithiasis	1(7%)		
Pre-dialysis CKD	CAKUT	4(44%)	Asthma	1(11%)
	Renal dysplasia	2(22%)		
	Miscellaneous causes	4 (44%)		

8.4.2 Vascular function

Blood pressure was significantly elevated in dialysis groups compared to healthy controls. Diastolic and mean BP were similarly elevated in all CKD groups, with a trend towards an increased SBP (p=0.068) (Table 8.3). This pattern was also reflected by elevated SBP and DBP centiles. However, there was no difference in PP between the groups.

Systemic vascular resistance was significantly elevated in the dialysis groups, with the greatest SVR observed in the PD population (p=0.004). Conversely, there was no difference in total arterial compliance between the groups (p=0.71). There was also no significant difference in measures of local (ascending) aorta stiffness like AoC or AoS. Although CO was lower in both dialysis groups, this did not reach statistical significance (Table 8.3). However, stroke volume was significantly lower in dialysis cohorts with the lowest SV observed in the PD group.

Both SVR and SV remained significantly associated with dialysis modality even after correcting for sex and age.

Table 8.3: Vascular phenotype of study population.

	Controls n=10	CKD stage 5 n=10	HD n=9	PD n=8	P-value
SBP (mmhg)	104±9.6	118±15	122±19	117±16	0.068
DBP (mmhg)	50±5.4	72±12	76±14	75±16	<0.001†
MBP (mmhg)*	73±1.1	89±1.1	93±1.2	90±1.2	<0.001†
PP (mmhg)	54±13	47±12	46±10	43±9.6	0.22
SBP percentile*	28±2.2	70±1.6	83±1.4	81±1.2	0.008†
DBP percentile*	12±2	64±1.8	78±1.4	67±1.8	<0.001
CO ($l/min/m^2$)*	4±1.2	3.5±1.2	3.6±1.2	3.3±1.3	0.30
SVR ($WU.m^2$)	19±3.7	26±4	27±9.6	29±9.4	0.004†
TAC ($ml/mmHg.\ m^2$)*	0.56±1.4	0.61±1.3	0.59±1.3	0.53±1.3	0.71
AoS (%)*	49±1.4	56±1.6	45±1.7	40±1.9	0.53
AoC ($cm^2.mmHg^{-1}.10^{-2}$)	3.4±1.1	3.4±1.2	3.2±1.2	2.9±1.4	0.81

Data presented as mean ± standard deviation. *- Logarithmic transformation was applied. †-ANOVA Welch (W) test was used. Abbreviations: CKD=Chronic kidney disease, HD= Haemodialysis group, PD=Peritoneal dialysis group, SBP=Systolic blood pressure, DBP=Diastolic blood pressure, MBP=Mean blood pressure, PP=Pulse pressure, CO=Cardiac output, SVR=Systemic vascular resistance, TAC=Total arterial compliance, AoS=Ascending aortic strain, AoC=Ascending aortic compliance.

8.4.3 Cardiac structure and global function

Left ventricular EDV and ESV were lower in the dialysis groups with the lowest seen in the PD patients ($p<0.01$). There was no significant LV hypertrophy in the dialysis groups (Table 8.4). There was also no difference in global systolic function, i.e. EF (Table 8.5).

There was evidence of diastolic dysfunction (Table 8.5). The E/A ratio was significantly lower in dialysis patients (lowest E/A ratio seen in PD patients). However, the significance was lost after correcting for age and sex. There was also a trend towards increased IRT ($p=0.09$) and myocardial performance index ($p=0.095$), with the most marked changes seen in the PD cohort.

8.4.4 Myocardial mechanics

Radial and longitudinal systolic velocity was impaired in all CKD groups ($p\leq0.002$). However, there was no apparent difference in systolic velocities between HD and pre-dialysis groups. Conversely, PD patients displayed the lowest radial and longitudinal systolic velocities (Table 8.6).

Similarly, impairment in early radial and longitudinal relaxation was evident in the CKD groups ($p\leq0.003$), with the most marked reduction seen in the PD cohort. There was no difference in late diastolic relaxation velocity (A') between the groups. Consequently, longitudinal E'/A' was reduced in both HD and PD groups ($p\leq0.003$).

Table 8.4: Left ventricular structure assessment.

	Controls n=10	CKD stage 5 n=10	HD n=9	PD n=8	P-value
LVEDV (ml/m^2)*	76±1.2	64±1.1	66±1.2	52±1.2	<0.001
LVESV (ml/m^2)*	24±1.3	18±1.3	20±1.2	16±1.3	0.01
LVSV (ml/m^2)	52±6.9	45±6.2	46±8.7	36±5.4	<0.001
$LVMht^{2.7}$ ($g/m^{2.7}$)	22±3.8	25±4.7	23±3.7	20±1.9	0.08
RAA (cm^2/m^2)	12±1.9	11±1.2	12±1.4	10±2.3	0.078
LAA (cm^2/m^2)*	12±1.3	11±1.2	12±1.2	11±1.3	0.61

Data presented as mean ± standard deviation. *- Logarithmic transformation was applied. Abbreviations: CKD=Chronic kidney disease, HD= Haemodialysis group, PD=Peritoneal dialysis group, LVEDV=Left ventricular end-diastolic volume, LVESV= Left ventricular end-systolic volume, LVSV= Left ventricular stroke volume, LVMht(2.7)=Left ventricular mass indexed to height to the power of 2.7, RAA=Right atrial area, LAA=Left atrial area.

Table 8.5: Left ventricular global systolic and diastolic function assessment.

	Controls n=10	CKD stage 5 n=10	HD n=9	PD n=8	P-value
EF (%)*	67±1.1	71±1.1	69±1.1	68±1.1	0.67
IRT (ms)	62±11	72±8.8	73±17	84±21	0.092†
ICT (ms)	48±23	33±15	37±21	48±21	0.27
Mitral E flow (mls)*	46±1.2	48±1.2	49±1.4	34±1.4	0.049
Mitral A flow (mls)	20±4.2	23±3.5	24±6.4	22±3.6	0.28
E/A ratio*	2.4±1.2	2.1±1.2	2.1±1.5	1.5±1.4	0.048
ET (ms)	271±15	277±19	265±30	249±30	0.11
Tei	0.41±0.1	0.38±0.085	0.43±0.16	0.54± 0.17	0.095

Data presented as mean ± standard deviation. ⁎- Logarithmic transformation was applied. †-ANOVA Welch (W) test was used. Abbreviations: CKD=Chronic kidney disease, HD= Haemodialysis group, PD=Peritoneal dialysis group, EF=Ejection fraction, IRT=Isovolumic relaxation time, ICT=Isovolumic contraction time, E flow=Early diastolic flow, A flow=Late diastolic flow, ET=Ejection time, Tei=Myocardial performance index.

Table 8.6: Myocardial velocity assessment.

	Controls n=10	CKD stage 5 n=10	HD n=9	PD n=8	P-value
Rad S' (cm/s)	2.8±0.33	2.4±0.28	2.4±0.35	2.2±0.42	0.0078
Rad E' (cm/s)	4.4±0.57	3.3±0.52	3.0±0.63	2.9±0.52	<0.001
Rad A' (cm/s)*	1.4±1.3	1.2±1.3	1.2±1.4	1.3±1.3	0.54
Long S' (cm/s)*	4.8±1.3	3.0±1.5	2.9±1.4	2.8±1.2	0.002
Long E' (cm/s)	7.9±1.1	6.7±1.6	5.5±2.2	5.1±1.3	0.003
Long A' (cm/s)	2.1±0.5	2.6±0.72	2.5±0.99	2.6±0.76	0.45
Long E'/A' ratio	3.8±0.94	2.6±0.58	2.4±1.0	2.2±1.2	0.003
Long E/E' ratio	5.9±0.87	7.7± 2.7	10± 4.1	7.4±2.0	0.015

Data presented as mean ± standard deviation. *- Logarithmic transformation was applied. Abbreviations: CKD=Chronic kidney disease, HD= Haemodialysis group, PD=Peritoneal dialysis group, Rad=Radial, Long=Longitudinal, S'=Peak systolic velocity, E'=Early diastolic velocity, A'=Late diastolic velocity, E'/A'=Ratio of E' over A', E/E' ratio=Ratio of early diastolic mitral flow to early diastolic myocardial velocity.

In addition, E/E', a surrogate marker of LV end-diastolic pressure, was elevated in the CKD groups. Notably, it was highest in the HD patients rather than in PD patients. All these differences remained significant even after adjusting for sex and age.

8.4.5 Relationship between vascular & myocardial function

Radial and longitudinal systolic and early diastolic velocities were all inversely related to BP (SBP, DBP and MBP), after adjusting for age and sex. There was also an inverse association between longitudinal E'/A' ratio and BP, independent of age and sex. There was no association between longitudinal E/E' ratio and BP.

When only dialysis patients were included into the regression models, only the early relaxation velocities remained negatively associated with DBP and MBP. Longitudinal E'/A' ratio was inversely associated with MBP but not to SBP or DBP. There were no significant associations between any other myocardial mechanics indices and BP. (Table 8.7).

Table 8.7: Relationship between blood pressure and myocardial mechanics.

(Only dialysis population included into model, n=17)

	DBP			**MBP**		
	β-coefficient	P-value	Regression Model Adjusted-R^2	β-coefficient	P-value	Regression Model Adjusted-R^2
Rad E’	-16.7	0.001	0.63	-14.9	0.004	0.61
Long E’	-5.25	0.001	0.68	-4.44	0.004	0.60
Long E’/A’ ratio	-5.88	0.07	0.36	-7.09	0.004	0.44

Models were adjusted for age, and sex. Abbreviations: Rad=Radial, Long=Longitudinal, E’=Early diastolic velocity, A’=Late diastolic velocity, DBP=Diastolic blood pressure, MBP=Mean blood pressure.

8.5 Discussion

This is the first study to comprehensively assess associations between cardiovascular measures and dialysis in children using novel CMR sequences. Our key findings were: i) SVR was elevated in both dialysis groups but was highest in peritoneal dialysis, ii) Systolic and diastolic impairment was evident in dialysis patients and was most marked in peritoneal dialysis, and iii) There was an independent and inverse relationship between DBP and MBP with myocardial diastolic function in children on dialysis.

8.5.1 Vascular effects of dialysis

Hypertension is common in children on long-term dialysis (127) and its determinants are multi-factorial. Volume overload is undoubtedly an important factor (128, 129). Its contribution to high BP will vary at different times due to wide fluctuations in intravascular volume between dialysis sessions (129). Other key factors are thought to be arterial stiffness (i.e. low arterial compliance) and elevated SVR (13). However, their relative significance is unclear in the dialysis population. In order to determine this, the children were studied after dialysis in this study. To the best of my knowledge, this study is the first to simultaneously assess the key determinants of BP in a paediatric dialysis cohort using CMR.

As expected, preload was decreased in both dialysis cohorts, indicated by reduced EDV and SV. This was most marked in PD patients as they had a dwell volume in the peritoneum causing increase intra-abdominal pressure, in turn leading to reduced preload from reduced venous return (130). Despite that, elevated BP was present in HD and PD patients. Neither cardiac output nor aortic compliance was abnormal, indicating that volume overload and arterial stiffness were not important factors in the post-dialytic setting. Instead, an increased SVR was the only significant finding in both groups. This suggests that SVR may be the most likely explanation for elevated BP post-dialysis.

However, there are two caveats to this statement. Firstly, there are other methods to assess arterial stiffness apart from TAC. Numerous studies have documented abnormal stiffness in paediatric dialysis population using pulse wave velocity (45, 131, 132). As this was not recorded in this study, arterial stiffness may be present on PWV measurement and could be an important determinant of hypertension.

Secondly, vascular stiffness and SVR are dependent on loading conditions. Arterial stiffness is known to be increased in fluid overloaded dialysis patients (123, 133). The viscoelastic properties of arterial walls are such that the vessels become stiffer as they stretch. However, a low preload may be associated with increased SVR (86). It is likely that dialysis children in this study had a low preload as indicated by reduced EDV. If the children had been scanned before their dialysis session and were in an “overloaded” state,

abnormal TAC may have been a more prominent feature. Indeed, arterial stiffness may play a more important role in “overloaded” patients who are hypertensive before their dialysis session. This will need to be investigated in future studies.

In healthy individuals, afterload increases (i.e. vasoconstriction) to maintain ‘normal’ physiological blood pressure in a low preload state. The dialysis patients in this study had low preload, high SVR but an elevated BP, instead of ‘normal’ BP. This may reflect a resetting of baroreceptor reflex as seen in chronic essential hypertension (134). Nonetheless, my findings highlight that in children post-dialysis, raised SVR appears to be the key contributor to increased afterload and BP.

It is well recognised that there is a subset of haemodialysis patients that experience intra- or post-dialytic hypertension (135). This is associated with a worse CV mortality (136). Although the reasons for this are not known, its pathogenesis is thought to be complex and include mechanisms like sympathetic overactivity, renin-angiotensin system activation, endothelial dysfunction, and clearance of anti-hypertensive medications leading to increased vasoconstriction post-dialysis (135). The HD patients in this study do not fulfil the criteria for post-dialytic hypertension. Nevertheless, the observation of elevated post-dialysis BP (compared to controls) and raised SVR in these children is consistent with above mechanisms and may represent a “pre-hypertensive” phenotype. Further research is needed to

investigate how or if underlying elevation in SVR may lead to subsequent development of post-dialytic hypertension in haemodialysis.

Interestingly, the greatest SVR was observed in peritoneal dialysis. This finding is in keeping with other studies that used different methodologies and also demonstrated increased SVR in peritoneal dialysis (137, 138). Blood pressure and SVR has been shown to acutely rise on instillation of PD fluid. The exact cause for this is unclear. However, several explanations have been proposed such as, impaired baroreceptor sensitivity associated with instillation of glucose containing peritoneal dialysate fluid (139), compression of mesenteric vessels secondary to filling of the peritoneal cavity and the cooling effect of the dialysate fluid inducing mesenteric vasoconstriction (140). The PD patients were all scanned more than three hours after instillation of PD fluid. Any acute cooling effect arising from instillation of dialysate fluid would be negligible. The daytime dwell consisted of icodextrin containing dialysate in all patients, rather than glucose containing fluid. While glucose containing dialysates can cause impaired baroreceptor response, icodextrin dialysates have less of an effect as it is “glucose-sparing” and does not induced the hyperglycaemic and hyperinsulinaemic response thought to be responsible (141). Hence, I believe the most likely cause of raised SVR in PD is the compression effect of peritoneal dialysate fluid on the mesenteric arteries. Indeed, an increase in dialysate dwell volume has been demonstrated to be significantly associated with an increase in SVR (142). The presence of a dwell volume in situ throughout the day may mean that PD

patients are subjected to greater afterload for a prolonged duration. This in turn may contribute to adverse consequences on the myocardium.

8.5.2 Association between dialysis and myocardial measures

The finding of sub-clinical systolic and diastolic impairment is consistent with previous ECHO studies in both adults (143-145) and paediatric (146, 147) dialysis populations. This study confirms that subtle myocardial impairment is present in children on dialysis despite the absence of traditional cardiovascular risk factors typically seen in adults.

Reduced longitudinal systolic function is often the first indicator of sub-clinical impairment and may be accompanied by compensatory increase in radial function to preserve global LV function (121). In this study, both longitudinal and radial systolic mechanics were reduced in dialysis patients but EF remained preserved. This suggests impairment of myocardial mechanics in dialysis may be counteracted by other compensatory mechanisms in order to maintain global function. It is unclear from this study what these mechanisms are. However, one possibility is the compensatory increase in LV rotational function, which has been observed in patients with heart failure with preserved ejection fraction (148). This is worth investigating further in future studies.

Notably, myocardial impairment was most marked in the PD patients. This is slightly surprising as peritoneal dialysis is widely believed to have theoretical

advantages compared with HD, such as superior haemodynamic stability from continuous fluid removal, better clearance of medium sized uraemic toxins and less systemic inflammation (140, 149). Peritoneal dialysis also does not result in myocardial stunning due to the absence of intra-dialytic hypotension (150). In contrast, haemodialysis induces transient myocardial ischaemia through various mechanisms such as HD related hypotension and ultrafiltration related factors (151). The HD cohort in this study had also been receiving dialysis for a longer duration than the PD cohort, which meant greater exposure to repeated intra-dialytic ischaemic insults. Despite this, myocardial function appeared comparatively worse in PD patients. Part of this may be explained by the recovery of LV function in the HD cohort by the time of CMR scan. Myocardial stunning largely resolves within 30 minutes after dialysis (152, 153). This means LV function would have had sufficient time to recover back to baseline as CMR was performed one-hour post haemodialysis.

My findings suggest that the effect of increased afterload on the myocardium may be an important factor in dialysis related LV impairment, particularly in peritoneal dialysis. Previous studies have found that afterload (including both non-pulsatile and pulsatile components, measured by SVR and PWV respectively) is inversely related to myocardial function. This has been shown in hypertensive adults (125) and in larger cohorts such as the Framingham Heart Study (154). This study is the first to demonstrate a significant relationship between impaired LV relaxation and diastolic (and mean) blood pressure in children on dialysis. Thus, it is perhaps unsurprising that SVR was

greatest in the PD cohort while diastolic (and systolic) function was also the lowest.

However, it is important to point out that myocardial velocity, like SVR and BP, is preload dependent. This means that preload may be an important confounder in this relationship. Indeed, a low preload can be associated with reduced E' (155) and increased afterload (86) (Figure 8.1). More research is needed to understand how different preload conditions may affect the relationship between afterload and myocardial function. This study only looked at the relationship at a single time point (i.e. post-dialysis). Future work examining how this relationship changes during haemodialysis or with different dwell volumes in PD patients may be useful.

The acute effects of dialysis on the CV system have been relatively well described. Conversely, the long-term CV impact of these changes remains unclear. Survival differences between haemodialysis and peritoneal dialysis have been difficult to determine as different studies have produced conflicting results (156). Nonetheless, there is a general consensus PD survival is broadly similar to HD in the long-term (157, 158). The present findings suggest that the short-term effects of PD on the CV system may not be as benign as currently believed. Future studies are needed to examine if chronically increased afterload may translate to CV changes and increased long-term risk in peritoneal dialysis.

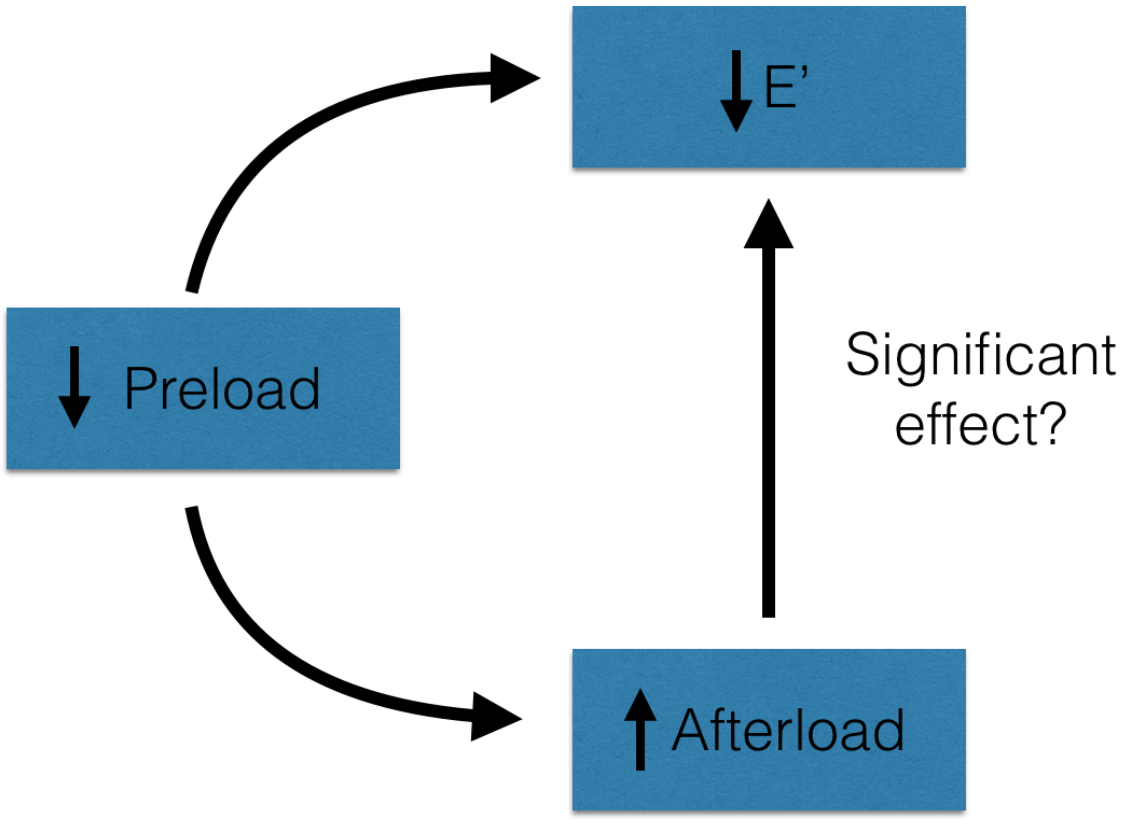

Figure 8.1: Confounding effect of preload: Is there a significant relationship between E' and afterload (Blood pressure/systemic vascular resistance), independent of pre-load? Abbreviations: E'=early diastolic myocardial velocity.

8.6 Limitations

The main limitation is the relatively small number of dialysis patients recruited into the study. Recruitment of these children was difficult. Given the rarity of paediatric end stage renal failure, there was a limited population of children available for recruitment in a single centre study. Furthermore, the high psychosocial and care burden associated with their condition meant that many of the children and families were reluctant to take part in research that required more hospital visits. In order to overcome that, we minimised inconvenience to patients by organising the CMR to coincide with outpatient appointments (in PD and pre-dialysis patients) and after their in-hospital dialysis sessions for HD patients. Despite the small numbers recruited, we were able to show differences in cardiovascular indices between the groups (although this study was not adequately powered to make a direct post-hoc comparison between dialysis modalities). Future studies will require multi-centre recruitment in order to increase study numbers.

8.7 Conclusion

In this study, I have found that elevated SVR and myocardial impairment is present in children on dialysis. Furthermore, SVR may be associated with myocardial impairment. Future studies are needed to investigate how vascular properties may vary between dialysis sessions as loading conditions changes. In addition, further investigation into how this in turn affects myocardial function is also required to better understand the impact of dialysis on myocardial function.

9 Conclusion and future work

9.1 Summary

Efforts to reduce cardiovascular risk in paediatric CKD have had minimal success over the past few decades. Identifying high-risk patients is difficult as conventional methods of cardiovascular assessment have limitations. Cardiovascular magnetic resonance imaging has numerous advantages and may be a more valuable tool for clinical assessment in this population. In this thesis, I investigated the utility of CMR for the cardiovascular phenotyping of pre-dialysis CKD in children. In addition, I also conducted two smaller exploratory studies on dialysis and renovascular hypertension children.

Using CMR, I was able to elicit clinically important findings in children with renal disease. Importantly, it did not require the use of MRI contrast, which is both unpleasant for children and contraindicated in CKD. The combination of sensitivity of novel CMR techniques like tissue phase mapping with precision of conventional sequences has made it an effective tool for the detection of subtle abnormalities. The other key advantage of the sequences used is the speed of acquisition. This enabled comprehensive cardiovascular assessment to be performed swiftly. All of this together helped improve the overall patient experience and made it a much more tolerable investigation for children.

9.2 Myocardial abnormalities in paediatric renal disease

A key aspect of this study was the novel detection of sub-clinical systolic and diastolic impairment with CMR. The ability to measure radial and longitudinal function allowed a detailed assessment of uraemic cardiomyopathy. Future studies should investigate how impairment in myocardial mechanics may evolve with disease progression. Larger studies are also needed to confirm the findings of this small exploratory study on dialysis patients. Examining how these parameters may change in dialysis may be helpful for a better understanding of the acute effect of haemodialysis on myocardial mechanics. This may help to improve current management of dialysis related complications such as myocardial ischaemic insults secondary to intra-dialytic hypotension.

Abnormalities in radial and longitudinal myocardial velocity are likely to be an early manifestation of myocardial involvement, as they appear to precede the development of LVH. Thus, myocardial velocity measured with tissue phase mapping may have a role as a potential imaging biomarker in the future. At present, there are no established normative values for myocardial velocity in children. This will need to be established. In the future, large prospective studies with long-term follow up are required to determine the prognostic significance of these indices and its ability to predict cardiovascular risk.

9.3 Role of systemic vascular resistance in hypertension in CKD

Although the mechanism for hypertension in CKD is multi-factorial, arterial stiffness is widely believed to be the key component in paediatric CKD. Previous studies have found evidence of increased arterial stiffness, which is consistent with the calcium and phosphate dysregulation and vascular remodelling so frequently seen in this population. Nonetheless, the role of arterial stiffness in the pathogenesis of hypertension is uncertain, even though it may be present. In this thesis, I have shown that it is possible to assess the key components of hypertension simultaneously using CMR in order to determine their relative importance.

Systemic vascular resistance appears to be the most important determinant of hypertension in renal disease in children. This suggests that treatment resistant hypertension in paediatric CKD or renovascular hypertension may be due to a significantly elevated SVR. Further investigation is needed to confirm this. If so, hypertension treatment in this population may be further optimised by therapies that reduce SVR, such as systemic vasodilators. Furthermore, SVR, measured by CMR, may also serve as a potential target to guide management of patients, particularly in resistant hypertension.

Although the dialysis study was exploratory in nature and the numbers were small, the markedly elevated SVR and its association with diastolic dysfunction in peritoneal dialysis were particularly interesting. My findings suggest that the daytime dwell volume may be an important factor, but preload may also be a confounding factor. Larger studies are needed to better understand how preload can affect SVR and if this may have any significant long-term consequences on the myocardium. If so, more work needs to be done to look at how this can be mitigated (such as studying if changing dwell volumes may reduce SVR).

The investigations in this thesis were limited to a cross-sectional evaluation of the determinants of hypertension at a single time point. However, these haemodynamic factors may change as the disease progresses, not least due to fluid accumulation in end stage disease. Understanding how this may evolve will allow clinicians to better tailor treatment to patients at different disease stages.

There are many different causes of elevated SVR in CKD. The relative significance of these mechanisms is uncertain. Future studies may combine CMR haemodynamic measures with other biomarkers (e.g. neurohumoral) to better understand the pathogenesis of raised SVR in CKD and renovascular hypertension. This may be useful for designing future therapies to effectively target key pathological mechanisms at a biochemical level.

The effect of aortic compliance on blood pressure does not appear to be important in paediatric renal disease. Nonetheless, the influence of arterial stiffness on afterload cannot be discounted. In fact, characteristic impedance is one of the key elements determining blood pressure (the other two being SVR and arterial compliance in the 3-element Windkessel model (85)). There is increasing recognition that arterial impedance, i.e. resistance to oscillatory flow, is an important factor in hypertension (159). Thus, methods for impedance analysis such as pulse wave velocity measurement will continue to be an important part of cardiovascular assessment. New CMR protocols have been developed that allow PWV measurements and have been used to demonstrate abnormal vascular function following coarctation of aorta repair (160). Future studies may incorporate this protocol to provide an even more comprehensive evaluation of vascular function in paediatric CKD.

9.4 Conclusion

In conclusion, CMR is a useful tool for the cardiovascular assessment of children with renal disease. The unique findings of vascular dysfunction and sub-clinical myocardial impairment in paediatric renal disease using CMR have clinically significant implications. Future studies are needed to determine the prognostic significance of these abnormalities and to evaluate its utility as potential imaging biomarkers.

10 References

1. Go AS, Chertow GM, Fan D, McCulloch CE, Hsu CY. Chronic kidney disease and the risks of death, cardiovascular events, and hospitalization. N Engl J Med. 2004;351(13):1296-305.

2. Collins AJ, Foley RN, Gilbertson DT, Chen SC. United States Renal Data System public health surveillance of chronic kidney disease and end-stage renal disease. Kidney Int Suppl (2011). 2015;5(1):2-7.

3. Sarnak MJ, Levey AS, Schoolwerth AC, Coresh J, Culleton B, Hamm LL, et al. Kidney disease as a risk factor for development of cardiovascular disease: a statement from the American Heart Association Councils on Kidney in Cardiovascular Disease, High Blood Pressure Research, Clinical Cardiology, and Epidemiology and Prevention. Circulation. 2003;108(17):2154-69.

4. Mitsnefes MM. Cardiovascular disease in children with chronic kidney disease. J Am Soc Nephrol. 2012;23(4):578-85.

5. Harambat J, van Stralen KJ, Kim JJ, Tizard EJ. Epidemiology of chronic kidney disease in children. Pediatr Nephrol. 2012;27(3):363-73.

6. Shroff R, Weaver DJ, Jr., Mitsnefes MM. Cardiovascular complications in children with chronic kidney disease. Nat Rev Nephrol. 2011;7(11):642-9.

7. Ronco C, Haapio M, House AA, Anavekar N, Bellomo R. Cardiorenal syndrome. J Am Coll Cardiol. 2008;52(19):1527-39.

8. Chirakarnjanakorn S, Navaneethan SD, Francis GS, Tang WH. Cardiovascular impact in patients undergoing maintenance hemodialysis: Clinical management considerations. Int J Cardiol. 2017;232:12-23.

9. Makar MS, Pun PH. Sudden Cardiac Death Among Hemodialysis Patients. Am J Kidney Dis. 2017;69(5):684-95.

10. Mitsnefes M, Flynn J, Cohn S, Samuels J, Blydt-Hansen T, Saland J, et al. Masked hypertension associates with left ventricular hypertrophy in children with CKD. J Am Soc Nephrol. 2010;21(1):137-44.

11. Flynn JT, Mitsnefes M, Pierce C, Cole SR, Parekh RS, Furth SL, et al. Blood pressure in children with chronic kidney disease: a report from the Chronic Kidney Disease in Children study. Hypertension. 2008;52(4):631-7.

12. Wong H, Mylrea K, Feber J, Drukker A, Filler G. Prevalence of complications in children with chronic kidney disease according to KDOQI. Kidney Int. 2006;70(3):585-90.

13. Hadtstein C, Schaefer F. Hypertension in children with chronic kidney disease: pathophysiology and management. Pediatr Nephrol. 2008;23(3):363-71.

14. Mitsnefes MM, Kimball TR, Kartal J, Witt SA, Glascock BJ, Khoury PR, et al. Cardiac and vascular adaptation in pediatric patients with chronic kidney disease: role of calcium-phosphorus metabolism. J Am Soc Nephrol. 2005;16(9):2796-803.

15. Drazner MH. The progression of hypertensive heart disease. Circulation. 2011;123(3):327-34.

16. Wilson AC, Mitsnefes MM. Cardiovascular disease in CKD in children: update on risk factors, risk assessment, and management. Am J Kidney Dis. 2009;54(2):345-60.

17. Lieb W, Gona P, Larson MG, Aragam J, Zile MR, Cheng S, et al. The natural history of left ventricular geometry in the community: clinical correlates and prognostic significance of change in LV geometric pattern. JACC Cardiovasc Imaging. 2014;7(9):870-8.

18. Halbach S, Flynn J. Treatment of hypertension in children with chronic kidney disease. Curr Hypertens Rep. 2015;17(1):503.

19. Kupferman JC, Aronson Friedman L, Cox C, Flynn J, Furth S, Warady B, et al. BP control and left ventricular hypertrophy regression in children with CKD. J Am Soc Nephrol. 2014;25(1):167-74.

20. Matteucci MC, Wuhl E, Picca S, Mastrostefano A, Rinelli G, Romano C, et al. Left ventricular geometry in children with mild to moderate chronic renal insufficiency. J Am Soc Nephrol. 2006;17(1):218-26.

21. Pierdomenico SD, Di Nicola M, Pierdomenico AM, Lapenna D, Cuccurullo F. Cardiovascular risk in subjects with left ventricular concentric remodeling at baseline examination: a meta-analysis. J Hum Hypertens. 2011;25(10):585-91.

22. Hoffmann R, Barletta G, von Bardeleben S, Vanoverschelde JL, Kasprzak J, Greis C, et al. Analysis of left ventricular volumes and function: a multicenter comparison of cardiac magnetic resonance imaging, cine ventriculography, and unenhanced and contrast-enhanced two-dimensional and three-dimensional echocardiography. J Am Soc Echocardiogr. 2014;27(3):292-301.

23. Chinali M, Matteucci MC, Franceschini A, Doyon A, Pongiglione G, Rinelli G, et al. Advanced Parameters of Cardiac Mechanics in Children with CKD: The 4C Study. Clin J Am Soc Nephrol. 2015;10(8):1357-63.

24. Johnstone LM, Jones CL, Grigg LE, Wilkinson JL, Walker RG, Powell HR. Left ventricular abnormalities in children, adolescents and young adults with renal disease. Kidney Int. 1996;50(3):998-1006.

25. Lindblad YT, Axelsson J, Balzano R, Vavilis G, Chromek M, Celsi G, et al. Left ventricular diastolic dysfunction by tissue Doppler echocardiography in pediatric chronic kidney disease. Pediatr Nephrol. 2013;28(10):2003-13.

26. Ten Harkel AD, Cransberg K, Van Osch-Gevers M, Nauta J. Diastolic dysfunction in paediatric patients on peritoneal dialysis and after renal transplantation. Nephrol Dial Transplant. 2009;24(6):1987-91.

27. Mitsnefes MM, Kimball TR, Border WL, Witt SA, Glascock BJ, Khoury PR, et al. Impaired left ventricular diastolic function in children with chronic renal failure. Kidney Int. 2004;65(4):1461-6.

28. Mencarelli F, Fabi M, Corazzi V, Doyon A, Masetti R, Bonetti S, et al. Left ventricular mass and cardiac function in a population of children with chronic kidney disease. Pediatr Nephrol. 2014;29(5):893-900.

29. Scoble JE, Maher ER, Hamilton G, Dick R, Sweny P, Moorhead JF. Atherosclerotic renovascular disease causing renal impairment--a case for treatment. Clin Nephrol. 1989;31(3):119-22.

30. de Silva R, Nikitin NP, Bhandari S, Nicholson A, Clark AL, Cleland JG. Atherosclerotic renovascular disease in chronic heart failure: should we intervene? Eur Heart J. 2005;26(16):1596-605.

31. Wright JR, Shurrab AE, Cheung C, Waldek S, O'Donoghue DJ, Foley RN, et al. A prospective study of the determinants of renal functional outcome and mortality in atherosclerotic renovascular disease. Am J Kidney Dis. 2002;39(6):1153-61.

32. Bayazit AK, Yalcinkaya F, Cakar N, Duzova A, Bircan Z, Bakkaloglu A, et al. Reno-vascular hypertension in childhood: a nationwide survey. Pediatr Nephrol. 2007;22(9):1327-33.

33. Tullus K, Brennan E, Hamilton G, Lord R, McLaren CA, Marks SD, et al. Renovascular hypertension in children. Lancet. 2008;371(9622):1453-63.

34. Nagueh SF, Smiseth OA, Appleton CP, Byrd BF, 3rd, Dokainish H, Edvardsen T, et al. Recommendations for the Evaluation of Left Ventricular Diastolic Function by Echocardiography: An Update from the American Society of Echocardiography and the European Association of Cardiovascular Imaging. Eur Heart J Cardiovasc Imaging. 2016;17(12):1321-60.

35. Daskalov IR, Petrovsky PD, Demirevska LD. Mitral annular systolic velocity as a marker of preclinical systolic dysfunction among patients with arterial hypertension. Cardiovasc Ultrasound. 2012;10:46.

36. Gorcsan J, 3rd, Tanaka H. Echocardiographic assessment of myocardial strain. J Am Coll Cardiol. 2011;58(14):1401-13.

37. Wetterslev M, Moller-Sorensen H, Johansen RR, Perner A. Systematic review of cardiac output measurements by echocardiography vs. thermodilution: the techniques are not interchangeable. Intensive Care Med. 2016;42(8):1223-33.

38. Schoenmaker NJ, van der Lee JH, Groothoff JW, van Iperen GG, Frohn-Mulder IM, Tanke RB, et al. Low agreement between cardiologists

diagnosing left ventricular hypertrophy in children with end-stage renal disease. BMC Nephrol. 2013;14:170.

39. Arnold R, Schwendinger D, Jung S, Pohl M, Jung B, Geiger J, et al. Left ventricular mass and systolic function in children with chronic kidney disease-comparing echocardiography with cardiac magnetic resonance imaging. Pediatr Nephrol. 2016;31(2):255-65.

40. Leischik R, Dworrak B, Hensel K. Intraobserver and interobserver reproducibility for radial, circumferential and longitudinal strain echocardiography. Open Cardiovasc Med J. 2014;8:102-9.

41. Sicari R. Relevance of tissue Doppler in the quantification of stress echocardiography for the detection of myocardial ischemia in clinical practice. Cardiovasc Ultrasound. 2005;3:2.

42. Shroff R, Degi A, Kerti A, Kis E, Cseprekal O, Tory K, et al. Cardiovascular risk assessment in children with chronic kidney disease. Pediatr Nephrol. 2013;28(6):875-84.

43. Calabia J, Torguet P, Garcia M, Garcia I, Martin N, Guasch B, et al. Doppler ultrasound in the measurement of pulse wave velocity: agreement with the Complior method. Cardiovasc Ultrasound. 2011;9:13.

44. Kis E, Cseprekal O, Horvath Z, Katona G, Fekete BC, Hrapka E, et al. Pulse wave velocity in end-stage renal disease: influence of age and body dimensions. Pediatr Res. 2008;63(1):95-8.

45. Shroff RC, Donald AE, Hiorns MP, Watson A, Feather S, Milford D, et al. Mineral metabolism and vascular damage in children on dialysis. J Am Soc Nephrol. 2007;18(11):2996-3003.

46. Benedetto FA, Mallamaci F, Tripepi G, Zoccali C. Prognostic value of ultrasonographic measurement of carotid intima media thickness in dialysis patients. J Am Soc Nephrol. 2001;12(11):2458-64.

47. Hundley WG, Li HF, Hillis LD, Meshack BM, Lange RA, Willard JE, et al. Quantitation of cardiac output with velocity-encoded, phase-difference magnetic resonance imaging. Am J Cardiol. 1995;75(17):1250-5.

48. Muthurangu V, Atkinson D, Sermesant M, Miquel ME, Hegde S, Johnson R, et al. Measurement of total pulmonary arterial compliance using invasive pressure monitoring and MR flow quantification during MR-guided cardiac catheterization. Am J Physiol Heart Circ Physiol. 2005;289(3):H1301-6.

49. Al-Naamani N, Chirinos JA, Zamani P, Ruthazer R, Paulus JK, Roberts KE, et al. Association of Systemic Arterial Properties With Right Ventricular Morphology: The Multi-Ethnic Study of Atherosclerosis (MESA)-Right Ventricle Study. J Am Heart Assoc. 2016;5(12).

50. Cavalcante JL, Lima JA, Redheuil A, Al-Mallah MH. Aortic stiffness: current understanding and future directions. J Am Coll Cardiol. 2011;57(14):1511-22.

51. Agarwal R, Brunelli SM, Williams K, Mitchell MD, Feldman HI, Umscheid CA. Gadolinium-based contrast agents and nephrogenic systemic fibrosis: a systematic review and meta-analysis. Nephrol Dial Transplant. 2009;24(3):856-63.

52. Clinical Cardiac MRI: Springer Verlag; 2016.

53. Wright KL, Hamilton JI, Griswold MA, Gulani V, Seiberlich N. Non-Cartesian parallel imaging reconstruction. J Magn Reson Imaging. 2014;40(5):1022-40.

54. Pruessmann KP, Weiger M, Scheidegger MB, Boesiger P. SENSE: sensitivity encoding for fast MRI. Magn Reson Med. 1999;42(5):952-62.

55. Steeden JA, Atkinson D, Hansen MS, Taylor AM, Muthurangu V. Rapid flow assessment of congenital heart disease with high-spatiotemporal-resolution gated spiral phase-contrast MR imaging. Radiology. 2011;260(1):79-87.

56. Muthurangu V, Lurz P, Critchely JD, Deanfield JE, Taylor AM, Hansen MS. Real-time assessment of right and left ventricular volumes and function in patients with congenital heart disease by using high spatiotemporal resolution radial k-t SENSE. Radiology. 2008;248(3):782-91.

57. Kowalik GT, Knight DS, Steeden JA, Tann O, Odille F, Atkinson D, et al. Assessment of cardiac time intervals using high temporal resolution real-time spiral phase contrast with UNFOLDed-SENSE. Magn Reson Med. 2015;73(2):749-56.

58. Scatteia A, Baritussio A, Bucciarelli-Ducci C. Strain imaging using cardiac magnetic resonance. Heart Fail Rev. 2017;22(4):465-76.

59. Steeden JA, Knight DS, Bali S, Atkinson D, Taylor AM, Muthurangu V. Self-navigated tissue phase mapping using a golden-angle spiral acquisition-proof of concept in patients with pulmonary hypertension. Magn Reson Med. 2014;71(1):145-55.

60. Knight DS, Steeden JA, Moledina S, Jones A, Coghlan JG, Muthurangu V. Left ventricular diastolic dysfunction in pulmonary

hypertension predicts functional capacity and clinical worsening: a tissue phase mapping study. J Cardiovasc Magn Reson. 2015;17:116.

61. National High Blood Pressure Education Program Working Group on High Blood Pressure in C, Adolescents. The fourth report on the diagnosis, evaluation, and treatment of high blood pressure in children and adolescents. Pediatrics. 2004;114(2 Suppl 4th Report):555-76.

62. Odille F, Steeden JA, Muthurangu V, Atkinson D. Automatic segmentation propagation of the aorta in real-time phase contrast MRI using nonrigid registration. J Magn Reson Imaging. 2011;33(1):232-8.

63. de Simone G, Devereux RB, Daniels SR, Koren MJ, Meyer RA, Laragh JH. Effect of growth on variability of left ventricular mass: assessment of allometric signals in adults and children and their capacity to predict cardiovascular risk. J Am Coll Cardiol. 1995;25(5):1056-62.

64. Foley RN, Parfrey PS, Harnett JD, Kent GM, Murray DC, Barre PE. The prognostic importance of left ventricular geometry in uremic cardiomyopathy. J Am Soc Nephrol. 1995;5(12):2024-31.

65. Laurent S, Cockcroft J, Van Bortel L, Boutouyrie P, Giannattasio C, Hayoz D, et al. Expert consensus document on arterial stiffness: methodological issues and clinical applications. Eur Heart J. 2006;27(21):2588-605.

66. Steeden JA, Atkinson D, Taylor AM, Muthurangu V. Assessing vascular response to exercise using a combination of real-time spiral phase contrast MR and noninvasive blood pressure measurements. J Magn Reson Imaging. 2010;31(4):997-1003.

67. Groothoff JW, Gruppen MP, Offringa M, Hutten J, Lilien MR, Van De Kar NJ, et al. Mortality and causes of death of end-stage renal disease in children: a Dutch cohort study. Kidney Int. 2002;61(2):621-9.

68. Guerin AP, Pannier B, Metivier F, Marchais SJ, London GM. Assessment and significance of arterial stiffness in patients with chronic kidney disease. Curr Opin Nephrol Hypertens. 2008;17(6):635-41.

69. Litwin M, Wuhl E, Jourdan C, Trelewicz J, Niemirska A, Fahr K, et al. Altered morphologic properties of large arteries in children with chronic renal failure and after renal transplantation. J Am Soc Nephrol. 2005;16(5):1494-500.

70. Litwin M, Wuhl E, Jourdan C, Niemirska A, Schenk JP, Jobs K, et al. Evolution of large-vessel arteriopathy in paediatric patients with chronic kidney disease. Nephrol Dial Transplant. 2008;23(8):2552-7.

71. Oh J, Wunsch R, Turzer M, Bahner M, Raggi P, Querfeld U, et al. Advanced coronary and carotid arteriopathy in young adults with childhood-onset chronic renal failure. Circulation. 2002;106(1):100-5.

72. Tasdemir M, Eroglu AG, Canpolat N, Konukoglu D, Agbas A, Sevim MD, et al. Cardiovascular alterations do exist in children with stage-2 chronic kidney disease. Clin Exp Nephrol. 2016;20(6):926-33.

73. Van Craenenbroeck AH, Van Craenenbroeck EM, Van Ackeren K, Hoymans VY, Verpooten GA, Vrints CJ, et al. Impaired vascular function contributes to exercise intolerance in chronic kidney disease. Nephrol Dial Transplant. 2016;31(12):2064-72.

74. Schaefer F, Doyon A, Azukaitis K, Bayazit A, Canpolat N, Duzova A, et al. Cardiovascular Phenotypes in Children with CKD: The 4C Study. Clin J Am Soc Nephrol. 2016.

75. Sinha MD, Keehn L, Milne L, Sofocleous P, Chowienczyk PJ. Decreased arterial elasticity in children with nondialysis chronic kidney disease is related to blood pressure and not to glomerular filtration rate. Hypertension. 2015;66(4):809-15.

76. Lin IC, Hsu CN, Lo MH, Chien SJ, Tain YL. Low urinary citrulline/arginine ratio associated with blood pressure abnormalities and arterial stiffness in childhood chronic kidney disease. J Am Soc Hypertens. 2016;10(2):115-23.

77. Pennell DJ, Sechtem UP, Higgins CB, Manning WJ, Pohost GM, Rademakers FE, et al. Clinical indications for cardiovascular magnetic resonance (CMR): Consensus Panel report. J Cardiovasc Magn Reson. 2004;6(4):727-65.

78. Mortensen KH, Jones A, Steeden JA, Taylor AM, Muthurangu V. Isometric stress in cardiovascular magnetic resonance-a simple and easily replicable method of assessing cardiovascular differences not apparent at rest. Eur Radiol. 2016;26(4):1009-17.

79. McCrindle BW. Assessment and management of hypertension in children and adolescents. Nat Rev Cardiol. 2010;7(3):155-63.

80. Gupta-Malhotra M, Banker A, Shete S, Hashmi SS, Tyson JE, Barratt MS, et al. Essential hypertension vs. secondary hypertension among children. Am J Hypertens. 2015;28(1):73-80.

81. Briet M, Boutouyrie P, Laurent S, London GM. Arterial stiffness and pulse pressure in CKD and ESRD. Kidney Int. 2012;82(4):388-400.

82. Shroff R, Quinlan C, Mitsnefes M. Uraemic vasculopathy in children with chronic kidney disease: prevention or damage limitation? Pediatr Nephrol. 2011;26(6):853-65.

83. Shroff R, Long DA, Shanahan C. Mechanistic insights into vascular calcification in CKD. J Am Soc Nephrol. 2013;24(2):179-89.

84. Pfaltzgraff ER, Bader DM. Heterogeneity in vascular smooth muscle cell embryonic origin in relation to adult structure, physiology, and disease. Dev Dyn. 2015;244(3):410-6.

85. Saouti N, Westerhof N, Postmus PE, Vonk-Noordegraaf A. The arterial load in pulmonary hypertension. Eur Respir Rev. 2010;19(117):197-203.

86. Van Biesen W, Verbeke F, Devolder I, Vanholder R. The relation between salt, volume, and hypertension: clinical evidence for forgotten but still valid basic physiology. Perit Dial Int. 2008;28(6):596-600.

87. Grassi G, Quarti-Trevano F, Seravalle G, Arenare F, Volpe M, Furiani S, et al. Early sympathetic activation in the initial clinical stages of chronic renal failure. Hypertension. 2011;57(4):846-51.

88. Brewster UC, Perazella MA. The renin-angiotensin-aldosterone system and the kidney: effects on kidney disease. Am J Med. 2004;116(4):263-72.

89. Schlaich MP, Socratous F, Hennebry S, Eikelis N, Lambert EA, Straznicky N, et al. Sympathetic activation in chronic renal failure. J Am Soc Nephrol. 2009;20(5):933-9.

90. Raimann J, Liu L, Tyagi S, Levin NW, Kotanko P. A fresh look at dry weight. Hemodial Int. 2008;12(4):395-405.

91. Garfinkle MA. Salt and essential hypertension: pathophysiology and implications for treatment. J Am Soc Hypertens. 2017;11(6):385-91.

92. Flynn JT, Daniels SR, Hayman LL, Maahs DM, McCrindle BW, Mitsnefes M, et al. Update: ambulatory blood pressure monitoring in children and adolescents: a scientific statement from the American Heart Association. Hypertension. 2014;63(5):1116-35.

93. Flynn JT, Pierce CB, Miller ER, 3rd, Charleston J, Samuels JA, Kupferman J, et al. Reliability of resting blood pressure measurement and classification using an oscillometric device in children with chronic kidney disease. J Pediatr. 2012;160(3):434-40 e1.

94. Cheng HM, Sung SH, Shih YT, Chuang SY, Yu WC, Chen CH. Measurement of central aortic pulse pressure: noninvasive brachial cuff-based estimation by a transfer function vs. a novel pulse wave analysis method. Am J Hypertens. 2012;25(11):1162-9.

95. Groothoff J, Gruppen M, de Groot E, Offringa M. Cardiovascular disease as a late complication of end-stage renal disease in children. Perit Dial Int. 2005;25 Suppl 3:S123-6.

96. Paoletti E, De Nicola L, Gabbai FB, Chiodini P, Ravera M, Pieracci L, et al. Associations of Left Ventricular Hypertrophy and Geometry with Adverse Outcomes in Patients with CKD and Hypertension. Clin J Am Soc Nephrol. 2016;11(2):271-9.

97. Hickson LJ, Negrotto SM, Onuigbo M, Scott CG, Rule AD, Norby SM, et al. Echocardiography Criteria for Structural Heart Disease in Patients With End-Stage Renal Disease Initiating Hemodialysis. J Am Coll Cardiol. 2016;67(10):1173-82.

98. Paoletti E, Specchia C, Di Maio G, Bellino D, Damasio B, Cassottana P, et al. The worsening of left ventricular hypertrophy is the strongest predictor of sudden cardiac death in haemodialysis patients: a 10 year survey. Nephrol Dial Transplant. 2004;19(7):1829-34.

99. Nagueh SF, Appleton CP, Gillebert TC, Marino PN, Oh JK, Smiseth OA, et al. Recommendations for the evaluation of left ventricular diastolic function by echocardiography. Eur J Echocardiogr. 2009;10(2):165-93.

100. Mitsnefes MM, Daniels SR, Schwartz SM, Meyer RA, Khoury P, Strife CF. Severe left ventricular hypertrophy in pediatric dialysis: prevalence and predictors. Pediatr Nephrol. 2000;14(10-11):898-902.

101. Silverberg DS, Wexler D, Iaina A. The role of anemia in congestive heart failure and chronic kidney insufficiency: the cardio renal anemia syndrome. Perspect Biol Med. 2004;47(4):575-89.

102. Rostand SG, Drueke TB. Parathyroid hormone, vitamin D, and cardiovascular disease in chronic renal failure. Kidney Int. 1999;56(2):383-92.

103. Muller-Brunotte R, Kahan T, Malmqvist K, Edner M, Swedish ibesartan left ventricular hypertrophy investigation vs a. Blood pressure and left ventricular geometric pattern determine diastolic function in hypertensive myocardial hypertrophy. J Hum Hypertens. 2003;17(12):841-9.

104. Amann K, Breitbach M, Ritz E, Mall G. Myocyte/capillary mismatch in the heart of uremic patients. J Am Soc Nephrol. 1998;9(6):1018-22.

105. Opdahl A, Remme EW, Helle-Valle T, Lyseggen E, Vartdal T, Pettersen E, et al. Determinants of left ventricular early-diastolic lengthening velocity: independent contributions from left ventricular relaxation, restoring forces, and lengthening load. Circulation. 2009;119(19):2578-86.

106. Gimpel C, Jung BA, Jung S, Brado J, Schwendinger D, Burkhardt B, et al. Magnetic resonance tissue phase mapping demonstrates altered left ventricular diastolic function in children with chronic kidney disease. Pediatr Radiol. 2017;47(2):169-77.

107. Khan R, Sheppard R. Fibrosis in heart disease: understanding the role of transforming growth factor-beta in cardiomyopathy, valvular disease and arrhythmia. Immunology. 2006;118(1):10-24.

108. Jellis CL, Kwon DH. Myocardial T1 mapping: modalities and clinical applications. Cardiovasc Diagn Ther. 2014;4(2):126-37.

109. Chade AR, Brosh D, Higano ST, Lennon RJ, Lerman LO, Lerman A. Mild renal insufficiency is associated with reduced coronary flow in patients with non-obstructive coronary artery disease. Kidney Int. 2006;69(2):266-71.

110. Amann K, Ritz E, Wiest G, Klaus G, Mall G. A role of parathyroid hormone for the activation of cardiac fibroblasts in uremia. J Am Soc Nephrol. 1994;4(10):1814-9.

111. Stadermann MB, Montini G, Hamilton G, Roebuck DJ, McLaren CA, Dillon MJ, et al. Results of surgical treatment for renovascular hypertension in children: 30 year single centre experience. Nephrol Dial Transplant. 2010;25(3):807-13.

112. Shroff R, Roebuck DJ, Gordon I, Davies R, Stephens S, Marks S, et al. Angioplasty for renovascular hypertension in children: 20-year experience. Pediatrics. 2006;118(1):268-75.

113. Cameli M, Mondillo S, Solari M, Righini FM, Andrei V, Contaldi C, et al. Echocardiographic assessment of left ventricular systolic function: from ejection fraction to torsion. Heart Fail Rev. 2016;21(1):77-94.

114. Yano Y, Stamler J, Garside DB, Daviglus ML, Franklin SS, Carnethon MR, et al. Isolated systolic hypertension in young and middle-aged adults and 31-year risk for cardiovascular mortality: the Chicago Heart Association Detection Project in Industry study. J Am Coll Cardiol. 2015;65(4):327-35.

115. Smulyan H, Mookherjee S, Safar ME. The two faces of hypertension: role of aortic stiffness. J Am Soc Hypertens. 2016;10(2):175-83.

116. Parikh SA, Shishehbor MH, Gray BH, White CJ, Jaff MR. SCAI expert consensus statement for renal artery stenting appropriate use. Catheter Cardiovasc Interv. 2014;84(7):1163-71.

117. Martinez-Maldonado M. Pathophysiology of renovascular hypertension. Hypertension. 1991;17(5):707-19.

118. Bountioukos M, Schinkel AF, Bax JJ, Lampropoulos S, Poldermans D. The impact of hypertension on systolic and diastolic left ventricular function. A tissue Doppler echocardiographic study. Am Heart J. 2006;151(6):1323 e7-12.

119. Chavers BM, Li S, Collins AJ, Herzog CA. Cardiovascular disease in pediatric chronic dialysis patients. Kidney Int. 2002;62(2):648-53.

120. Parekh RS, Carroll CE, Wolfe RA, Port FK. Cardiovascular mortality in children and young adults with end-stage kidney disease. J Pediatr. 2002;141(2):191-7.

121. Green D, Kalra PR, Kalra PA. Echocardiographic abnormalities in dialysis patients with normal ejection fraction. Nephrol Dial Transplant. 2012;27(12):4256-9.

122. Hayashi SY, Brodin LA, Alvestrand A, Lind B, Stenvinkel P, Mazza do Nascimento M, et al. Improvement of cardiac function after haemodialysis.

Quantitative evaluation by colour tissue velocity imaging. Nephrol Dial Transplant. 2004;19(6):1497-506.

123. Kocyigit I, Sipahioglu MH, Orscelik O, Unal A, Celik A, Abbas SR, et al. The association between arterial stiffness and fluid status in peritoneal dialysis patients. Perit Dial Int. 2014;34(7):781-90.

124. Odudu A, McIntyre C. Volume is not the only key to hypertension control in dialysis patients. Nephron Clin Pract. 2012;120(3):c173-7.

125. Borlaug BA, Melenovsky V, Redfield MM, Kessler K, Chang HJ, Abraham TP, et al. Impact of arterial load and loading sequence on left ventricular tissue velocities in humans. J Am Coll Cardiol. 2007;50(16):1570-7.

126. Maroules CD, Khera A, Ayers C, Goel A, Peshock RM, Abbara S, et al. Cardiovascular outcome associations among cardiovascular magnetic resonance measures of arterial stiffness: the Dallas heart study. J Cardiovasc Magn Reson. 2014;16:33.

127. Mitsnefes M, Stablein D. Hypertension in pediatric patients on long-term dialysis: a report of the North American Pediatric Renal Transplant Cooperative Study (NAPRTCS). Am J Kidney Dis. 2005;45(2):309-15.

128. Konings CJ, Kooman JP, Schonck M, Dammers R, Cheriex E, Palmans Meulemans AP, et al. Fluid status, blood pressure, and cardiovascular abnormalities in patients on peritoneal dialysis. Perit Dial Int. 2002;22(4):477-87.

129. Lins RL, Elseviers M, Rogiers P, Van Hoeyweghen RJ, De Raedt H, Zachee P, et al. Importance of volume factors in dialysis related hypertension. Clin Nephrol. 1997;48(1):29-33.

130. Krediet RT, Balafa O. Cardiovascular risk in the peritoneal dialysis patient. Nat Rev Nephrol. 2010;6(8):451-60.

131. Covic A, Mardare N, Gusbeth-Tatomir P, Brumaru O, Gavrilovici C, Munteanu M, et al. Increased arterial stiffness in children on haemodialysis. Nephrol Dial Transplant. 2006;21(3):729-35.

132. Kis E, Cseprekal O, Biro E, Kelen K, Ferenczi D, Kerti A, et al. Effects of bone and mineral metabolism on arterial elasticity in chronic renal failure. Pediatr Nephrol. 2009;24(12):2413-20.

133. Tycho Vuurmans JL, Boer WH, Bos WJ, Blankestijn PJ, Koomans HA. Contribution of volume overload and angiotensin II to the increased pulse wave velocity of hemodialysis patients. J Am Soc Nephrol. 2002;13(1):177-83.

134. Lohmeier TE, Iliescu R. The baroreflex as a long-term controller of arterial pressure. Physiology (Bethesda). 2015;30(2):148-58.

135. Locatelli F, Cavalli A, Tucci B. The growing problem of intradialytic hypertension. Nat Rev Nephrol. 2010;6(1):41-8.

136. Losito A, Del Vecchio L, Del Rosso G, Locatelli F. Postdialysis Hypertension: Associated Factors, Patient Profiles, and Cardiovascular Mortality. Am J Hypertens. 2016;29(6):684-9.

137. Tian JP, Du FH, Cheng LT, Tian XK, Axelsson J, Wang T. Peripheral resistance modulates the response to volume overload in peritoneal dialysis patients. Perit Dial Int. 2008;28(6):604-10.

138. Schurig R, Gahl GM, Becker H, Schiller R, Kessel M, Paeprer H. Hemodynamic studies in long-term peritoneal dialysis patients. Artif Organs. 1979;3(3):215-8.

139. John SG, Selby NM, McIntyre CW. Effects of peritoneal dialysis fluid biocompatibility on baroreflex sensitivity. Kidney Int Suppl. 2008(108):S119-24.

140. McIntyre CW. Hemodynamic effects of peritoneal dialysis. Perit Dial Int. 2011;31 Suppl 2:S73-6.

141. Paniagua R, Orihuela O, Ventura MD, Avila-Diaz M, Cisneros A, Vicente-Martinez M, et al. Echocardiographic, electrocardiographic and blood pressure changes induced by icodextrin solution in diabetic patients on peritoneal dialysis. Kidney Int Suppl. 2008(108):S125-30.

142. Ivarsen P, Povlsen JV, Jensen JD. Increasing fill volume reduces cardiac performance in peritoneal dialysis. Nephrol Dial Transplant. 2007;22(10):2999-3004.

143. Liu YW, Su CT, Huang YY, Yang CS, Huang JW, Yang MT, et al. Left ventricular systolic strain in chronic kidney disease and hemodialysis patients. Am J Nephrol. 2011;33(1):84-90.

144. Sun M, Kang Y, Cheng L, Pan C, Cao X, Yao H, et al. Global longitudinal strain is an independent predictor of cardiovascular events in patients with maintenance hemodialysis: a prospective study using three-dimensional speckle tracking echocardiography. Int J Cardiovasc Imaging. 2016;32(5):757-66.

145. Antlanger M, Aschauer S, Kopecky C, Hecking M, Kovarik JJ, Werzowa J, et al. Heart Failure with Preserved and Reduced Ejection Fraction in Hemodialysis Patients: Prevalence, Disease Prediction and Prognosis. Kidney Blood Press Res. 2017;42(1):165-76.

146. Rumman RK, Ramroop R, Chanchlani R, Ghany M, Hebert D, Harvey EA, et al. Longitudinal assessment of myocardial function in childhood chronic kidney disease, during dialysis, and following kidney transplantation. Pediatr Nephrol. 2017;32(8):1401-10.

147. Bakkaloglu SA, Saygili A, Sever L, Noyan A, Akman S, Ekim M, et al. Assessment of cardiovascular risk in paediatric peritoneal dialysis patients: a Turkish Pediatric Peritoneal Dialysis Study Group (TUPEPD) report. Nephrol Dial Transplant. 2009;24(11):3525-32.

148. Omar AM, Vallabhajosyula S, Sengupta PP. Left ventricular twist and torsion: research observations and clinical applications. Circ Cardiovasc Imaging. 2015;8(6).

149. Sens F, Schott-Pethelaz AM, Labeeuw M, Colin C, Villar E, Registry R. Survival advantage of hemodialysis relative to peritoneal dialysis in patients with end-stage renal disease and congestive heart failure. Kidney Int. 2011;80(9):970-7.

150. Selby NM, McIntyre CW. Peritoneal dialysis is not associated with myocardial stunning. Perit Dial Int. 2011;31(1):27-33.

151. Burton JO, Jefferies HJ, Selby NM, McIntyre CW. Hemodialysis-induced repetitive myocardial injury results in global and segmental reduction in systolic cardiac function. Clin J Am Soc Nephrol. 2009;4(12):1925-31.

152. Selby NM, Burton JO, Chesterton LJ, McIntyre CW. Dialysis-induced regional left ventricular dysfunction is ameliorated by cooling the dialysate. Clin J Am Soc Nephrol. 2006;1(6):1216-25.

153. Selby NM, Lambie SH, Camici PG, Baker CS, McIntyre CW. Occurrence of regional left ventricular dysfunction in patients undergoing standard and biofeedback dialysis. Am J Kidney Dis. 2006;47(5):830-41.

154. Kaess BM, Rong J, Larson MG, Hamburg NM, Vita JA, Cheng S, et al. Relations of Central Hemodynamics and Aortic Stiffness with Left Ventricular Structure and Function: The Framingham Heart Study. J Am Heart Assoc. 2016;5(3):e002693.

155. Dincer I, Kumbasar D, Nergisoglu G, Atmaca Y, Kutlay S, Akyurek O, et al. Assessment of left ventricular diastolic function with Doppler tissue imaging: effects of preload and place of measurements. Int J Cardiovasc Imaging. 2002;18(3):155-60.

156. Shroff R. Can dialysis modality influence cardiovascular outcome? Pediatr Nephrol. 2012;27(11):2001-5.

157. Yeates K, Zhu N, Vonesh E, Trpeski L, Blake P, Fenton S. Hemodialysis and peritoneal dialysis are associated with similar outcomes for end-stage renal disease treatment in Canada. Nephrol Dial Transplant. 2012;27(9):3568-75.

158. Mehrotra R, Chiu YW, Kalantar-Zadeh K, Bargman J, Vonesh E. Similar outcomes with hemodialysis and peritoneal dialysis in patients with end-stage renal disease. Arch Intern Med. 2011;171(2):110-8.

159. Segers P, Rietzschel ER, De Buyzere ML, Vermeersch SJ, De Bacquer D, Van Bortel LM, et al. Noninvasive (input) impedance, pulse wave velocity, and wave reflection in healthy middle-aged men and women. Hypertension. 2007;49(6):1248-55.

160. Quail MA, Short R, Pandya B, Steeden JA, Khushnood A, Taylor AM, et al. Abnormal Wave Reflections and Left Ventricular Hypertrophy Late After Coarctation of the Aorta Repair. Hypertension. 2017;69(3):501-9.